Discovery and Characterization of Next-Generation Antibody and Vaccine Candidates

By

Kelsey Angelica Pilewski

Dissertation

Submitted to the Faculty of the

Graduate School of Vanderbilt University

in partial fulfillments of the requirements

for the degree of

DOCTOR OF PHILOSOPHY

in

Molecular Pathology & Immunology

May 13, 2022

Nashville, Tennessee

Approved:

Amy Major, PhD

James W. Thomas, MD

Maria Hadjifrangiskou, PhD

Tina Iverson, PhD

Ivelin S. Georgiev, PhD

Copyright © 2022 Kelsey Angelica Pilewski

All Rights Reserved.

This dissertation is dedicated to my parents, Lisa and Tom Pilewski.

Acknowledgements

First, I'd like to thank my advisor, Ivelin Georgiev. There have been quite a few times over the last few years when I've wondered why you let me join your lab, but I will be forever grateful for it. Beyond helping me reach this huge professional milestone, you taught me to me think bigger than I had ever imagined and to make the best out of every situation. Thank you to my committee members: Amy Major, Tom Thomas, Maria Hadjifrangiskou, and Tina Iverson, for your support, advice, criticisms, and time. Each of you have made me a better scientist.

Thank you to every Georgiev lab member, past and present. Kevin, lab buddy, buffer boy (the list goes on)…thank you for helping make the most stressful times of our lives fun, LTD. Andrea Shiakolas, not only are you a brilliant scientist ant beautiful human, you make those around you better. Thank you for commiserating, crying, and cheering with me. Thank you Lauren Walker, for always reminding me of the bigger picture. Thank you to previous lab member Ian Setliff, for questioning every one of my ideas, you made me a better scientist. To Steven Wall, thank you so much for all of your hard work, patience, and humor. I've loved watching the scientist you've become and I can't wait to see all that you do.

Finally, I could not be more grateful for the friends and family that helped get me to this moment. Thank you, Abbie Neininger and Geena Ildefonso, for being the definition of a true friend, we've laughed and cried our way through this whole adventure together, and I'm better because of you both. Thank you to my "oldest" friends -Jenn Duppert, Amanda Ceravolo, Elizabeth Stone, Alex Sarenski, and Courtney Mcgee- and my "older" friends- Anna Kozlowski, Cailin Schupbach, Grace Western, and Alex Febrizio- for your support and friendship, especially when I couldn't reciprocate. Thank

you to my siblings Dan and Brendan, for sitting through over a decade of dance recitals just to have to listen to me talk about science forever. To Livie, you are my best friend, I'm not sure which one of us is the big sister. Thank you to my parents, Lisa and Tom Pilewski, you have made all of this possible. Few people would be equally supportive when driving me to college dance major auditions and hearing about biomedical PhD interviews. You have been extraordinary role models of strength, hardwork, and humor. In everything I do, I hope only to make you proud. Finally, thank you to my person, Joey Balsamo. You have made me laugh louder, love bigger, and think harder than I could've imagined. You are the reason I made it through this crazy adventure, and we're just getting started.

TABLE OF CONTENTS

Figure List Page #

Chapter 1: Introduction

OVERVIEW

This dissertation contains my primary body of work focused on applying advancements in high-throughput antigen-specific antibody and B cell characterization, and modern rational vaccine design strategies towards the discovery and development of protective vaccines or antibody therapeutics against Human Immunodeficiency Virus (HIV-1), Hepatitis C Virus (HCV), and *Staphylococcus aureus*. In this document, I describe the human adaptive immune system, primarily focused on mechanisms of the humoral, or antibody-mediated immune response. Further, I discuss how this system can be exploited by vaccination to elicit long-lasting, protective immunity. One goal of this work was to profile the B cell receptor antigen specificity during chronic HIV-1/HCV co-infection using LIBRA-seq, the first study to examine antibody specificities in the relatively common infection setting of HIV-1/HCV co-infection. Further, I describe the discovery of the first HIV-1/HCV cross-reactive monoclonal antibodies which have the potential to aid cross-reactive vaccine design or serve as therapeutics themselves for both HIV-1 and HCV. Moreover, design and testing of a protective vaccine against *S. aureus* would significantly lessen the morbidity and mortality of this dangerous pathogen. Finally, I explore the relationship between cocktail vaccination and development of antigen-specific antibody responses, highlighting that factors outside direct antigen choice strongly influence vaccine-induced antibody responses. Discussing each direction outlined above, I have organized my dissertation into five chapters describing my thesis research performed under the direct mentorship of Dr. Georgiev, along with support from numerous Vanderbilt and external collaborators.

In Chapter I, I present the fundamental immunological principles that underlie the humoral, or B cell-mediated, arm of human adaptive immunity, and how knowledge of this system can be exploited to provide long lasting prophylaxis of infectious disease through vaccination.

In Chapter II, I investigate the antibody repertoire of a chronically HIV-1/HCV co-infected individual using LIBRA-seq, a technology that enables the simultaneous screening of B cells against a diverse library of antigen targets. This work resulted in the discovery of the first cross-functional HIV-1/HCV cross-reactive antibodies. This chapter required significant technical effort, including aiding in the development and original application of LIBRA-seq, and designing and optimizing flow cytometry panels for antigen-specific cell sorting. I also designed lab protocols for the use of human samples containing BSL2+ infectious agents including HIV-1. Further, I developed and implemented several techniques to measure antibody binding including cell surface display and biolayer interferometry (BLI) along with standard and competition ELISA. External collaborators aided in the functional characterization (Fc effector, neutralization) and auto/polyreactivity testing. Beyond serving as potential therapeutic candidates or vaccine scaffolds, the HIV-1/HCV cross-reactive antibodies described in this chapter challenge our understanding of antibody binding breadth.

In Chapter III, I sought to design a *S. aureus* vaccine that overcomes limitations of previous investigations by testing a multi-subunit vaccine that targets nutrient metal acquisition. In this study, I found that immunization with antigens targeting iron, zinc, and manganese acquisition induce superior *S. aureus* killing over mock-immunized controls. For this effort, I designed cloning and recombinant protein expression strategies for the generation of different vaccine combinations. Further, I wrote and executed the mouse immunization protocols and helped adapt whole blood killing assays. Together this

investigation provides important support for the development of a successful *S. aureus* vaccine.

Chapter IV examines how simultaneous immunization with multiple diverse immunogens affects the development of antigen-specific IgG antibody responses using pathogen-derived antigens and a prime/two boost vaccination regimen in mice. we discovered that although cocktail-immunized mice initially elicited more robust antibody responses, the rate of titer development decreases significantly over time compared to single antigen-immunized mice. Further, we found that single antigen-immunized mice showed an increased rate of IgG antibody development over cocktail antigen-immunized mice. These efforts demonstrate the contribution of formulation to elicitation of robust antibody responses. Understanding basic properties that govern the development of antigen-specific antibody responses is crucial to the design of future vaccines.

Chapter V summarizes the data and observations presented in the preceding chapters and proposes relevant directions of future study. Given the continued emergence of infectious agents, highlighted by the current pandemic, development of effective vaccines is critical to the control and prevention of disease.

INTRODUCTION

The human immune system

The human immune system is capable of mounting a response against nearly antigen, ideally resulting in lifelong protection (Chaplin, 2010; Nicholson, 2016). This process is orchestrated by a number of cells body-wide that can be divided into two arms: the innate and adaptive immune systems (Chen & Amigorena, 2015). The innate immune system is the body's first defense and is critical to the earliest stages of an immune

response. Innate immunity is not antigen-specific, but rather relies on a network of receptors recognizing conserved pathogen- and damage-associated molecular patterns (PAMPs/DAMPs) (Jain & Pasare, 2017; Tang et al., 2012). The triggering of these innate immune cells then recruits adaptive immunity, the slow but long-lasting, antigen-specific arm of the immune system (Iwasaki & Medzhitov, 2015). The adaptive immune response can be further divided into two classes, cellular/T cell-mediated immunity or humoral/B cell-mediated immunity (Garcia, 2019). The coordination of these arms generates antigen-specific adaptive immune cells capable of clearing infection or diseased tissue by multiple different mechanisms (Janeway, 2001b).

Humoral immunity

The humoral, or B cell-mediated immune response, acts by generating antigen-specific cellular receptors and their secreted forms, antibodies (Blattner & Tucker, 1984). Antibodies are Y-shaped proteins composed of two identical copies of “heavy” and “light” chain polypeptides and are the primary effector molecules of the humoral immune system (Chiu et al., 2019; Harkness, 1970). The antigen-binding (or Fab) area of the antibody is responsible for recognizing a region on their cognate antigen known as the epitope. Each antibody expresses a unique Fab structure, appropriately named the variable region, allowing each antibody to recognize a distinct antigen or epitope (Burton, 1985). On the other end of the antibody molecule is the constant region (or Fc), a sequence that is conserved and allows for antibody recognition by innate immune effectors such as complement and phagocytes (Dorrington & Klein, 1982; Jefferis et al., 1998). Through neutralization, opsonization, and complement activation (among other mechanisms), antibodies are critical effectors of humoral immunity (Lu et al., 2018).

B cell repertoire development

As introduced above, each B cell expresses a unique receptor sequence bearing a distinct antigen-binding site that allows the humoral immune system to recognize nearly any antigen. The extraordinary diversity of the human B cell repertoire is generated, in part, by somatic DNA recombination mechanisms during cell development (Rose, 1982). The B cell receptor (BCR) is made up of two identical copies of a heavy and a light chain that are expressed from three distinct genetic loci: the heavy chain, and two equivalent, but distinct, light chain gene clusters termed kappa and lambda (**κ, λ**). Both the heavy and light chains have variable (V_H or V_L) and constant regions ($C_{H1\text{-}3}$ or C_L), where the variable region of both chains is generated by the random recombination of Variable (V) and Joining (J) gene segments, and the heavy chain contains an additional gene termed the Diversity (D) segment (Gally & Edelman, 1970). The diversity generated by this random genetic recombination, termed V(D)J recombination, along with the random pairing of heavy and light chains together, is termed combinatorial diversity. Junctional diversity provides a further source of heterogeneity and refers to the addition and subtraction of random nucleotides at the junctions of gene segments induced by the DNA recombination process (Janeway, 2001a). After DNA recombination, the variable region (V_H or V_L) is transcribed, and the constant region gene segments are added by alternative mRNA splicing. A **κ** or **λ** constant gene segment is combined with the V_L region to form the kappa or lambda light chain, and, initially, a **μ** (and **δ**) constant gene segment is combined with the V_H region to form the IgM (and IgD) heavy chain. Together, these mechanisms generate more potential BCR sequences than there are naïve B cells circulating at any given time (Imkeller & Wardemann, 2018; Jackson et al., 2013).

Germinal center reactions and generation of high affinity antibody responses

B cells that generate a productive BCR sequence and pass relevant developmental checkpoints (summarized elsewhere), make up the naïve B cell repertoire and search the periphery for their cognate antigen (Nemazee, 2017; Notidis et al., 2002). Once a B cell has bound its antigen via recognition by the BCR, these cells migrate from the periphery towards secondary lymphoid structures (lymph nodes or spleen) for further activation. B cells that engage antigen will then seek help from a specialized subset of T cells called T follicular helper cells (T_{FH}), through a process termed linked recognition (Breitfeld et al., 2000; Mintz & Cyster, 2020). B cells can also be activated to secrete antibody in a T cell-independent manner by mechanisms described elsewhere (Allman et al., 2019). If a B cell finds a T_{FH} cell that has been activated by the same antigen (linked recognition), it may receive the appropriate survival signals and terminally-differentiate into a mature antibody-secreting cell (ASC) or proliferate to help form a germinal center (Mitchison, 1971a, 1971b, 1971c). Within the germinal center, B cells are able to remodel and diversify their BCRs through a directed-evolutionary process termed affinity maturation (Tonegawa, 1983). Affinity maturation is mediated by somatic hypermutation (SHM), where additional mutations are added throughout the variable region of the BCR. If these mutations increase the affinity of the BCR for its given antigen, the B cell is positively selected by survival signals and T cell help. During this phase of the immune response, B cells can also change their constant region to another isotype by a process termed class-switching (Sakano et al., 1980). This process is mediated by the same enzymatic mechanism as SHM but is activated by distinct cytokine signals. Both the affinity and antigen-specificity, as well as isotype, of the BCR have critical impacts on the development of protective immunity (Allen et al., 1987).

Mechanisms of antibody-mediated anti-pathogen immunity

Antibodies produced by B cells contribute to immunity by a number of different mechanisms, including neutralization, opsonization, and complement activation. Antibody recognition of pathogen epitopes critical for host entry or adherence can directly neutralize or block infection (Bachmann & Zinkernagel, 1997). Further, antibody-binding can opsonize, or tag pathogens for clearance by innate immune cells through mechanisms such as antibody-dependent cellular phagocytosis (ADCP) and antibody-dependent cellular cytotoxicity (ADCC). These processes are mediated through recognition of the antibody constant region (Fc) by Fc receptors. As introduced above, the Fc region of the antibody determines the isotype, which in turn greatly affects which immune cells and effector mechanisms are recruited (Forthal, 2014; J V Ravetch & Kinet, 1991). For example, although IgM is capable of neutralization and opsonization, this antibody isotype is most effective at activating complement. IgG isotype antibodies by contrast, have the most functional potential, capable of activating all of the pathways described thus far. Overall, antibodies contribute to immunity both by directly binding and inhibiting pathogens, as well as coordinating their clearance by innate immune cells.

Vaccine-induced immunity and reverse vaccinology 2.0

Since Edward Jenner's pioneering experiments with smallpox, immunization has become the most effective public health intervention, preventing, and in some cases eradicating, infection by multiple pathogens (Hajj Hussein et al., 2015; Plotkin, 2014). Notably, nearly all licensed vaccines confer protection by eliciting pathogen-specific humoral immunity (Amanna & Slifka, 2011; Plotkin, 2010). Traditional vaccine strategies have involved the injection of live-attenuated or inactivated versions of the pathogen, or portion of the pathogen, to induce long lasting protection (Pöyhönen et al., 2019; Wareing & Tannock, 2001). However, the emergence of highly mutable (e.g. Human

Immunodeficiency Virus (HIV-1) and Hepatitis C Virus (HCV)) and antibiotic-resistant (e.g. *Staphylococcus aureus*) pathogens has highlighted the need for additional approaches (Hargrave et al., 2021; Kennedy et al., 2020; Li et al., 2015). Fortunately, advancements in high-throughput antibody profiling, next-generation sequencing, and structural characterization technologies have enabled the contemporary era of vaccinology often referred to as reverse vaccinology 2.0 (Rappuoli et al., 2016; Sette & Rappuoli, 2010).

Modern immunization strategies aim to rationally engineer a single antigen or cocktail of antigens to generate a more focused, protective antibody response. This process involves defining protective epitopes or antigens by studying natural infection and immunization and applying these observations to inform design of vaccines that elicit desired immune responses (Burton, 2010; Moxon et al., 2019). Understanding mechanisms of vaccine-induced humoral immunity is crucial to the design of effective immunization regimens. Highlighted by the current pandemic, development of protective vaccines is essential to the control and prevention of infectious disease.

Chapter 2: Functional HIV-1/HCV Cross-Reactive Antibodies Isolated from a Chronically Co-infected Donor

This chapter is adapted from the following manuscript:

Pilewski, KA et al., “Functional HIV-1/HCV Cross-Reactive Antibodies Isolated from a Chronically Co-infected Donor”, *In revision*, 2022.

Contributions: Steven Wall aided in the expression and purification of both antibodies and antigens used throughout this study, as well as performing ELISA binding assays. Simone Richardson performed Fc effector functional assays. Kaitlyn Clark, Nicole Frumento, and Jordan Salas performed HCV neutralization assays. Tandile Hermanus and Rutendo Mapengo performed HIV-1 neutralization assays. Elad Binshtein performed nsEM and 2D averaging studies of Fab+ HIV-1 trimer. Rohit Venkat, Ian Setliff, and Nagarajan Raju provided bioinformatic support. Kevin Kramer tested antibody binding to CoV antigens by ELISA. Andrea Shiakolas tested antibody binding to Influenza A antigens by ELISA. Giuseppe Sautto performed influenza neutralization and HAI assays. Naveen Suryadevara performed SARS CoV-2 neutralization assays. John Brannon and Connor Beebout performed *E. coli* inhibition assays. Rob Parks performed antibody autoreactivity experiments. Lauren Walker, Emilee Friedman Fechter and Juliana Qin provided control antibodies and antigens. Spyros Kalams provided VC10014 donor samples. I performed all aspects of the LIBRA-seq experiment, expression/purification of antigens and antibodies, antibody testing by ELISA and BLI, and coordinated all collaborator experiments. Ivelin Georgiev and I designed the study and wrote the paper.

INTRODUCTION

Human immunodeficiency virus (HIV-1) and hepatitis C virus (HCV) are two of the most diverse human pathogens, ever-evolving to evade immune system pressure, typically establishing chronic, life-long infection (Burke & Cox, 2010; Chen et al., 2009; Gandhi & Walker, 2002; Tester et al., 2005; Tonegawa). Furthermore, due to the shared routes of transmission, HIV-1/HCV co-infection is relatively common, affecting an estimated 5 million individuals worldwide (Operskalski & Kovacs, 2011; Platt et al., 2016). Although the last 30+ years have seen significant advances in the treatment of both viruses, there are still no licensed vaccines or other prophylactic countermeasures (Hernandez & Sherman, 2011; Pineda et al., 2007). Moreover, there is a cure for HCV available, yet less than 50% of infected individuals know of their positive status, highly limiting its utility (Martinello et al.). Poor medication and diagnostic access, as well as high re-infection rates, for which HIV-1/HCV co-infected individuals experience the highest re-infection rates with either virus, strongly motivate the development of alternative therapeutic and prophylactic tools (Chohan et al., 2005; Ingiliz et al., 2017; Lambers et al., 2011). Such new tools will be of important utility in the setting of HIV-1/HCV co-infection, where the chronic exposure to two mutating pathogens leads to significantly exacerbated health problems compared to mono-infection (Feuth et al., 2013; Lin et al., 2013; Vivithanaporn et al., 2012).

Although these highly mutable viruses have rendered classical vaccine design difficult, investigating the human antibody response to HIV-1 and HCV mono-infection has led to the identification of antibodies that are effective in therapy and prophylaxis, and that have served as templates for antibody-specific vaccine development (Balazs et al., 2012; Bricault et al., 2019; Keck et al., 2019; Pierce et al., 2017). The clinical setting of

HIV-1/HCV co-infection has been far less explored, with little understanding about antibody responses in the chronic presence of two diverse, constantly evolving, antigen

A.

VC10014

LIBRA-seq Antigen Screening Panel		
Virus	*Strain*	*Protein*
HIV-1	BG505	gp140
	B41	gp140
	ConC	gp120
	A244	gp120
HCV	H77	E1E2
	H77	E2c
	JFH1	E2c

B.

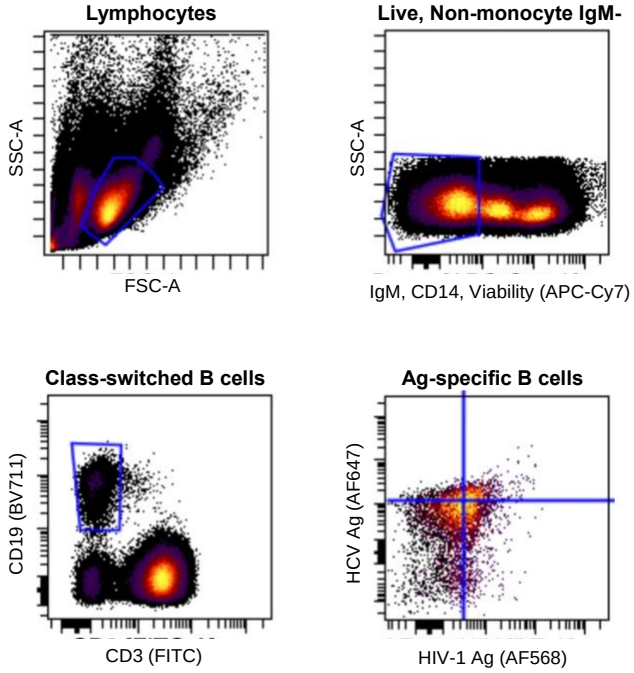

C.

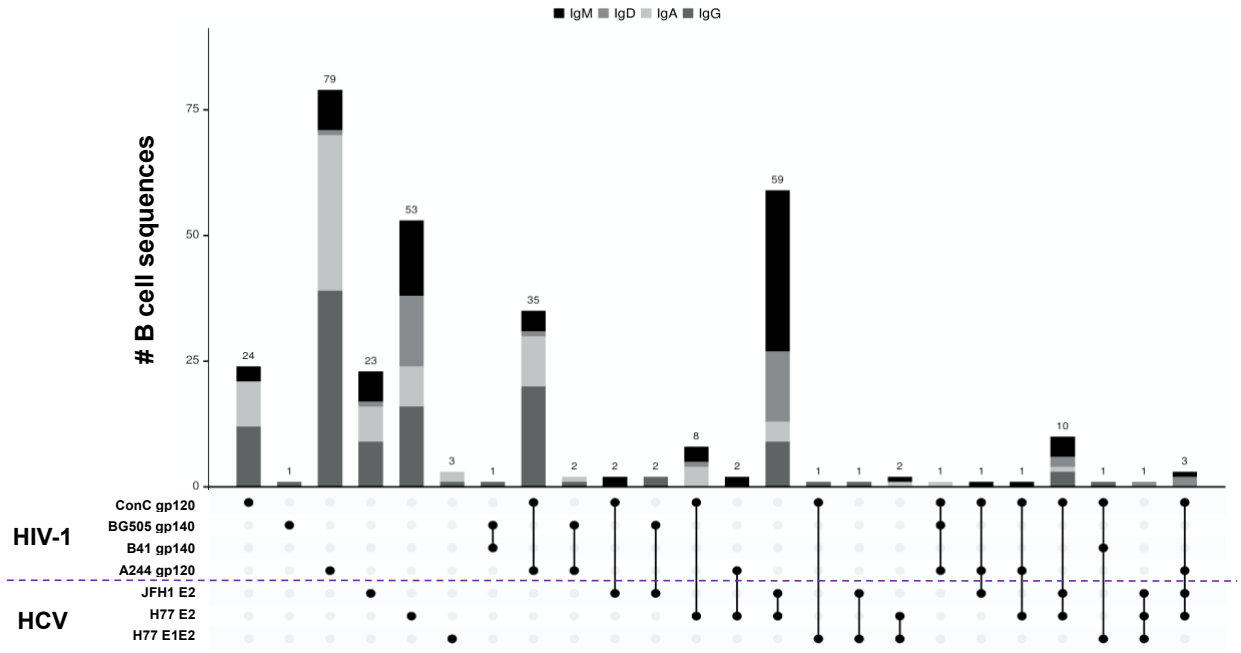

Figure 2-1. Strategy for the Identification of HIV-1/HCV Cross-reactive B cells using LIBRA-seq.

(A) Diverse, DNA-barcoded envelope proteins from the indicated strains of both HIV-1 and HCV were used to isolate antigen-specific B cells from Vanderbilt HIV-1 cohort donor VC10014. (B) Flow sorting strategy for the identification of antigen-specific B cells. First, the lymphocyte population was identified by scatter, followed by exclusion of dead cells, monocytes, and IgM-expressing cells. Next, the B cell population was identified, and Dead$^-$, CD14$^-$, IgM$^-$, CD3$^-$, CD19$^+$, Antigen$^+$ cells were sorted for subsequent single-cell sequencing. (C) Frequency of B cells (y-axis) that were positive for each combination (filled circles connected by lines) of antigens (rows), colored by isotype. B cells with calculated LIBRA-seq scores >1 for a given antigen were considered positive.

targets (Danta et al., 2008; Lara et al., 2018; Reiche et al., 2014). In this study, we sought to investigate the antibody repertoire of a chronically HIV-1/HCV co-infected individual using LIBRA-seq, a technology that enables the simultaneous screening of B cells against a diverse library of antigen targets (Setliff et al., 2019). Notably, we show that LIBRA-seq identified antibodies with binding and functional cross-reactivity between HIV-1 and HCV, without exhibiting typical traits of promiscuous antigen recognition. These results challenge our long-standing understanding of the exclusiveness of antibody-antigen specificity and pave the way toward the development of effective therapeutics and vaccines with an unparalleled breadth of reactivity.

RESULTS

Discovery of HIV-1/HCV Cross-reactive Antibodies from a Chronically HIV-1/HCV Co-infected Donor

To probe the development of antibody responses produced by the unique immunological challenge of HIV-1/HCV co-infection, we sought to profile the antigen-specific B cell compartment using LIBRA-seq. As previously described, LIBRA-seq is a technology that allows for high-throughput mapping of antigen specificity to B cell receptor sequence by leveraging oligo-barcoded antigens and single-cell sequencing (Setliff et al., 2019). We identified a donor, VC10014 from the Vanderbilt HIV-1 infection cohort, who had been chronically HIV-1/HCV co-infected for >3 years at the time of sample collection and had never taken anti-viral or anti-retroviral medication. Previous studies investigating key events leading to early development of broad HIV-1 neutralization established that VC10014 developed broad serum neutralization approximately one year after HIV-1 infection and that this phenotype could largely be traced to a CD4 binding site-directed antibody response (Sather et al., 2009; Sather et al., 2014). Monoclonal antibody

discovery efforts in this donor failed to identify any broadly neutralizing antibodies, instead attributing the observed serum breadth to a diverse but cooperative antibody lineages (Chukwuma et al., 2018). Given the ability of LIBRA-seq to screen tens of thousands of B cells against a large panel of diverse antigens, including those from unrelated pathogens, we sought to apply this technology to HIV-1/HCV co-infected donor VC10014. The application of LIBRA-seq provides a unique opportunity to interrogate the antibody repertoire in the setting of chronic exposure to diverse – and constantly evolving – antigens.

To identify virus-specific B cell sequences from VC10014, we applied LIBRA-seq with a diverse panel of seven antigens including four HIV-1 envelope (Env) glycoprotein

A.

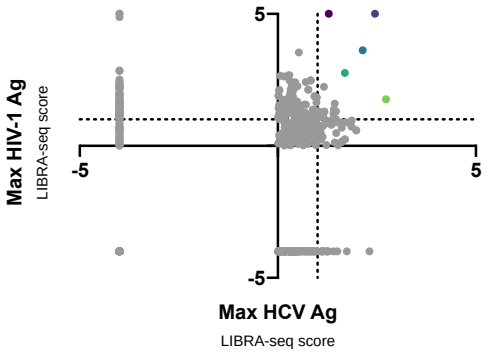

B.

mAb name	IGHV gene	% SHM	CDRH3	IGLV gene	% SHM	CDRL3	Isotype
mAb180	*IGHV3-48*	11.2	CARSEKRVTMTRKIKGRWFGPW	*IGLV3-21*	7.2	CQVWDSSSEHVVF	IgG1
mAb692	*IGHV1-46*	8.8	CARVAPPGVVNNKWFDIW	*IGLV2-11*	9.7	CCLYAGSYSWVF	IgG1
mAb688	*IGHV3-23*	12.5	CAKGLTTESRLEFW	*IGKV1-39*	12.4	CQQSYNVPTF	IgG3
mAb803	*IGHV3-21*	4.9	CVSSWGPESPYYFDYW	*IGKV6-21*	3.6	CHQSSSLPFTF	IgA
mAbKP1-8	*IGHV1-8*	9.7	CAREYCTGGDCHFFLDYW	*IGKV4-1*	6.7	CQHFYSSPPTF	IgA

C.

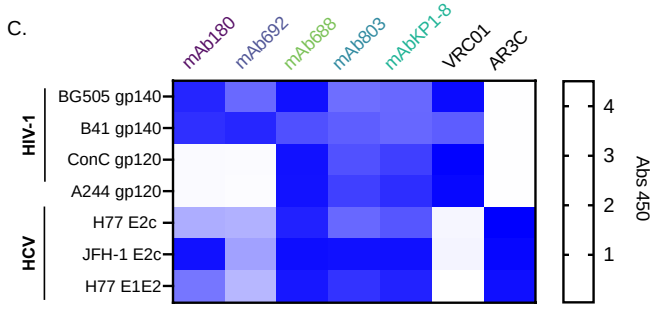

D.

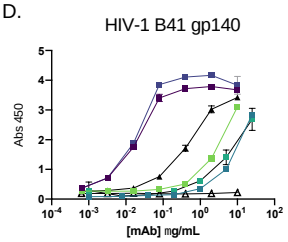

E.

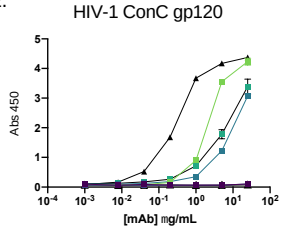

F.

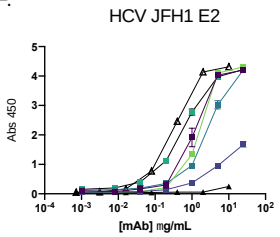

G.

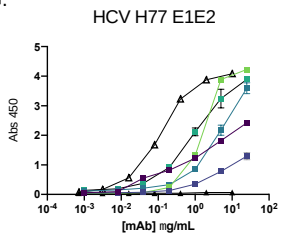

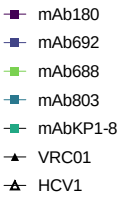

Figure 2-2. Discovery of Exceptionally Broad Anti-viral Antibodies from a Chronically HIV-1/HCV Co-infected Donor.
(A) Plot of maximum LIBRA-seq score for an HIV antigen (Ag) vs. HCV antigen where each dot represents a single class-switched (IgG, IgA) cell. Colored dots represent antibodies selected for further study. Cells with antigen values <0 were set to -4. (B) Genetic features of identified HIV-1/HCV cross-reactive BCRs. Color of antibody name corresponds to LIBRA-seq score colors in A. (C) Binding of HIV/HCV cross-reactive recombinant antibodies to the panel of viral antigens (shown on the left) at 10ug/mL as measured by ELISA. The following antibodies are shown as controls: AR3C (HCV E2), VRC01 (HIV-1 gp120). (D-E) Recombinantly-expressed lead antibody binding to clade B (B41) and clade A (BG505) HIV envelope glycoproteins; and (F-G) genotype 2a (JFH1) and genotype 1a (H77) HCV envelope glycoproteins, measured by ELISA.

antigens each from a unique clade (A/BG505 gp140, B/B41 gp140, C/ConC gp120, AE/A244 gp120), and three HCV envelope glycoprotein antigens from two distinct genotypes (1a/ H77 E2c, H77 E1E2, and 2a/ JFH1 E2c) (**Figure 2-1A**). The inclusion of multiple antigen variants for each of HIV-1 and HCV allows for the identification of antibodies with broad diversity of antigen specificities. LIBRA-seq recovered paired VH:VL B cell receptor (BCR) sequences with associated antigen specificity mapping for 886 cells (**Figure 2-1B, C**). Of the identified class-switched BCR sequences, ~75% were HIV-1 antigen-specific, and ~23% were HCV antigen-specific. Interestingly, we also identified a small population of cells positive for at least one HIV-1 and at least one HCV antigen (**Figure 2-1C**). Within this population of cross-reactive B cells, we focused on the class-switched cells with the highest LIBRA-seq scores for any HIV-1 and HCV antigen (**Figure 2-2A**). We identified five genetically unique sequences with varied levels of somatic hypermutation (SHM) and HIV-1 antigen+/HCV antigen+ specificity phenotypes for further study (**Figure 2-2B**). We expressed these five paired heavy-light chain sequences as recombinant antibodies and confirmed their reactivity against a panel of HIV-1 and HCV envelope glycoproteins by ELISA (**Figure 2-2C-G**). The results confirmed that LIBRA-seq successfully predicted the HIV-1/HCV envelope antigen cross-reactivity of the identified antibodies.

HIV-1/HCV Cross-reactive Antibodies Recognize Distinct Epitopes on the HIV-1 and HCV Envelope Glycoproteins

Given the unique antibody-antigen cross-reactivity, we sought to map the epitope of these antibodies on the two antigen targets. We first wanted to define the five cross-reactive antibody epitope targets on the HCV envelope. All antibodies bound recombinant HCV E1E2 with recognition directed to the E2 subunit of the glycoprotein, with only

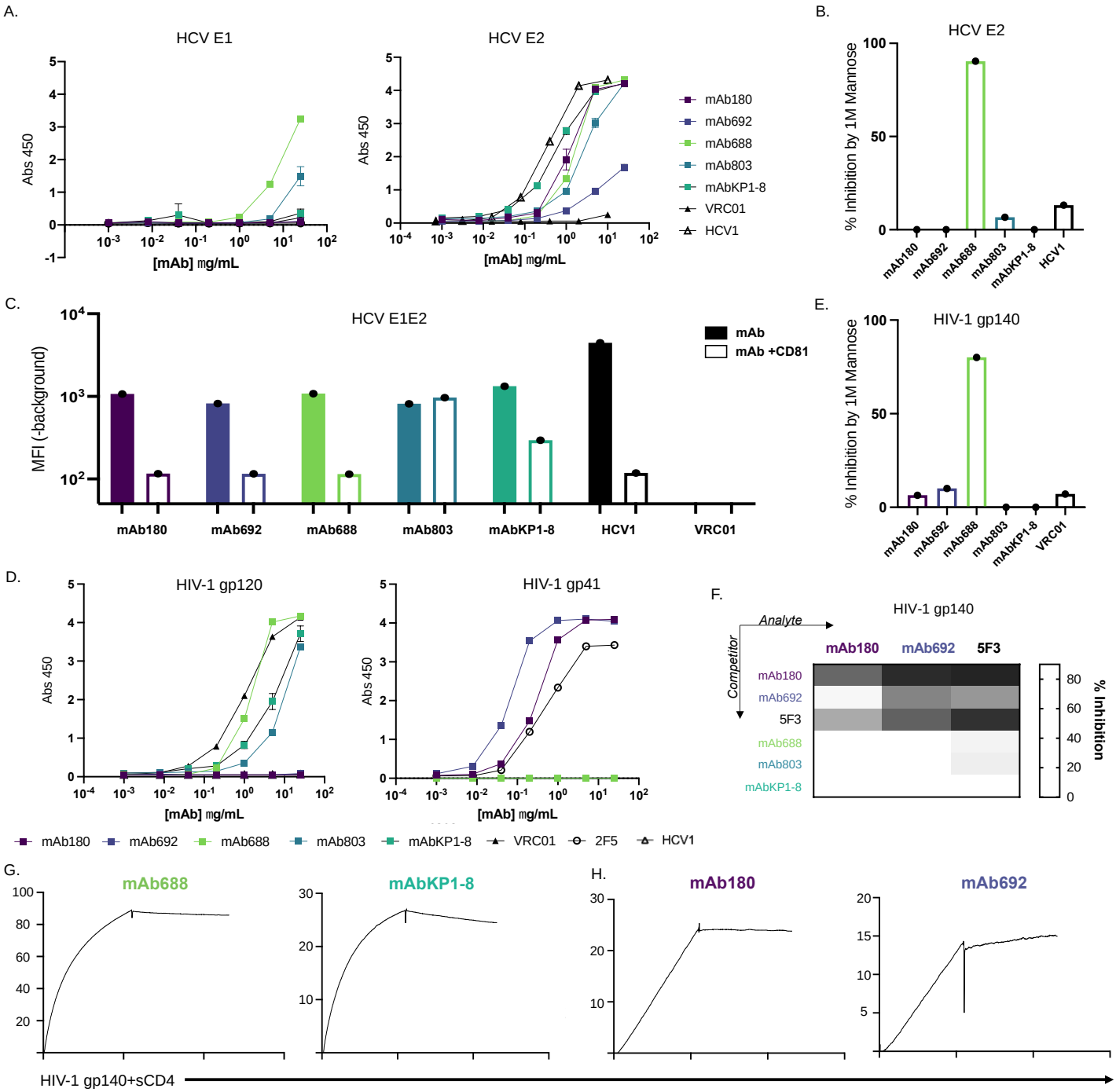

Figure 2-3. HIV-1/HCV Cross-reactive Antibodies Recognize Distinct Epitopes on the HIV-1 and HCV Envelope Glycoproteins.

(A) Antibody binding to the E1 (strain: HC-J4; left) and E2 (strain: JFH-1; right) subunits of the HCV envelope glycoprotein measured by ELISA. The HCV1 E2-specific antibody HCV1 is shown as a positive control, and the HIV-1-specific antibody VRC01 is shown as a negative control. (B) Antibody binding to HCV E2 glycoprotein (strain: JFH-1) in the presence of 1M D-(+)-Mannose. Data plotted as % inhibition as compared to binding in PBS buffer. Antibodies demonstrating negative % inhibition values were set to 0 (C) Antibody binding to cell surface-expressed HCV E1E2 (strain: H77) measured by flow cytometry. Cells were either pre-incubated with PBS (filled bar) or CD81-LEL (open bar) before detection by fluorescent secondary. Data shown as background-subtracted mean fluorescence intensity (MFI). (D) Antibody binding to the gp120 (strain AE.A244) (left) and gp41 (strain: MN) (right) subunits of the HIV-1 envelope glycoprotein measured by ELISA. The gp120-specific and gp41-specific antibodies VRC01 and 2F5, respectively, are shown as positive controls, and the HCV-specific antibody HCV1 is shown as a negative control. (E) Antibody binding to HIV-1 gp140 (strain: BG505) in the presence of 1M D-(+)-Mannose measured ELISA. Data plotted as % inhibition as compared to binding in PBS buffer. The mannose-independent HIV-1 antibody VRC01 is shown as a control. Antibodies demonstrating negative % inhibition values were set to 0. (F) Antibody binding to HIV-1 gp140 (strain: BG505) in the presence of competitor antibodies measured by ELISA. Competitor antibodies (shown on the Y axis) were added first, and subsequently binding of biotinylated analyte antibodies (shown on the X axis) was detected. Data displayed as % inhibition, calculated as a function of no competition controls. Antibody binding to HIV-1 gp140 (strain: BG505) with soluble CD4 (sCD4), measured by SPR (G) mAb688 and mAbKP1-8, (H) mAb180 and mAb692. HIV-1 gp140 antigen was incubated with sCD4 before antibody was added.

further map the epitopes targeted, we measured antibody competition with CD81, the cognate HCV entry receptor (**Figure 2-3C**). We discovered that binding of four of the five HIV-1/HCV cross-reactive antibodies was inhibited by pre-incubation with CD81-LEL (**Figure 2-3C**). Interestingly, mAb803 binding was slightly increased in the presence of receptor (**Figure 2-3C**).

Given the extensive glycan shield that decorates both the HIV-1 and HCV envelope glycoproteins, we also sought to define the glycan-dependence of HIV-1/HCV cross-reactive recognition. We found that only mAb688 was inhibited by both 1M D-(+)-mannose and PNGaseF de-glycosylation (**Figure 2-3B, Figure 2-4A**). Additionally, in experiments with HCV E2 protein produced in the presence of kifunensine, a class I α-mannosidase inhibitor that results in the majority presence of high mannose-type glycans, mAb688 binding was decreased, suggesting that recognition requires additional contacts or glycan processing (**Figure 2-4B**). In summary, we discovered that HIV-1/HCV cross-reactive antibodies recognize at least three distinct epitopes on the HCV envelope protein including CD81-independent (mAb803), as well as glycan-dependent (mAb688) and -independent (mAb180, mAb692, mAbKP1-8) CD81-blocking regions.

Next, we sought to map the epitopes of these antibodies on the HIV-1 envelope protein. All five antibodies bound soluble HIV-1 gp140, albeit to various degrees (**Figure 2-2D**). Intriguingly, two of the five antibodies (mAb180, mAb692) recognized the gp41 subunit of HIV-1 Env, while the other three antibodies recognized gp120 (**Figure 2-3D, Figure 2-4C**). In competition ELISA experiments we found that mAb180 and mAb692 recognized epitopes overlapping with that of 5F3 (**Figure 2-3F**). 5F3 has previously been reported to interact with both the C-terminal heptad repeat region (CHR) and the fusion peptide proximal region (FPPR) (Buchacher et al., 1994; Corti et al., 2010). Importantly,

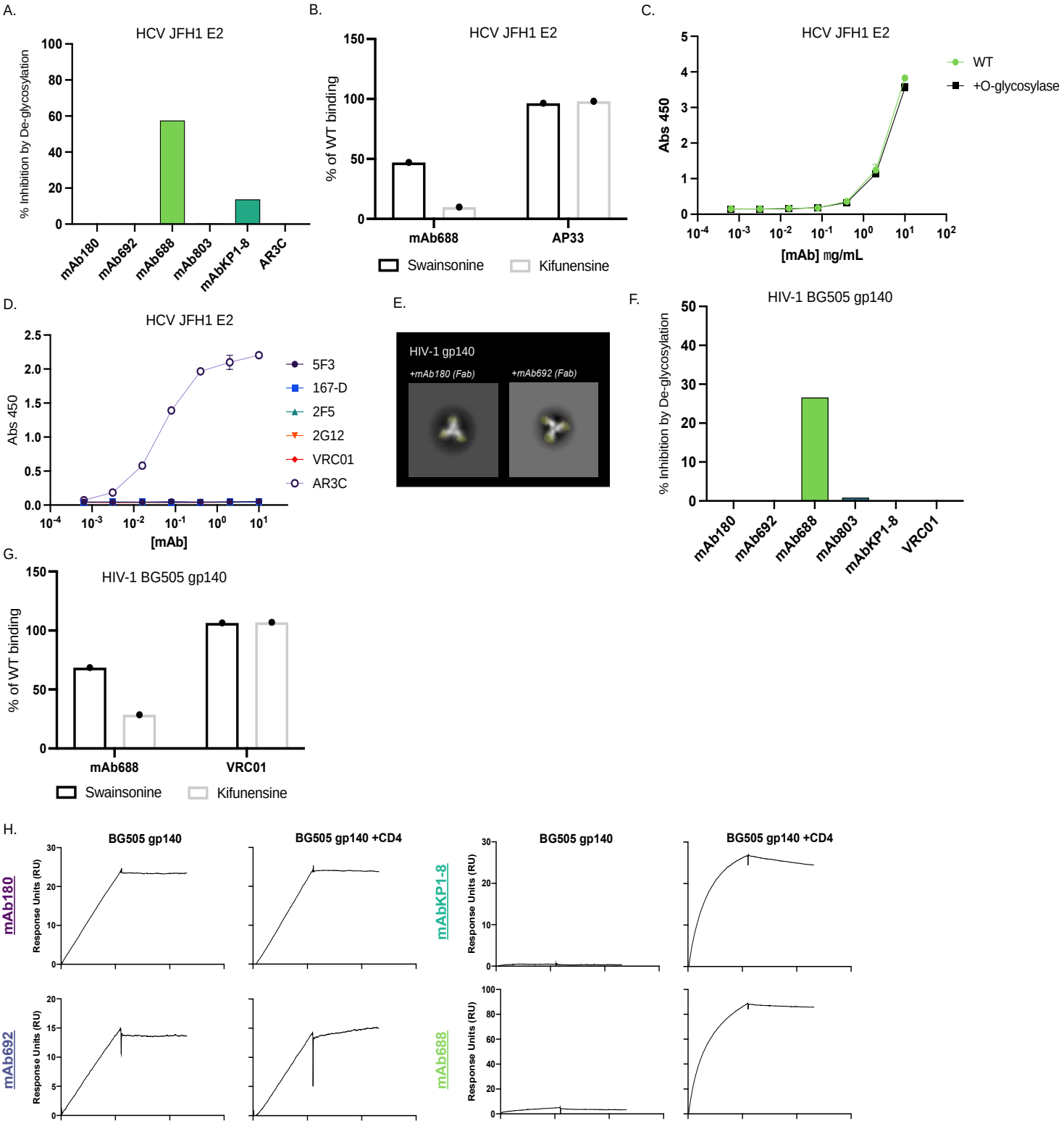

Figure 2-4. Characteristics of HCV and HIV-1 Envelope Recognition by HIV-1/HCV Antibodies.
(A) Antibody binding to PNGaseF de-glycosylated HCV E2 (strain: JFH1) measured by ELISA was compared to wild type (WT) binding. HCV-specific antibody AR3C is shown as a control. (B) Antibody binding to HCV E2 (strain:JFH1) after mannosidase inhibitor treatment with either swainsonine (black bars) or kifunensine (gray bars). AP33 is shown as a control. (C) Antibody binding to O-glycosylase de-glycosylated and WT HCV E2 (strain: JFH1) measured by ELISA. (D) HIV-specific antibody binding to HCV envelope protein measured by ELISA. HCV-specific antibody AR3C is shown as a control. (E) nsEM images of HIV-1 gp140 in complex with either mAb180 (left: Fab, colored yellow) or mAb692 (right: Fab, colored yellow). (F) Antibody binding to PNGaseF de-glycosylated HIV-1 gp140 (strain: BG505) measured by ELISA was compared to wild type (WT) binding. HIV-specific antibody VRC01 is shown as a control. (F) Antibody binding to HIV-1 Env (BG505) after mannosidase inhibitor treatment. VRC01 is shown as a control. (H) Antibody binding to HIV-1 gp140 (strain: BG505) with and without soluble CD4 (sCD4), measured by SPR. *HIV-1 gp140 antigen was either incubated with PBS (left) or sCD4(right) before antibody was added.

(167-D, F240) to the HCV envelope protein, suggesting our LIBRA-seq-identified antibodies represent a unique binding modality (**Figure 2-4D**). As expected from their gp120 reactivity, mAbs 688, 803, and KP1-8 did not compete with the gp41-reactive mAb180 and mAb692 for binding to HIV-1 gp140 (**Figure 2-3F**). Next, we assessed HIV-1/HCV cross-reactive antibody binding to HIV-1 envelope in the presence of soluble CD4 receptor (**Figure 2-3G-H**). Notably, two of the antibodies (mAb688 and mAbKP1-8)

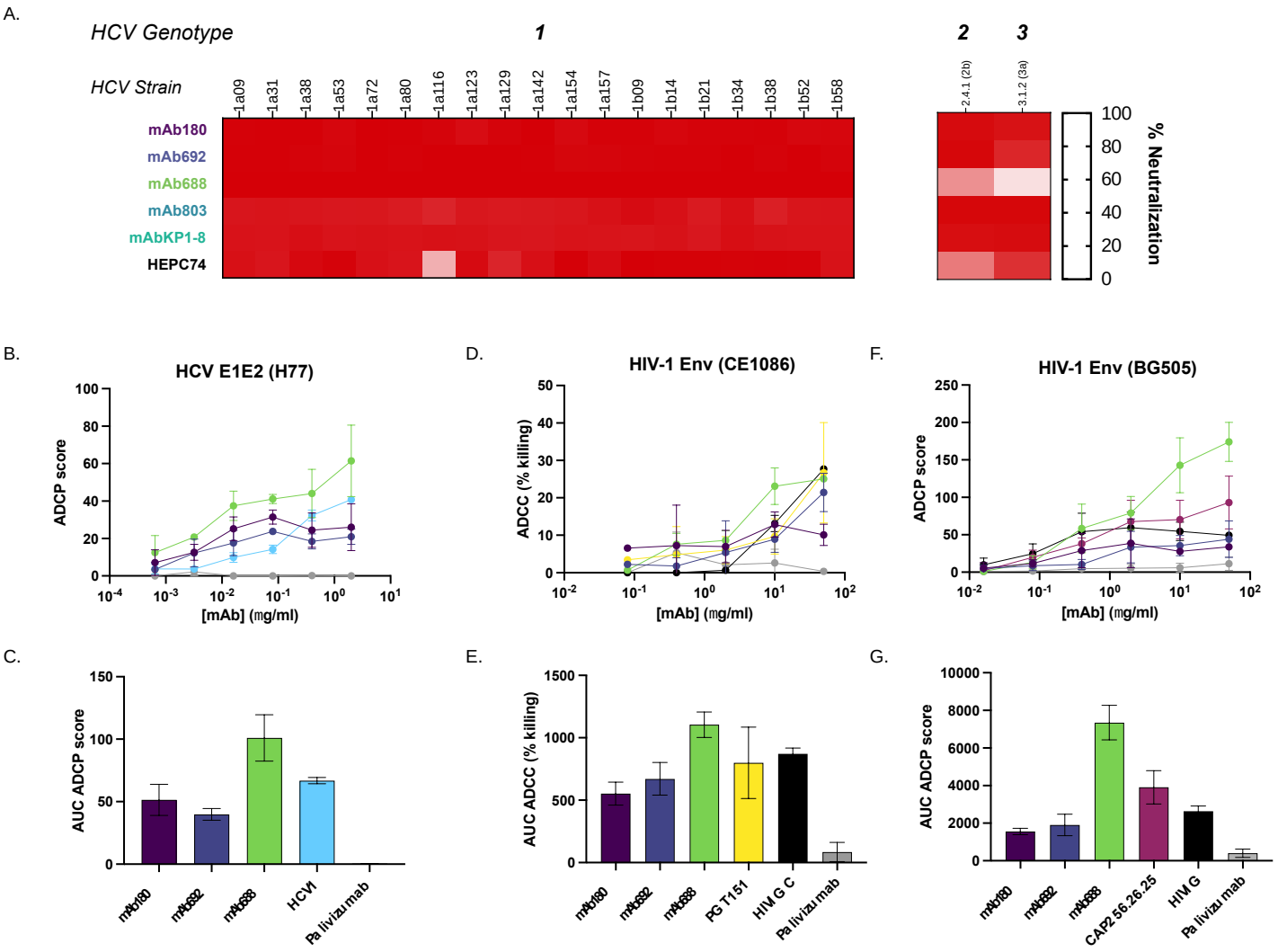

Figure 2-5. HIV-1/HCV Cross-reactive antibodies Show Diverse Neutralization and Fc-mediated Effector Functions.
(A) In vitro neutralization of a panel of diverse genotype 1 HCV virus strains by HIV-1/HCV-reactive antibodies and control antibody HEPC74 at 100µg/mL. % Neutralization calculated in comparison to unrelated IgG control. (B) Antibody-dependent cellular phagocytosis (ADCP) by either HIV-1/HCV cross-reactive or control antibodies (HCV1: positive; Palivizumab: negative) against HCV E1E2 envelope protein (H77). (C) Area under the curve (AUC) values computed from (B). (D) Antibody-dependent cellular cytotoxicity (ADCC) potentiated by either HIV-1/HCV cross-reactive or control antibodies (PGT151/HIVIG C: positive; Palivizumab: negative) against infectious HIV-1 envelope protein (CE1086). (E) Area under the curve (AUC) values computed from (D). (F) Antibody-dependent cellular phagocytosis (ADCP) by either HIV-1/HCV cross-reactive or control antibodies (CAP256.26.25/HIVIG C: positive; Palivizumab: negative) against HIV-1 envelope protein (BG505). (G) Area under the curve (AUC) computed from (F).

recognized CD4-induced epitopes on the HIV-1 envelope (**Figure 2-3G**). Binding of gp41-targeting HIV-1/HCV antibodies mAb180 and mAb692 was not affected by CD4, by contrast (**Figure 2-3H**). We did not observe strong HIV-1 envelope recognition by mAb803 measured by SPR in either condition.

As with HCV, we also investigated glycan-dependence of antibody binding to HIV-1 gp140, a viral protein ornamented with under-processed glycans. We discovered that only mAb688 binding to HIV-1 gp140 was inhibited by PNGaseF de-glycosylation and competition with 1M D-(+)-mannose (**Figure 2-3E, Figure 2-4F**). Similar to experiments with HCV E1E2, mAb688 recognition of HIV-1 gp140 was significantly decreased after treatment with the class I α-mannosidase inhibitor kifunensine (**Figure 2-4G**). Taken together, these data support the discovery of antibodies recognizing at least three distinct regions on the HIV-1 Env glycoprotein encompassing gp41 (mAb180, 692), and both glycan-dependent (mAb688) and -independent (mAb803, KP1-8) gp120 epitopes.

HIV-1/HCV Cross-reactive mAbs Show Diverse Neutralization and Fc-mediated Effector Functions

After evaluating HIV-1 and HCV antigen specificity, we next set out to assess the functional abilities of the HIV-1/HCV cross-reactive antibodies in both neutralization and Fc-mediated effector function assays. First, we investigated the ability of HIV-1/HCV cross-reactive antibodies to neutralize a panel of representative genotype 1 HCV strains. Notably, we observed that all five HIV-1/HCV cross-reactive antibodies showed exceptional HCV neutralization breadth, neutralizing all 19 genotype 1 viruses tested at 100 μg/mL (**Figure 2-5A, Figure 2-6A, B**). This is particularly striking when compared to the previously reported broadly neutralizing

A.

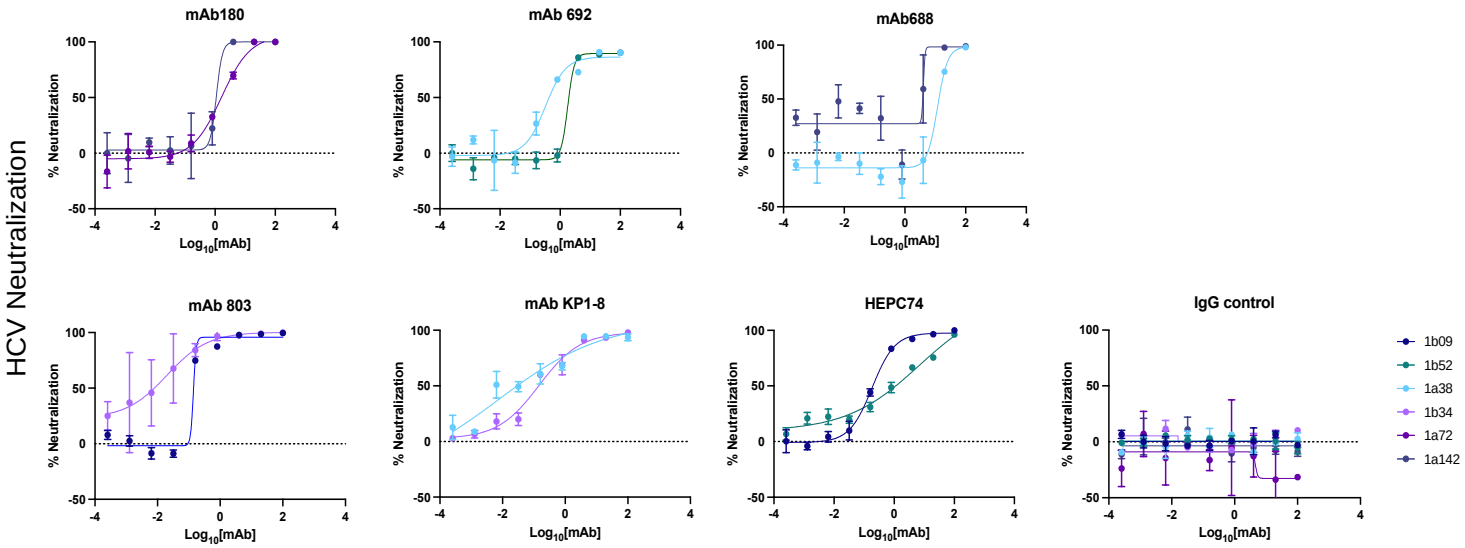

B.

IC_{50} (μg/mL)

	HCV virus					
Antibody	*1a72*	*1a142*	*1a38*	*1b52*	*1b09*	*1b34*
mAb180	1.63	1.09	ND	ND	ND	ND
mAb692	ND	ND	0.32	1.77	ND	ND
mAb688	ND	3.99	2.58	ND	ND	ND
mAb803	ND	ND	ND	ND	0.14	0.02
mAbKP1-8	ND	ND	0.008	ND	ND	0.66
HEPC74	ND	ND	ND	6.93	0.18	ND

C.

IC_{50} (μg/mL)

			Antibody				
Tier	Clade	Strain	mAb180	mAb692	mAb688	mAb803	mAbKP1-8
HIV-1 Virus							
1	B	MW965	>50	>50	>50	>10	>10
	A	BG505 T332N	>50	>50	>50	>10	>10
	A	BG505 N332T	>50	>25	>25	>25	>25
	C	ZM197	>50	>50	>50	>25	>25
	B	B41	ND	>25	>25	>25	>25
	C	HIV-1 25710	>25	>25	>25	ND	ND
2	B	X2278	>25	>25	>25	ND	ND
	C	Ce1176	>25	>25	>25	ND	ND
	C	Ce0217	>25	>25	>25	ND	ND
	B	TRO.11	ND	>25	>25	ND	ND
	CRF07	CH119	ND	>25	>25	ND	ND
	CRF01	CNE55	ND	>25	>25	ND	ND
	A	398 F1	ND	>25	>25	ND	ND

Figure 2-6. HIV-1 and HCV Antibody Neutralization Phenotypes.

(A) Neutralization of HCV-pseudotyped viruses by HIV-1/HCV cross-reactive antibodies and human IgG control. For each antibody (panel) and concentration (x-axis) against each virus (colored curve), shown is % neutralization (y-axis) calculated as a function of no-antibody control. (B) Half-maximal inhibitory concentration (IC_{50}, μg/mL) of each antibody against the respective genotype 1 HCV virus strains from (A). ND= Not determined. (C) Neutralization (IC_{50}, μg/mL) of a panel of HIV-1-pseudotyped viruses by HIV-1/HCV cross-reactive antibodies.

panel, respectively (Bailey et al., 2017; Giang et al., 2012). Further, four of the five HIV-1/HCV cross-reactive antibodies were also able to neutralize both genotype 2b and 3a strains in an infectious cell culture-generated virus (HCV_{CC}) assay (**Figure 2-5A**). we sought to measure anti-HCV function for these antibodies. We next sought to test whether the IgG antibodies mAb180, mAb692, and mAb688 could mediate anti-HCV E1E2 Fc effector functions. We discovered that all tested antibodies (mAb180, mAb692, mAb688) mediated antibody-dependent cellular phagocytosis (ADCP) against HCV E1E2 (genotype 1a; strain H77) (**Figure 2-5B, C**).

Next, we sought to characterize the anti-HIV-1 functions of HIV-1/HCV cross-reactive antibodies and discovered that none of the antibodies showed neutralizing activity against the HIV-1 strains tested (**Figure 2-6C**). However, we discovered that all tested antibodies (mAb180, mAb692, mAb688) were capable of potentiating antibody-dependent cellular cytotoxicity (ADCC) against infectious HIV-1 envelope (strain CE1086) (**Figure 2-5D, E**). Moreover, we observed that all three antibodies mediated antibody-dependent cellular phagocytosis (ADCP) against HIV-1 gp140 (strain BG505) (**Figure 2-5F, G**). Taken together, beyond binding of diverse viral envelope glycoproteins, the identified antibodies revealed extraordinary cross-functionality. The IgA isotype antibodies (mAb803, KP1-8) were not tested in the Fc effector assays against either virus, as this isotype plays a less significant role in serological anti-viral Fc-mediated immunity (Astronomo et al., 2016; Davis et al., 2020).

<u>mAb688 Reveals Exceptionally Broad Anti-Viral Functions</u>

Next, we asked whether the LIBRA-seq-identified antibodies were solely HIV-1/HCV cross-reactive, or whether they could recognize additional viral envelope glycoproteins. To that end, we tested these antibodies against a panel of antigens from a

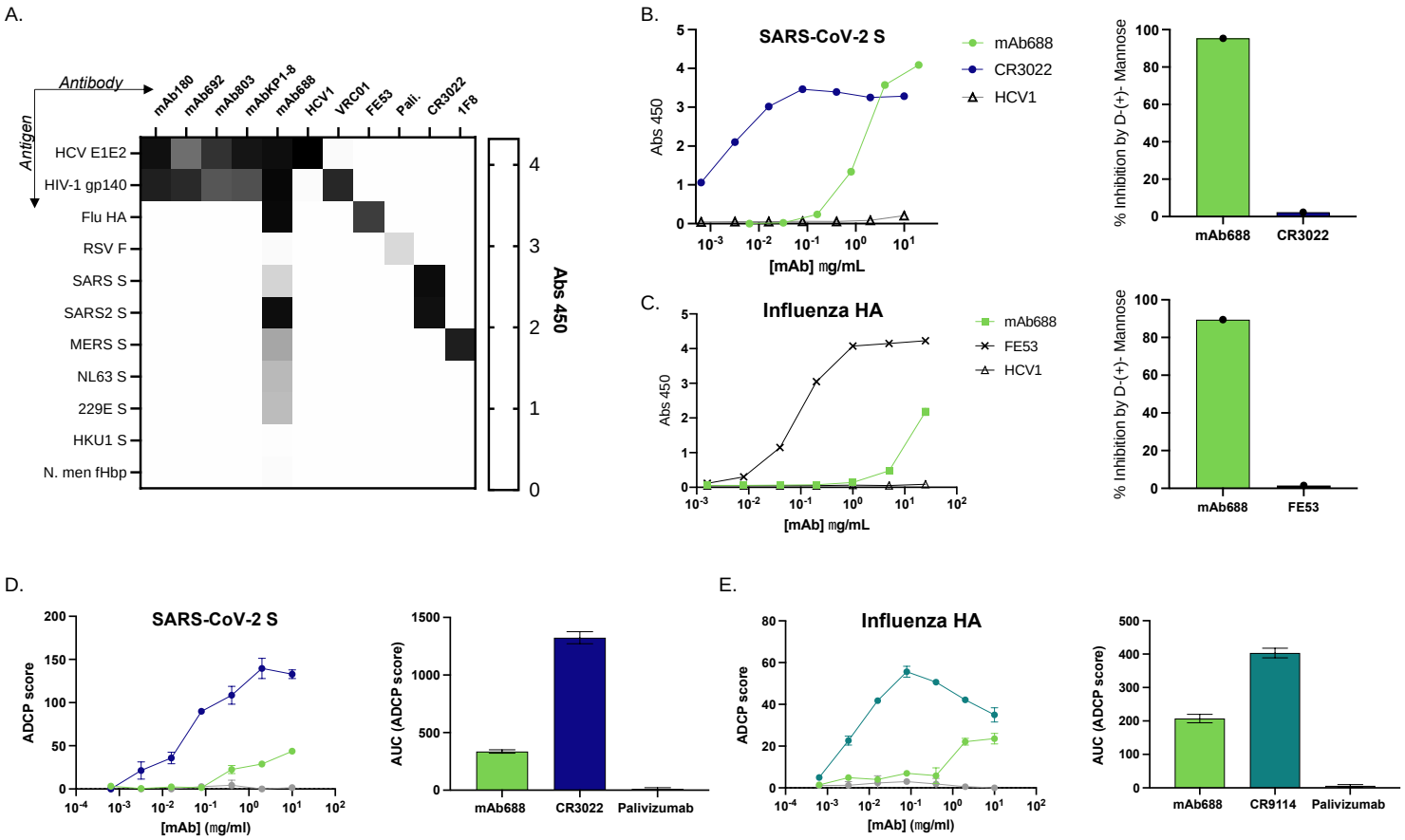

Figure 2-7. Cross-reactive mAb688 Reveals Exceptionally Broad Anti-viral Functions Achieved by Glycan Recognition.
(A) Binding of HIV-1/HCV cross-reactive antibodies (columns) to a panel of diverse viral antigens (rows) at 10μg/mL, as measured by ELISA. The following antibodies are shown as controls: HCV1 (HCV E2), VRC01 (HIV-1 gp120), FE53 (HA), Palivizumab (RSV F), CR3022 (SARS-CoV/SARS-CoV-2 S), 1F8 (MERS S). (B) mAb688 binding to SARS-CoV-2 spike protein with PBS (left) and competition in presence of 1M D-(+)-Mannose (right), displayed as %inhibition (y-axis) in the presence of mannose. (C) mAb688 binding to Influenza A HA (strain H1N1/New Caledonia/1999) envelope glycoprotein with PBS (left) and competition in presence of 1M D-(+)-Mannose (right), displayed as %inhibition (y-axis) in the presence of mannose. (D) Antibody-dependent cellular phagocytosis (ADCP) of SARS-CoV-2 envelope glycoprotein (left), with data displayed as area under the curve (AUC, right). CR3022 is shown as a positive control, and Palivizumab is shown as a negative control. (E) Antibody-dependent cellular phagocytosis (ADCP) of Influenza A HA (strain H1N1/New Caledonia/1999) envelope glycoprotein (left), with data displayed as AUC (right). CR9114 is shown as a positive control, and Palivizumab is shown as a negative control.

diverse set of pathogens, and found that mAb 180, 692, 803, and KP1-8 indeed bound only the HIV-1 and HCV antigens tested (**Figure 2-7A**). By contrast, mAb688 recognized a broad diversity of other viral antigens including glycoproteins from Influenza A, alphacoronaviruses NL63 and 229E, and betacoronaviruses MERS-CoV, SARS-CoV, and notably, SARS-CoV-2 (**Figure 2-7A**). As observed with HIV-1 and HCV, we found that mAb688 recognition of both influenza A hemagglutinin and SARS-CoV-2 spike was mannose-dependent (**Figure 2-7B, C**). Previous studies suggested that the anti-HIV-1 antibody 2G12 is also able to bind the SARS-CoV-2 spike, by recognition of a high

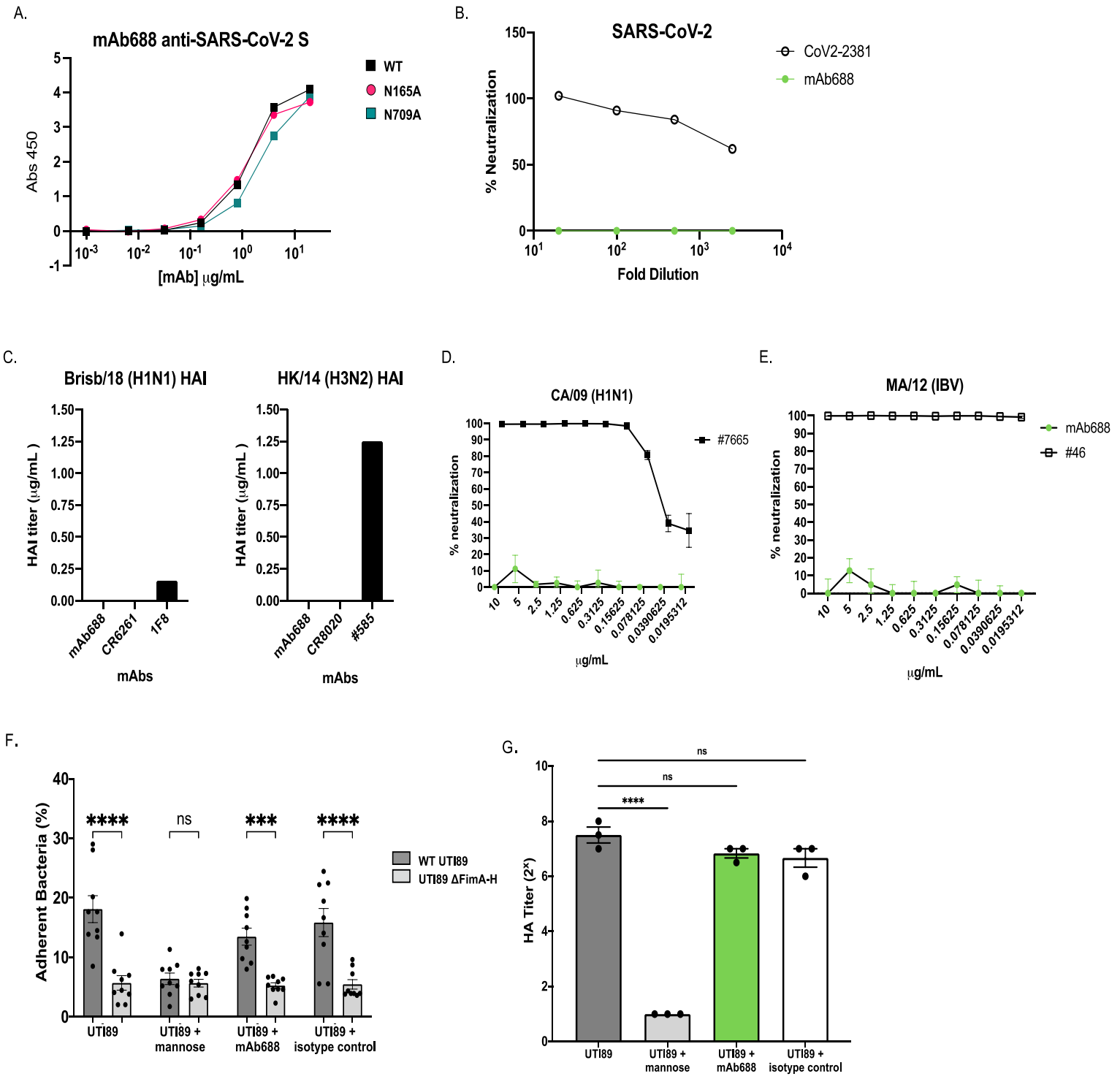

Figure 2-8. mAb688 Functional Assays Against SARS-CoV-2, Influenza, and *Escherichia coli.*

(A) mAb688 binding to WT or specific glycan-mutated SARS-CoV-2 S. (B) Antibody-mediated neutralization of SARS-CoV-2-pseudotyped VSV particles. Antibody CoV2-2381 is shown as a positive control. (C) Antibody inhibition of hemagglutination mediated by Influenza A HA (left: A/Brisbane/02/2018 (CA/09 pdm-like H1N1), right: A/Hong Kong/4801/2014 (H3N2)). Stem-specific antibodies CR6261 and CR8020 are shown as negative controls. Head-specific antibodies 1F8 and #585 are shown as positive controls. (D-E) Antibody-mediated neutralization of (D) Influenza A (IAV; A/California/07/2009 (pdm H1N1) or (E) Influenza B (IBV; B/Massachusetts/02/2012). Antibodies #7665, #1664, and #46 are shown as positive controls. (F) Bacterial cell adherence to bladder epithelial cells was measured for both the WT UPEC strain UTI89 and bacteria lacking FimA-H, in the presence of either media, mannose or antibody. Bacterial adherence in the presence of 20µg/mL mAb688 or the isotype control HCV1 is shown. Statistical significance determined by t-test. *** denotes p<0.001 ;**** denotes p<0.0001. (G) Measurement of *E. coli strain* UTI89-mediated hemagglutination in the presence of either media, mannose or antibody. Hemagglutination in the presence of 20µg/mL mAb688 or the isotype control HCV1 is shown. Statistical significance determined by one-way ANOVA with Dunnett's test for multiple comparisons. **** denotes p<0.0001.

found that mAb688 binding to SARS-CoV-2 spike was not inhibited by N709A mutation (**Figure 2-8A**). mAb688 was unable to neutralize SARS-CoV-2 but showed ADCP activity against the SARS-CoV-2 spike protein (**Figure 2-7D, Figure 2-8B**). Similarly, mAb688 was unable to neutralize influenza virus but showed ADCP against the influenza A hemagglutinin protein (**Figure 2-7E, Figure 2-8C-E**). Together with the mAb688 HIV-1 and HCV functional activity, these data indicate that mAb688 is capable of diverse functions against a broad range of viral targets.

To determine whether the observed broad functional abilities of mAb688 spanned beyond virus targets, we sought to investigate whether mAb688 could inhibit the most common etiological agent of urinary tract infection (UTI), Uropathogenic *Escherichia coli*

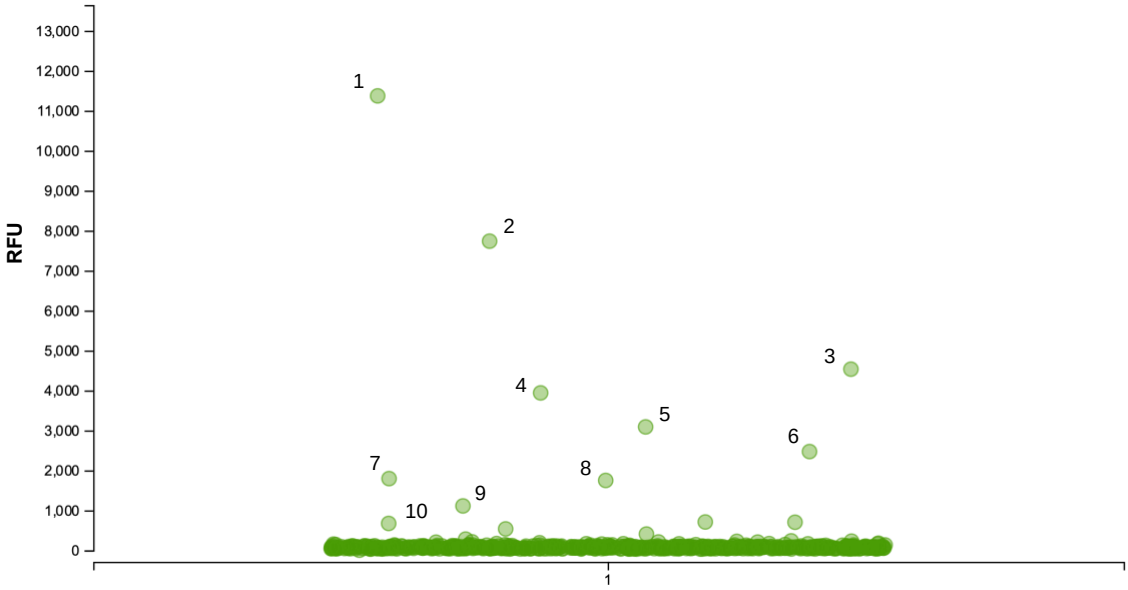

Label	Glycan
1	GlcNAca1-6Galb1-4GlcNAcb-Sp8
2	GlcNAcb1-6(GlcNAcb1-3)GalNAca-Sp8
3	GlcNAcb1-6GalNAca-Sp8
4	GlcNAcb1-6(GlcNAcb1-2)Mana1-6(GlcNAcb1-2Mana1-3)Manb1-4GlcNAcb1-4(Fuca1-6)GlcNAcb-Sp24
5	GlcNAcb1-2(GlcNAcb1-6)Mana1-6(GlcNAcb1-2Mana1-3)Manb1-4GlcNAcb1-4GlcNAcb-Sp19
6	GlcNAcb1-6(Galb1-3)GalNAca-Sp8
7	Neu5Aca2-6Galb1-4GlcNAcb1-6(Neu5Aca2-6Galb1-4GlcNAcb1-2)Mana1-6(GlcNAcb1-4)(Neu5Aca2-6Galb1-4GlcNAcb1-4(Neu5Aca2-6Galb1-4GlcNAcb1-2)Mana1-3)Manb1-4GlcNAcb1-4GlcNAcb-Sp21
8	GlcNAcb1-2Mana1-6(GlcNAcb1-2Mana1-3)Manb1-4GlcNAcb1-4GlcNAcb-Sp13
9	GlcNAcb1-3Man-Sp10
10	GlcNAcb1-3Fuca-Sp21

Figure 2-9. mAb688 Achieves Broad Anti-viral Binding via Recognition of Immature Glycans
Binding of mAb688 to the printed CFG v5.4 glycan microarray was tested at 50µg/mL. Antibody binding was detected using fluorescent secondary antibody and data is shown as the average Relative Fluorescence Units (RFU). Glycan structures corresponding to numbered green circles are shown below.

(UPEC). UPEC potentiates infection using fimbriae to recognize mannosylated bladder host cell surface glycoprotein and red blood cells (Pizarro-Cerda & Cossart, 2006). As this interaction between bacteria and host is free mannose-inhibitable, we tested whether mAb688 recognition of host mannose could block function. Importantly, we discovered that neither mAb688 nor the isotype control were able to impede UPEC adherence or hemagglutination (**Figure 2-8F, G**), suggesting that mAb688 recognizes a mannose structure that may be specific to viral glycosylation and/or may require additional antigen interactions.

Finally, to define specific glycan architecture that mediates broad mAb688 recognition, we tested binding to a glycan microarray consisting of >580 distinct structures developed by the Center for Functional Glycomics (CFG, v5.4 microarray). Interestingly, the majority of observed glycan hits contained a terminal N-acetyl glucosamine with β1-6 linkage, suggesting this is critical for mAb688 binding (**Figure 2-9**). Further, these data demonstrate mAb688 preferentially recognizes immature, hybrid-type glycans, a form of glycosylation that's enriched on viral glycoproteins (**Figure 2-9**).

Diverse polyreactivity profiles of HIV-1/HCV cross-reactive mAbs

To investigate whether the cross-reactive antibodies may achieve diverse binding phenotypes via antigen polyreactivity, or non-specific interactions, we first measured reactivity to a panel of nuclear self-antigens using the Luminex AtheNA Multi-analyte ANA assay (**Figure 2-10A**) (Liu et al., 2015). Similar to previously described gp41 antibodies, we observed autoreactivity for both mAb180 and mAb692. Further, we found that mAb180, but not the other antibodies, bound non-infected, whole (un-permeabilized) HEp-2 cells in a fluorescent assay (**Figure 2-10B, C**). Therefore, from the set of five cross-reactive antibodies, only mAb180 and mAb692 showed binding in polyreactivity assays, suggesting that the broadly reactive anti-viral phenotype of the other antibodies –

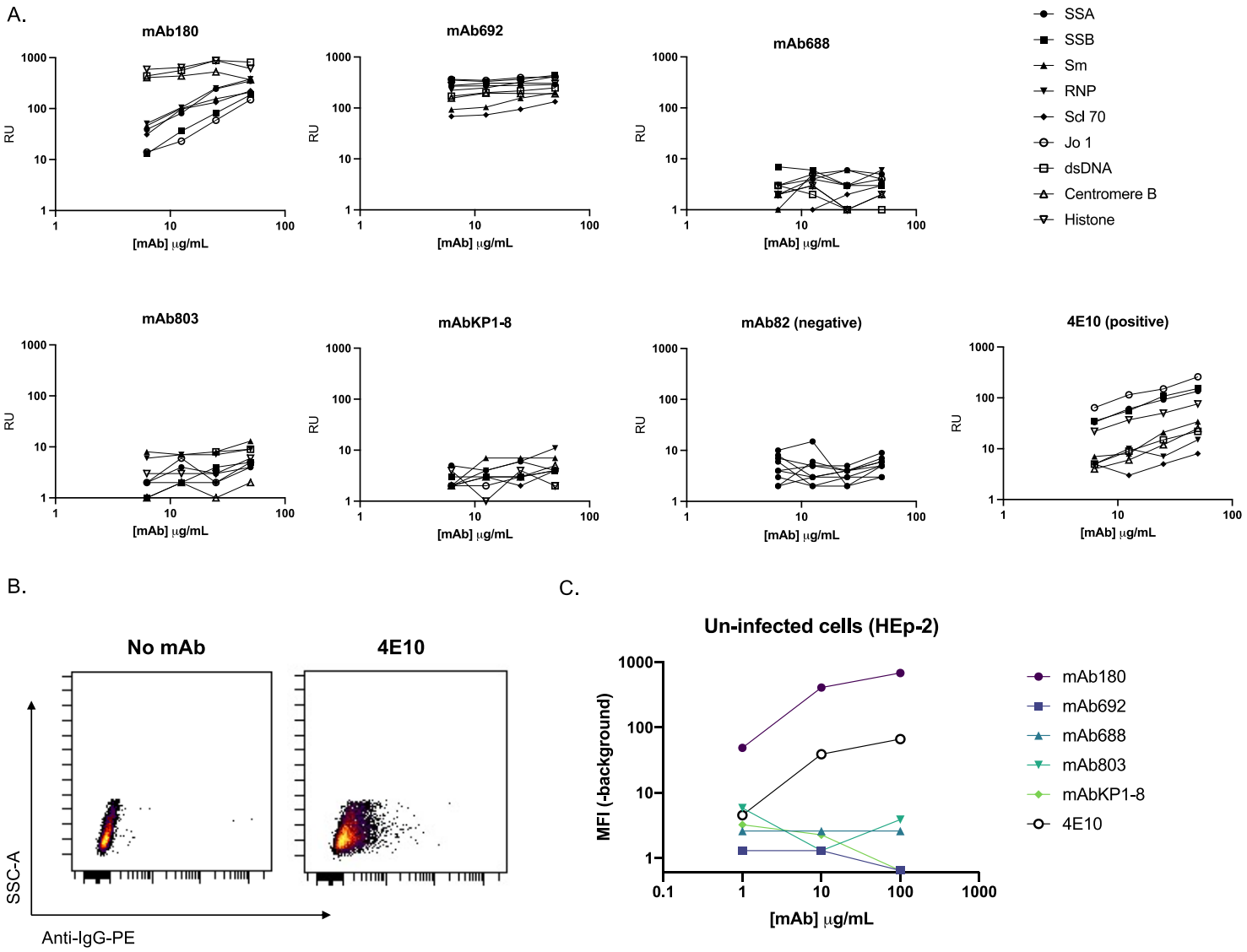

Figure 2-10. Autoreactivity of HIV-1/HCV Cross-reactive Antibodies.
(A) Antibody binding to a panel of autoantigens using the AtheNA multiplex assay, over a concentration gradient. Relative units (RU) > 100 are considered positive. The HIV-1 antibody 4E10 is shown as a positive control, and mAb82 is shown as a negative control. (B-C) Antibody binding to whole, unpermeabilized, un-infected HEp-2 cells detected by anti-IgG-PE (anti-IgA-PE; mAb803, mAbKP1-8). (B) Secondary only (negative) and 4E10 (positive) control plots. (C) Binding of HIV/HCV cross-reactive antibodies depicted as MFI of the PE channel (-MFI unstained control) at the shown concentration of antibody.

including the exceptionally broad mAb688 – could not be explained by promiscuous, non-specific, antigen interactions.

Somatic hypermutation establishes and enhances cross-reactivity

We finally interrogated the effect of affinity maturation on the development of HIV-1/HCV cross-reactivity. High affinity HIV-1-specific antibody responses often require the

accumulation of mutations through multiple rounds of somatic hypermutation over the course of chronic infection. We therefore assessed binding of germline-reverted IgG antibody mutants to both HIV-1 and HCV envelope proteins (**Figure 2-11A, B, Figure 2-12A,**). These mutants lack all acquired mutants but bear the CDR3 sequences of the mature antibody. Interestingly, when somatic mutations were removed from mAb688, this antibody was no longer capable of recognizing either HIV-1 or HCV (**Figure 2-12A**). By contrast, when mAb180 and mAb692 were germline-reverted, they retained binding to HCV envelope protein, and demonstrated distinct HIV-1 envelope reactivities (**Figure 2-**

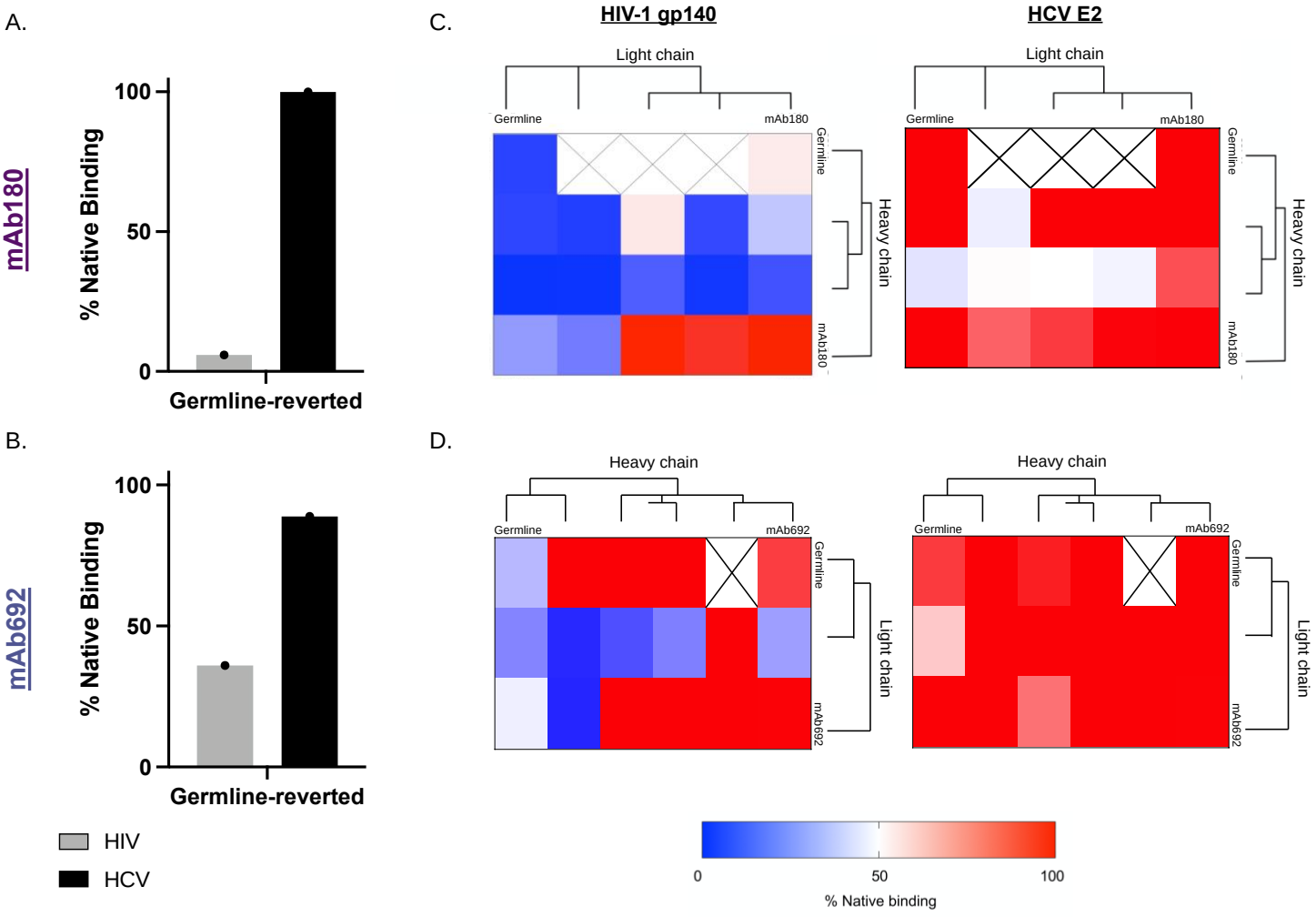

Figure 2-11. Somatic hypermutation establishes and enhances cross-reactivity
Binding of germline-reverted antibody mutants (A) mAb180 and (B) mAb692 to HIV-1 gp140 (strain: BG505, gray bars) and HCV E2 (strain: JFH1, black bars) measured by ELISA. Data shown was calculated by dividing the area under the ELISA curve (AUC) of the germline-reverted antibody by the AUC of the native antibody (% Native binding). Binding of early sequences clonally related to (C) mAb180 or (D) mAb692 to HIV-1 gp140 (strain: BG505, left) or HCV E2 (strain: JFH1, right) measured by ELISA. Data is shown as a heatmap where % Native binding is calculated as in (A-B). Each heatmap square represents a unique combination of heavy and light chain sequences. The phylogenetic relationship between each set of sequences was determined using PhyML, not shown to scale.

11A, B). Together, these data suggest that affinity maturation is essential for both establishing and developing HIV-1/HCV cross-reactive antibody binding.

Finally, to trace the early development of HIV-1/HCV cross-reactivity, we performed deep, unpaired BCR sequencing of donor VC10014 approximately 0.59 years post co-infection (~3 years before the sample used for LIBRA-seq). From this dataset we identified multiple heavy and light chain sequences clonally related to both mAb180 and mAb692. We then sought to define the effect of these early acquired mutations on HIV-1/HCV antigen cross-reactivity, by expressing pairwise combinations of heavy and light chain sequences as recombinant antibodies (**Figure 2-11C, D**). Overall, we observed distinct binding patterns when various mutation-containing heavy and light chain sequences were combined (**Figure 2-11C, D**). Notably, HCV envelope recognition by both mAb180 and mAb692 was significantly more tolerant of variable somatic hypermutation than HIV-1 envelope recognition (**Figure 2-11C, D**). Together, these results suggest that different acquired-mutations or regions of the mAb180 and mAb692 paratope are essential for recognition of HCV vs. HIV-1 envelope glycoprotein.

DISCUSSION

Although antibodies are generally utilized for their incredible specificity, flexibility in the antigen binding site can provide a unique advantage in the fight against highly mutable pathogens such as HIV-1 and HCV (Mouquet & Nussenzweig, 2012; Planchais et al., 2019). This is exemplified by the discovery of broadly reactive or broadly neutralizing antibodies (bNAbs) and their documented utility as prophylactic therapeutics and vaccine design scaffolds (Burton, 2010; He et al., 2015; Jardine et al., 2015; Ofek et al., 2010). In this study, we expand the concept of broadly reactive antibodies by

discovering the first HIV-1/HCV cross-functional antibodies. Using the LIBRA-seq technology, we identified five genetically unique, class-switched, paired heavy-light chain sequences positive for at least one HIV-1 and one HCV envelope glycoprotein, and then confirmed this unique antigen cross-reactivity by expression as recombinant human antibodies. Remarkably, we observed that all five antibodies were capable of potentiating anti-HIV-1 and anti-HCV functions. Further, we discovered that when native antibody isotype (either IgG3-mAb688 or IgA-mAb803/mAbKP1-8) was switched to IgG1, antibody binding was reduced or ablated (**Figure 2-12**). These results indicate that antigen recognition by these antibodies can be influenced by a number of factors outside of direct antibody-epitope interactions. Additional structural and paratope characterization will be needed to examine differences in how the identified antibodies interact with HIV-1 vs. HCV envelope glycoproteins.

Previous studies have noted roles for poly- and auto-reactive antibodies in immune responses against highly diverse viruses, most notably observing common cross-reactivity between HIV-1

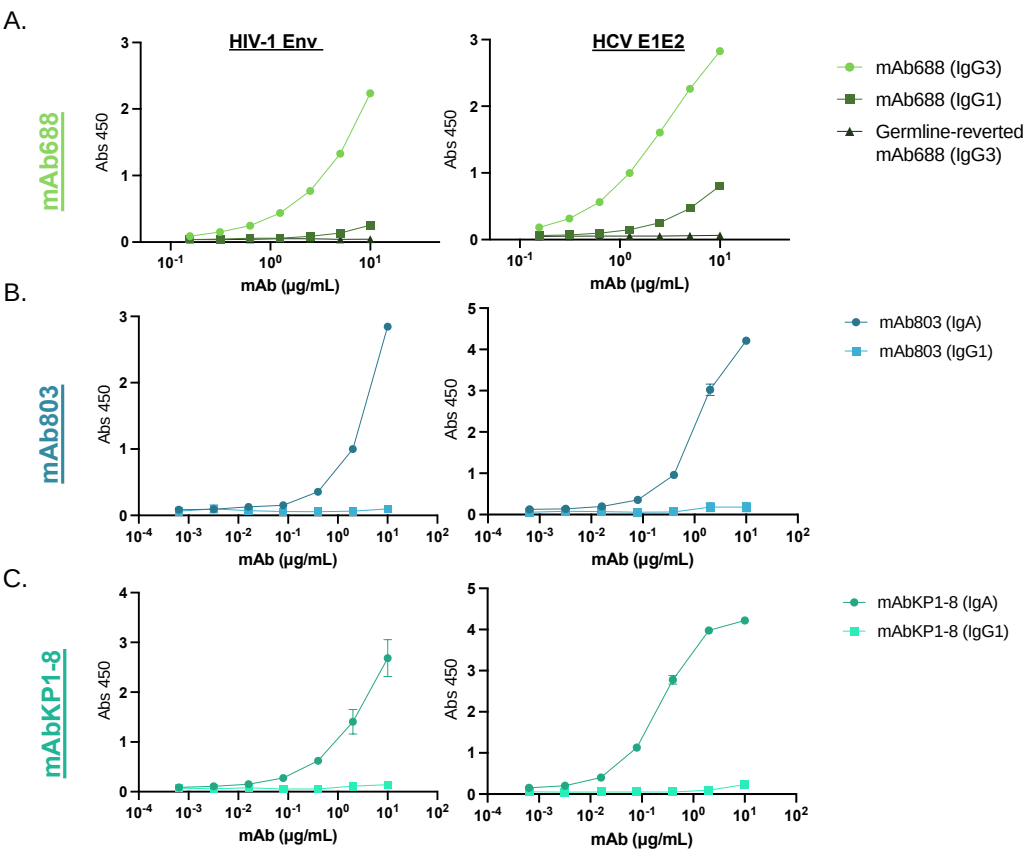

Figure 2-12. Native Antibody Features Are Crucial to Binding Viral Envelopes
Binding of germline-reverted (A) mAb688 and/or isotype antibody mutants (B) mAb803, and (C) mAbKP1-8 to HIV-1 gp140 (strain: BG505, left) and HCV E1E2 (strain: H77, right) by ELISA.

gp41-specific antibodies with host and microbiome antigens (Finney & Kelsoe, 2018; Williams et al., 2018; Williams et al., 2015). However, these antibodies are often IgM, non-functional, or difficult to elicit by vaccination due to immune tolerance mechanisms (Finney et al., 2019; Kelsoe & Haynes, 2017; Verkoczy & Diaz, 2014). Notably, three of the five antibodies described in this study did not show evidence for polyreactivity. While the other two, mAb180 and mAb692, showed reactivity with host antigens, they nevertheless exhibited anti-viral functions against both HIV-1 and HCV, suggesting such antibodies could still contribute to cross-viral clearance. In addition, all five antibodies regardless of autoreactivity showed exceptional HCV neutralization, inhibiting infection with 19/19 genotype 1 strains. Further, all five antibodies displayed exceptional HCV neutralization breadth, with four of the five antibodies capable of neutralizing viral strains from HCV genotypes 1-3. This is particularly striking as genotypes 1-3 account for >95% of all HCV infections in the United States (McHutchison et al., 1998; Rustgi, 2007). Beyond neutralization, these antibodies may still impede or reduce infection by Fc-mediated effector functions or by targeting glycan structures outside the receptor binding site to prevent viral interaction with host cell lectin receptors (DC-SIGN and L-SIGN both interact with HIV-1 and HCV) (Hijazi et al., 2011; Pohlmann et al., 2001; Pöhlmann et al., 2003). We note that the current study investigated one HIV-1/HCV co-infected donor more than three years post co-infection, and whether these unconventional cross-reactive antibody specificities are common, protective, or found in settings other than chronic co-infection remains to be examined.

Recent reports have outlined a class of glycan-reactive antibodies capable of recognizing, and in particular cases potentiate effector functions against, HIV-1, coronavirus, and influenza antigens, similar to the exceptionally broad antibody mAb688 isolated in our studies (Lee et al., 2021; Trkola et al., 1996; Williams et al., 2021). Although

some antibodies in this category displayed promiscuous polyreactivity against arbitrary unrelated antigens, we did not observe autoreactive binding for mAb688 (Williams et al., 2021). Glycan-reactive antibodies that avoid self-recognition may represent a general immune defense mechanism for effectively counteracting viral infections. In addition to this glycan-reactive “class” of cross-reactive antibodies, the discovery of multiple HIV-1/HCV cross-reactive antibodies targeting diverse epitope determinants shows that there are multiple mechanisms that may result in antibody cross-reactivity against unrelated antigens. These findings provide unexpected insights into the dynamic and flexible nature of the human antibody response. In the face of highly mutable threats, antibodies that can tolerate sequence variability, without triggering auto- or poly-reactivity, provide a selective advantage. Such antibodies have the potential to aid cross-reactive vaccine design or serve as therapeutics themselves for both HIV-1 and HCV, as well as emerging threats such as SARS-CoV-2 and other infectious diseases.

MATERIALS AND METHODS

Donor information

Donor VC10014 was identified and enrolled in the Vanderbilt cohort (VC) and samples isolated after informed consent. VC10014 was recruited with $CD4^+$ T-cell counts of ≥250/μl without antiretroviral therapy and with no AIDS-defining illness during the period of observation. The sample used for this study was collected on 03/21/2006, >3 years post onset of co-infection.

Purification of antigens

Plasmids encoding the following genes were transfected in FreeStyle293F (Thermo Fisher Scientific) cells via polyethyleneimine transfection; HIV-1/

BG505.664.SOSIP(Sanders et al., 2013), B41.664.SOSIP(Pugach et al., 2015), ConC gp120[61], A244 gp120[62], HCV/H77 E1E2[63], H77 E2c [17], JFH-1 E2c [64]. All antigens contained an AviTag sequence for subsequent biotinylation. Antigens were purified by Galanthus nivalis (GNA, Snowdrop) lectin affinity chromatography (Vector Labs), and further purified by gel filtration with Superdex200 Increase column (Cytiva). Fractions corresponding to correctly folded protein were collected and biotinylated using BirA (Avidity). Biotinylated HIV-1 antigens were fluorescently labeled by incubation with Streptavidin-AF568 (Invitrogen), and biotinylated HCV antigens fluorescently labeled by incubation with Streptavidin-AF647 (Invitrogen).

The following reagents were obtained through the NIH HIV Reagent Program, Division of AIDS, NIAID, NIH: Human Immunodeficiency Virus Type 1 MN gp41 Protein, Recombinant from Escherichia coli, ARP-12027, contributed by DAIDS/NIAID; produced by ImmunoDX, LLC; Human Immunodeficiency Virus 1 (HIV-1) gp120 Recombinant Protein (B.9021 D11gp120), ARP-12571, contributed by Drs. Barton F. Haynes and Hua-Xin Liao. The following antigens were acquired from Sino Biological: Hepatitis C virus Envelope Glycoprotein E1 / HCV-E1 (subtype 1b, strain HC-J4) Protein (His Tag); Human coronavirus (HCoV-229E) Spike Protein (S1+S2 ECD, His Tag); Human coronavirus (HCoV-NL63) Spike Protein (S1+S2 ECD, His Tag); SARS-CoV-2 (2019-nCoV) Spike S1+S2 ECD-His Recombinant Protein; SARS-CoV Spike S1+S2 ECD-His Recombinant Protein; Human coronavirus HKU1 (isolate N5) (HCoV-HKU1) Spike Protein (S1+S2 ECD, His Tag); MERS-CoV Spike Protein (S1+S2 ECD, aa 1-1297, His Tag). The following reagent was obtained through BEI Resources, NIAID, NIH: H1 Hemagglutinin (HA) Protein with C-Terminal Histidine Tag from Influenza Virus, A/New Caledonia/20/1999 (H1N1), Recombinant from Baculovirus, NR-48873; F Protein with C-

Terminal Histidine Tag from Respiratory Syncytial Virus, B1, Recombinant from Baculovirus, NR-31097.

DNA-barcoding of antigens

We used oligos that possess 15 bp antigen barcode, a sequence capable of annealing to the template switch oligo that is part of the 10X bead-delivered oligos and contain truncated TruSeq small RNA read 1 sequences in the following structure: 5'-CCTTGGCACCCGAGAATTCCANNNNNNNNNNNNCCCATATAAGA*A*A-3', where Ns represent the antigen barcode (Integrated DNA Technologies). For each antigen, a unique DNA barcode was directly conjugated to the antigen itself. In particular, 5'amino-oligonucleotides were conjugated directly to each antigen using the Solulink Protein-Oligonucleotide Conjugation Kit (Vector Labs) according to manufacturer's instructions. Briefly, the oligo and protein were desalted, and then the amino-oligo was modified with the 4FB crosslinker, and the biotinylated antigen protein was modified with S-HyNic. Then, the 4FB-oligo and the HyNic-antigen were mixed together. This causes a stable bond to form between the protein and the oligonucleotide. The concentration of the antigen-oligo conjugates was determined by a BCA assay (Pierce), and the HyNic molar substitution ratio of the antigen-oligo conjugates was analyzed using the NanoDrop according to the Solulink protocol guidelines. AKTA FPLC (Cytiva) was used to remove excess oligonucleotide from the protein-oligo conjugates, which were also verified using SDS-PAGE with a silver stain (Pierce). Antigen-oligo conjugates were also used in flow cytometry titration experiments.

Antigen-specific B cell sorting

Antigen-specific B cells were sorted from donor PBMCs by fluorescence-activated cell sorting. Briefly, frozen cells were quickly thawed at 37°C, and washed 3X with DPBS without Ca^{2+} or Mg^{+} (Gibco) supplemented with 1% BSA (Sigma) (DPBS-BSA) before counting. Cells were resuspended in DPBS-BSA and stained with antibodies against cell markers including viability dye (Ghost Red 780) (Tonbo Biosciences), CD14-APC-Cy7 (BD Biosciences), IgM-APC-Cy7 (BD Biosciences), CD3-FITC (BD Biosciences), CD19-BV711 (BD Biosciences), and IgG-PE-Cy5 (BD Biosciences). Additionally, fluorescently-labeled antigen-oligo conjugates were added to the stain. After staining in the dark for 20 minutes at room temperature, cells were washed three times with DPBS-BSA. Live, $CD14^{-}$, IgM^{-}, $CD3^{-}$, $CD19^{+}$, $Antigen^{+}$ cells were sorted using a FACSAria III flow sorter ((BD Biosciences) and to the Vanderbilt Technologies for Advanced Genomics (VANTAGE) sequencing core at an appropriate target concentration for 10X Genomics library preparation and subsequent sequencing.

Sample preparation, library preparation, and sequencing

Single-cell suspensions were loaded onto the Chromium Controller microfluidics device (10X Genomics) and processed using the B-cell Single Cell V(D)J solution according to manufacturer's suggestions for a target capture of 10,000 B cells per 1/8 10X cassette, with minor modifications in order to intercept, amplify and purify the antigen barcode libraries as previously described.

Sequence processing and bioinformatic analysis

We utilized a modified version of our previously described pipeline to use paired-end FASTQ files of oligo libraries as input, process and annotate reads for cell barcode, UMI, and antigen barcode, and generate a cell barcode - antigen barcode UMI count

matrix. BCR contigs were processed using Cell Ranger (10X Genomics) using GRCh38 as reference. Antigen barcode libraries were also processed using Cell Ranger (10X Genomics). The overlapping cell barcodes between the two libraries were used as the basis of the subsequent analysis. We removed cell barcodes that had only non-functional heavy chain sequences as well as cells with multiple functional heavy chain sequences and/or multiple functional light chain sequences, reasoning that these may be multiplets. Additionally, we aligned the BCR contigs (filtered_contigs.fasta file output by Cell Ranger, 10X Genomics) to IMGT reference genes using HighV-Quest38. The output of HighV-Quest was parsed using ChangeO and merged with an antigen barcode UMI count matrix. Finally, we determined the LIBRA-seq score for each antigen in the library for every cell as previously described (Setliff et al., 2019).

Antibody purification

For each antibody, variable genes were inserted into custom plasmids encoding the native (IgG1, IgG3, or IgA) constant region for the heavy chain as well as respective lambda or kappa light chains (pTwist CMV BetaGlobin WPRE Neo vector, Twist Bioscience). Antibodies were expressed in Expi293F mammalian cells (Thermo Fisher Scientific) by co-transfecting heavy chain and light chain expressing plasmids using polyethylenimine transfection reagent. Antibodies were purified from filtered cell supernatant by Protein A affinity chromatography, and stored in PBS, pH=7.4 unless otherwise noted. The following reagents were obtained through the NIH HIV Reagent Program, Division of AIDS, NIAID, NIH: Anti-Human Immunodeficiency Virus (HIV)-1 gp41 Monoclonal Antibody (2F5), ARP-1475, contributed by DAIDS/NIAID; Monoclonal Anti-Human Immunodeficiency Virus (HIV)-1 gp120 Protein (VRC01), ARP-12033,

contributed by Dr. John Mascola; Anti-Human Immunodeficiency Virus 1 (HIV-1) gp41 Monoclonal (5F3), ARP-6882, contributed by Polymun Scientific.

ELISA

To assess antibody binding, soluble protein was plated on Immulon 2HB plates (Thermo Fisher Scientific) at 2 µg/ml overnight at 4°C. In cases where capture ELISA was used, plates were pre-incubated for 2 hours at room temperature (RT) with 5µg/ml GNA lectin (Sigma) or 2µg/ml anti-AviTag (Genscript) and washed 3X with PBS+ 0.05% Tween-20 (PBS-T) before antigen plating overnight. Between each of the subsequent incubation steps, plates were washed 3X with PBS-T. Non-specific binding was blocked by incubation with 5% fetal bovine serum (FBS) (Gibco) diluted in PBS-T for 1 hour at RT. Primary monoclonal antibodies were diluted in 5% FBS-PBST starting at 20 µg/ml with a serial 1:5 dilution (unless otherwise specified) and then added to the plate for 1 hour at RT. Secondary antibody, either goat anti-human IgG (Southern Biotech) or goat anti-human IgA (Invitrogen), was diluted 1:10,000 in 5% FBS diluted in PBS-T and added for 1 hour at RT. Reaction was developed by 10 minute incubation with One Step Ultra-TMB (Thermo Fisher Scientific) and stopped with 1N sulfuric acid. Plate absorbances were read at 450 nm (Biotek). Data are represented as mean ± SEM for one ELISA experiment performed in duplicate. ELISA experiments were repeated with at least 2 different antibody preparation aliquots. The area under the curve (AUC) was calculated using GraphPad Prism 8.0.0.

Competition ELISA

Competition ELISA experiments were performed as above with minor modifications. After coating with antigen and blocking, non-biotinylated competitor

antibody was added to each well at 10 µg/ml and incubated at RT for 1 hour. After washing, biotinylated antibody (final concentration of 1 µg/ml) was added and incubated for 1 hour at RT. After washing three times with PBS-T, streptavidin-HRP (Thermo Fisher Scientific) was added at 1:10,000 dilution in 5% FBS in PBS-T and incubated for 1 hour at room temperature. Plates were washed and substrate and sulfuric acid were added as described above.

Mannose-competition ELISA

Mannose competition ELISAs were performed as described above with minor modifications. After antigen coating and washing, nonspecific binding was blocked by incubation with 5% FBS diluted in PBS for 1 hour at RT. Primary antibodies were diluted in 5% FBS-PBST +/- 1M D-(+)- Mannose (Sigma) starting at 10 µg/ml with a serial 1:5 dilution and then added to the plate for 1 hour at RT. After washing, antibody binding was detected with goat anti-human IgG-HRP (Southern Biotech) and added at 1:10,000 dilution in 5% FBS in PBS-T to the plates. After 1 hour incubation, plates were washed and substrate and sulfuric acid were added as described above. Data shown is representative of experiments performed in duplicate with at least 2 different antibody preparations.

Negative stain grid preparation

For screening and imaging of negatively stained (NS) HIV-1 gp140 in complex with Fab 180/692, ~3μl of the complex after SEC at concentrations of 10 to 15 μl g/ml were applied to glow-discharged grid with continuous carbon film on 400 square mesh copper EM grids (Electron Microscopy Sciences). The grids were stained with 0.75% Uranyl formate (UF) (Ohi et al., 2004).

Screening, data collection, and image processing

NS grids were screened on an FEI Morgagni (Thermo Fisher Scientific) microscope operating at 100kV with AMT 1k×1k CCD camera to verify sample and grid quality. Data collection from NS grids were done on FEI TF20 (Thermo Fisher Scientific) operate at 200kV with US4000 4kx4k CCD camera (Gatan) and controlled by SerialEM (Mastronarde, 2003). The data set was collected at nominal mag of 50Kx with A/pix of 2.18 with defocus range of 1.4-1.8 and a total dose of ~30.0e/A2.

Image processing was performed using the CryoSPARC software package (Punjani et al., 2017). The data set was imported, CTF estimated, and particles were picked. The particles were extracted with box size of 256 x 256 pixels and 2D classification was performed to generated clean homogeneous classes.

TZM-bl HIV-1 neutralization

Antibody neutralization was assessed using the TZM-bl assay as described (Sarzotti-Kelsoe et al., 2014). This standardized assay measures antibody-mediated inhibition of infection of JC53BL-13 cells (also known as TZM-bl cells) by molecularly cloned Env-pseudoviruses. Viruses that are highly sensitive to neutralization (Tier 1) and/or those representing circulating strains that are moderately sensitive (Tier 2) were included, plus additional viruses, including a subset of the antigens used for LIBRA-seq. Murine leukemia virus (MLV) was included as an HIV-specificity control and VRC01 was used as a positive control. Results are presented as the concentration of monoclonal antibody (in µg/ml) required to inhibit 50% of virus infection (IC_{50}).

Antibody-dependent cellular phagocytosis (ADCP), and antibody-dependent cellular cytotoxicity (ADCC)

The THP-1 phagocytosis assay was performed as previously described using 1μM neutravidin beads (Molecular Probes Inc) coated with antigen. Monoclonal IgG samples were titrated and tested at a final concentration of 100μg/ml. Additionally monoclonal antibodies were tested starting at 100μg/ml with 5-fold dilutions. Phagocytic scores were calculated as the geometric mean fluorescent intensity (MFI) of the beads that have been taken up multiplied by the percentage bead uptake. This, as well as all other flow cytometry work was completed on a FACSAria II (BD Biosciences). Pooled IgG from HIV-positive donors from the NIH AIDS Reagent programme (HIVIG) was used in all assays to normalize for plate to plate variation while samples from 10 Clade C-infected individuals was used as a positive control for all assays. Palivizumab (MedImmune) was used as negative control.

HCV pseudoparticle (HCV_{PP}) neutralization

A panel of 19 HCVpps were produced by lipofectamine-mediated transfection of HCV E1E2 plasmid, pNL4-3.Luc.R-E-plasmid containing the env-defective HIV proviral genome (NIH AIDS Reagent Program), and pAdVantage (Promega) into HEK293T cells. Mock pseudoparticles, generated with pNL4-3.Luc.R-E- and pAdVantage and without E1E2 plasmid, were used as a negative control for each transfection. For HCVpp testing, 8,000 Hep3B cells per well were plated in 96-well solid white flat bottom polystyrene TC-treated microplates (Corning) and incubated overnight at 37°C. For infectivity testing, HCVpp were incubated on Hep3B target cells for 5 hours. Following this incubation, medium was changed to 100μL of phenol-free Hep3B media and incubated for 72 hours at 37°C. Infectivity was quantified using a luciferase

assay as described below. All HCVpp used in neutralization assays produced RLU values at least 10-fold above background entry by mock pseudoparticles. For antibody breadth testing, HCVpp were incubated for 1 hour with mAb at 100μg/mL and then added in duplicate to Hep3B target cells for 5 hours. Following this incubation, medium was changed to 100μL of phenol-free Hep3B media and incubated for 72 hours at 37°C. Infectivity was quantified using a luciferase assay as described below. All HCVpp used in neutralization assays produced RLU values at least 10-fold above background entry by mock pseudoparticles. For antibody potency testing, antibodies were serially diluted five-fold, starting at a concentration of 100μg/mL and ending at $2.56x10^{-4}$ (leaving the last well as PBS only), and incubated with HCVpp for one hour at 37°C before the addition to HEP3B target cells in duplicate. Following this incubation, medium was changed to 100μL of phenol-free Hep3B media and incubated for 72 hours at 37°C. After incubation (for either breadth or potency testing), media was removed from the cells, 45μL of 1x cell culture lysis reagent (Promega) was added to each well and left to incubate for 5 minutes. The luciferase assay was measured in relative light units (RLUs) in Berthold Luminometer (Berthold Technologies Centro LB960). The percentage of neutralization for the antibody breadth was calculated as (1-(RLU_{mAb}/RLU_{IgG})) x 100). The percentage of neutralization for the dilution curves and was calculated as (1-(RLU_{mAb}/RLU_{PBS})) x 100. HEPC74 and Human IgG were run as controls.

Influenza A hemagglutination inhibition (HAI)

The hemagglutination inhibition (HAI) assay was used to assess the ability of mAb688 to inhibit agglutination of erythrocytes. The HAI assay was performed similarly to previously described protocols (Forgacs et al., 2021; Sautto et al., 2020) adapted from the World Health Organization (WHO) laboratory influenza surveillance manual. In brief,

mAb688 (expressed as IgG1 or IgG3) was diluted in a series of 2-fold serial dilutions in v-bottom microtiter plates (Greiner Bio-One) starting from 20 µg/ml. An equal volume of A/Brisbane/02/2018 (CA/09 pdm-like H1N1) or A/Hong Kong/4801/2014 (H3N2) virus, adjusted to ~8 hemagglutination units per 50 µl, was added to each well. The plates were covered and incubated at room temperature for 20 min, and then a 0.8% solution of turkey (for H1N1) or guinea pig (for H3N2) erythrocytes (Lampire Biologicals) in PBS was added. Erythrocytes were stored at 4°C and used within 72 h of preparation. The plates were mixed by agitation and covered, and the erythrocytes were settled for 30 min at room temperature. The HAI titer was determined by the reciprocal dilution of the last well that contained nonagglutinated erythrocytes. Positive and negative controls were included for each plate.

Focus reduction assay

Madin-Darby canine kidney (MDCK) cells stably-transfected with cDNA encoding human 2,6-sialtransferase (SIAT1) MDCK-SIAT1 (provided by Center for Disease Control and Prevention) were maintained in DMEM (Corning) supplemented with penicillin-streptomycin, BSA fraction V 7.5% solution (Thermo Fisher Scientific), 25 mM HEPES buffer, 10% heat-inactivated FBS and 1 mg/ml of geneticin (G418 sulfate; Thermo Fisher Scientific).

The focus reduction assay (FRA) was performed similarly to previously described protocols (Sautto et al., 2020). In brief, MDCK-SIAT1 cells were seeded at a density of 2.5-3×10^5 cells/ml in a 96-well plate (Greiner Bio-One) the day before the assay was run. The following day, the cell monolayers were rinsed with 0.01 M PBS (pH 7.2) (Thermo Fisher Scientific), followed by the addition of 2-fold serially diluted mAb688 (expressed as IgG1 or IgG3) at 50 µl per well starting with 20 µg/ml dilution in virus growth medium,

termed VGM-T (DMEM containing 0.1% BSA, penicillin-streptomycin, and 1 µg/ml L-(tosylamido-2-phenyl) ethyl chloromethyl ketone (TPCK)-treated trypsin (Sigma, St. Louis, MO, USA)). Afterwards, 50 µl of virus (A/California/07/2009 (pdm H1N1), A/Texas/50/2012 (H3N) or B/Massachusetts/02/2012 (influenza B virus) standardized to 1.2×10^4 focus forming units (FFU) per milliliter, and corresponding to 600 FFU per 50 µl, was added to each well, including control wells. Following a 2h incubation period at 37°C with 5% CO_2, the cells in each well were then overlaid with 100 µl of equal volumes of 1.2% Avicel RC/CL (Type RC581 NF; FMC Health and Nutrition, Philadelphia, PA) in 2× MEM (Thermo Fisher Scientific) containing 1 µg/ml TPCK-treated trypsin, 0.1% BSA, and antibiotics. Plates were incubated for 18-22h at 37°C, 5% CO_2. The overlays were then removed from each well and the monolayer was washed once with PBS to remove any residual Avicel. The plates were fixed with ice-cold 4% formalin in PBS for 30 min at 4°C, followed by a PBS wash and permeabilization using 0.5% Triton X-100 in PBS/glycine at room temperature for 20 min. Plates were washed three times with PBS supplemented with 0.1% Tween 20 (PBST) and incubated for 1h with a mAb against influenza A nucleoprotein (provided by the International Reagent Resource (IRR), Influenza Division, WHO Collaborating Center for Surveillance, Epidemiology and Control of Influenza, Centers for Disease Control and Prevention) in ELISA buffer (PBS containing 10% horse serum and 0.1% Tween 80 (Thermo Fisher Scientific)). Following washing three time with PBST, the cells were incubated with goat anti-mouse peroxidase-labeled IgG (SeraCare) in ELISA buffer for 1h at room temperature. Plates were washed three times with PBST, and infectious foci (spots) were visualized using TrueBlue substrate (SeraCare) containing 0.03% H2O2 incubated at room temperature for 10–15 min. The reaction was stopped by washing five times with distilled water. Plates were dried and foci were enumerated using an ImmunoSpot S6 ULTIMATE reader with ImmunoSpot 7.0.28.5

software (Cellular Technology Limited). The FRA titer was reported as the reciprocal of the highest dilution of serum corresponding to 50% foci reduction compared with the virus control minus the cell control.

SARS-CoV-2 pseudoparticle neutralization

To assess neutralizing activity against SARS-CoV-2 strain 2019 n-CoV/USA_WA1/2020 (obtained from the Centers for Disease Control and Prevention, a gift from N. Thornburg), we used the high-throughput RTCA assay and xCelligence RTCA HT Analyzer (ACEA Biosciences) as described previously. After obtaining a background reading of a 384-well E-plate, 6,000 Vero-furin cells were seeded per well. Sensograms were visualized using RTCA HT software version 1.0.1 (ACEA Biosciences). One day later, equal volumes of virus were added to antibody samples and incubated for 1ch at 37°C in 5%cCO2. mAbs were tested in triplicate with a single (1:20) dilution. Virus–mAb mixtures were then added to Vero-furin cells in 384-well E-plates. Controls were included that had Vero-furin cells with virus only (no mAb) and media only (no virus or mAb). E-plates were read every 8–12 h for 72 h to monitor virus neutralization. At 32 h after virus-mAb mixtures were added to the E-plates, cell index values of antibody samples were compared to those of virus only and media only to determine presence of neutralization.

Uropathogenic *E. coli* hemagglutination and adherence inhibition

Hemagglutination assays were performed as described previously (Hultgren et al., 1986). Bacterial cultures were grown statically at 37˚C for 24 hours in Lysogeny broth (LB), subcultured intro fresh LB, and grown another 24 hours. Cultures were normalized to optical density (600 nm) of 1.0 in PBS, concentrated 10x, and resuspended in PBS or PBS containing 4% mannose (to competitively inhibit the type 1 pili), 20 µg/mL mAb688,

or 20 µg/mL isotype control. Bacteria were added to a 96 well plate and diluted in two-fold increments. Next, guinea pig erythrocytes (Innovative Research, Inc.) were washed and suspended in PBS or PBS containing 4% mannose, 20 µg/mL mAb688, or 20 µg/mL isotype control. Erythrocytes were added to the diluted bacterial culture and incubated statically overnight at 4˚C. Hemagglutination titer was determined by measuring the lowest dilution that visibly inhibited hemagglutination. Data are representative of three biological replicates performed in technical duplicate.

Autoreactivity

Monoclonal antibody reactivity to nine autoantigens (SSA/Ro, SS-B/La, Sm, ribonucleoprotein (RNP), Scl 70, Jo-1, dsDNA, centromere B, and histone) was measured using the AtheNA Multi-Lyte® ANA-II Plus test kit (Zeus scientific, Inc.). Antibodies were incubated with AtheNA beads for 30min at concentrations of 50, 25, 12.5 and 6.25 µg/mL. Beads were washed, incubated with secondary and read on the Luminex platform as specified in the kit protocol. Data were analyzed using AtheNA software. Positive (+) specimens received a score >120, and negative (-) specimens received a score <100. Samples between 100-120 were considered indeterminate.

HEp-2 cell binding

We measured antibody binding to whole (un-permeabilized) un-infected HEp-2 cells by flow cytometry. Briefly, we collected HEp-2 cells and washed 3X with DPBS-BSA before counting. ~1 million cells/condition were stained with a final concentration of 100µg/ml, 10µg/ml, or 1µg/ml antibody diluted in DPBS-BSA for 20 minutes at 4C. Cells were then washed 3X with DPBS-BSA and stained with either goat anti-human IgG labeled with PE (Southern Biotech) or goat anti-human IgA (Southern Biotech) labeled

with PE diluted 1:1000 in DPBS-BSA for 20 minutes at 4C. Cells were washed a final time and fluorescence acquired on a 4-Laser Fortessa (BD Biosciences). FCS files were analyzed and figures generated using CytoBank. Data shown is representative of at least 2 separate experiments with different antibody preparations. The following reagent was obtained through the NIH HIV Reagent Program, Division of AIDS, NIAID, NIH: Anti-Human Immunodeficiency Virus (HIV)-1 gp41 Monoclonal Antibody (4E10), ARP-10091, contributed by DAIDS/NIAID.

Chapter 3: Multi-component Vaccine Targeting Metal Acquisition Kills *Staphylococcus aureus*

CONTRIBUTIONS: I helped choose the vaccine antigens, I designed the primers and cloning strategy, performed antigen cloning from *S. aureus* DNA, antigen expression and purification, immunization studies, mouse handling and euthanasia, sample preparation, and ELISA binding assays. Jessica Sheldon helped choose the vaccine antigens, design the cloning primers, and performed all whole blood killing assays. Steven Wall helped design and perform antigen cloning, helped with antigen expression and purification, and mouse euthanasia/sample collection. Kevin Kramer and Amyn Murji helped with mouse euthanasia and final sample collection. I coordinated all collaborator experiments, made the figures and wrote the manuscript.

INTRODUCTION

Staphylococcus aureus is a facultative anaerobic Gram-positive bacterium that colonizes up to one-third of the population (Kang et al., 2011; Lowy, 1998). Although frequently commensal, *S. aureus* can cause a range of illnesses from mild skin and soft tissue infection (SSTI) to endocarditis and sepsis (Kang et al., 2011; Krismer et al., 2017; Tong et al., 2015). Moreover, the rise of antibiotic-resistance has made *S. aureus* one of the most dangerous human pathogens, compelling the development of additional therapeutic and prophylactic options (Gu et al., 2020; Guo et al., 2020; Vestergaard et al., 2019).

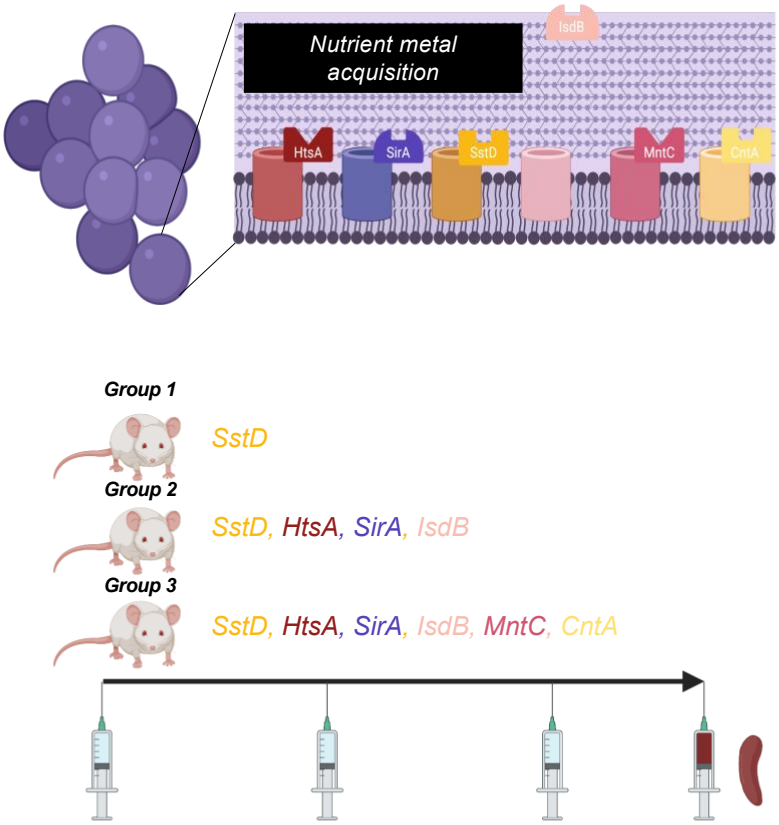

Figure 3-1. Multi-subunit vaccination strategy targeting *S.aureus* metal acquisition
Selection of surface-accessible antigens involved in metal acquisition for vaccination. Three groups of mice (plus a control mock-immunized group) were vaccinated with the antigens shown and boosted with additional injections at 21-day intervals. Study conclusion was two weeks after the last immunization.

Vaccination and immunotherapies offer a particularly attractive solution against *S. aureus*, but traditional strategies, including immunization with whole-inactivated bacteria or subunit toxin antigens, have failed to elicit sterilizing immunity in humans (Broughan et al., 2011). Among significant impediments to vaccine design summarized elsewhere, small animal models have failed to effectively predict protection in clinical trials (Salgado-Pabón & Schlievert, 2014). Although there are no human vaccines licensed against *S. aureus*, the decades of research have uncovered several paths forward (Ansari et al., 2019; Bagnoli et al., 2012; Broughan et al., 2011).

Previous studies, and *S. aureus*' diverse arsenal of virulence and host evasion factors, suggest that a successful vaccine will need to target multiple antigens (Jansen et

al., 2013). One particularly promising study, which failed during Phase IIB clinical trials, comprised four antigens conjugated to diphtheria toxin (capsular polysaccharide serotypes 5 and 8 (CP5 and CP8), clumping factor A (ClfA), and recombinant manganese transporter C (MntC)) (Frenck et al., 2017; Miller et al., 2020). Although this trial induced high levels of opsonophagocytic antibodies against the diverse immunogens, it failed to meet protection endpoints (Begier et al., 2017). One hypothesis for the limited success of this study could be that the sheer diversity of virulence factors and number of functionally redundant systems allows *S. aureus* to evade vaccine-induced immunity by tuning down expression of vaccine immunogens and/or using other pathways (Deng et al., 2019; Klimka et al., 2021; Teymournejad & Montgomery, 2021).

In this study, we sought to overcome the limitations of previous investigations by designing a multi-subunit vaccine that targets an entire essential *S. aureus* system. Specifically, we hypothesized that using antigens from each nutrient metal acquisition pathway would *limit S. aureus* escape, and promote bacterial clearance through normal immune mechanisms, (opsonogenic antibodies, cytokines etc.) as well as bacterial metal starvation. To investigate this, we immunized BALB/c mice with either a single antigen (SstD), all iron acquisition antigens (SstD, SirA, HtsA, IsdB), or all metal acquisition antigens (SstD, SirA, HtsA, IsdB, CntA, MntC) and assessed vaccine-induced *S. aureus* immunity and killing.

RESULTS

Multi-subunit vaccination strategy targeting *S. aureus* metal acquisition

Metal ion acquisition is critical to the survival of all life, including bacterial pathogens (Cassat & Skaar, 2012; Jenkins et al., 2015). *S. aureus* possesses multiple pathways to accomplish this critical process including the Sst, Sir, Hts, and Isd systems

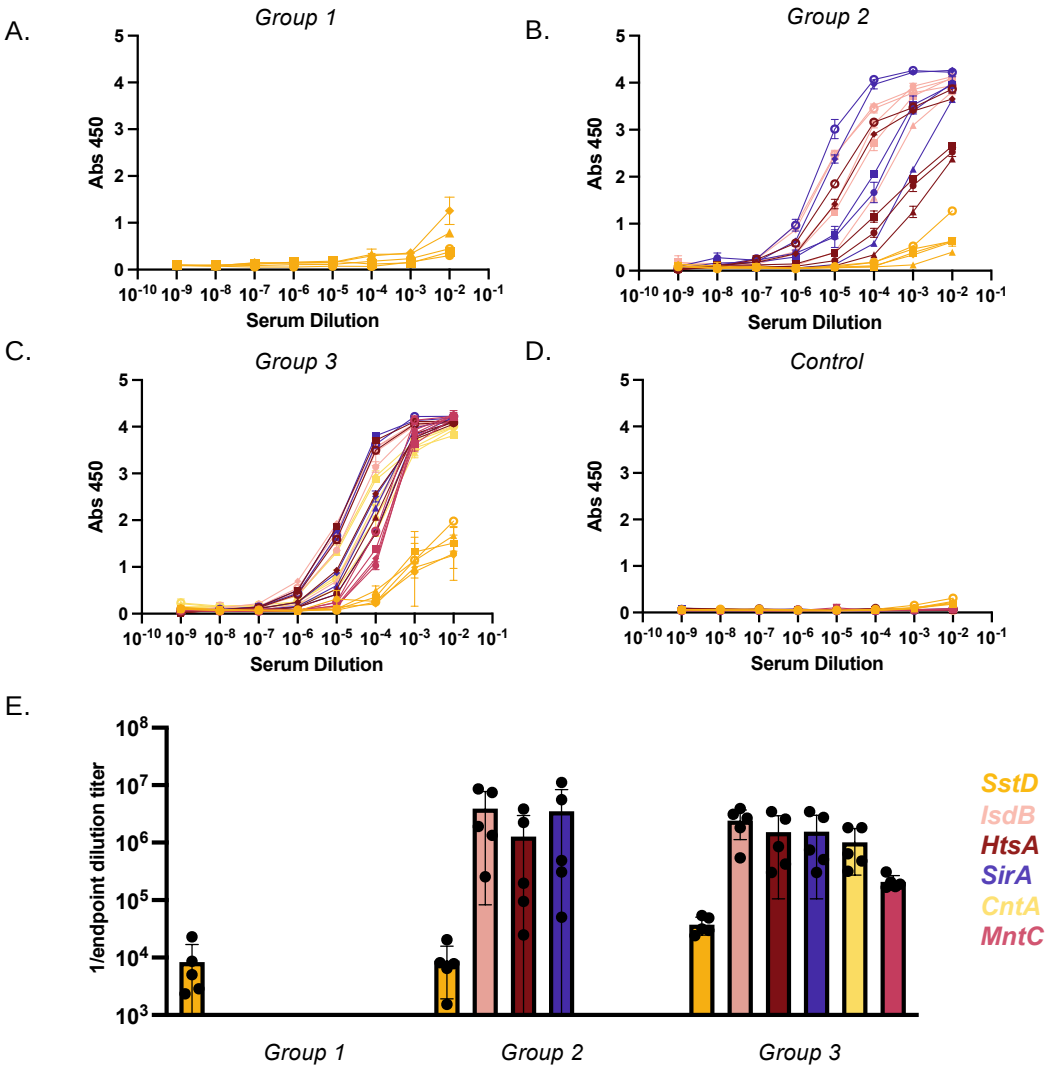

Figure 3-2. Metal acquisition immunogens induce variable IgG responses
Antibody responses of each immunization group against vaccine antigens measured by ELISA. (A) Serological IgG antibody response to SstD (dark yellow) elicited by group 1. (B) Serological IgG antibody response as described in (A) plus IsdB (light pink), HtsA (red), and SirA (purple) elicited by group 2. (C) Serological IgG antibody response described as in (B) including CntA (light yellow), and MntC (dark pink) elicited by group 3. (D) Serological IgG antibody responses as described in (C) elicited by mock-immunized control mice. (E) Quantification of reciprocal endpoint dilution antibody titers calculated from (A-C).

to acquire iron, the Cnt system to acquire zinc, and the Mnt system to acquire manganese (Beasley et al., 2011; Grim et al., 2017; Kehl-Fie et al., 2013; Salazar et al., 2014; Sheldon & Heinrichs, 2012). To interrogate the effect of vaccination with metal acquisition antigens on the development of *S. aureus* immunity, we chose a surface accessible antigen from each of the pathways described above, and immunized BALB/c mice with equimolar quantities of each metal acquisition antigens (SstD, SirA, HtsA, IsdB, CntA, MntC) (Figure

1; group 3). We also vaccinated additional groups with either SstD alone, iron-acquisition antigens (SstD, SirA, HtsA, IsdB), or mock-immunized with PBS (Figure 1; group 1, group 2, control). We vaccinated mice with the recombinant soluble antigen combinations described, followed by two booster injections three weeks apart (Day 0, 21, 42). Vaccine-induced *S. aureus* immunity and killing was assessed at study conclusion (day 56) (**Figure 3-1**).

Metal acquisition immunogens induce variable IgG responses

After completing the described immunization regimens, we first sought to assess the elicitation of vaccine-specific IgG antibodies (**Figure 3-2**). We measured the

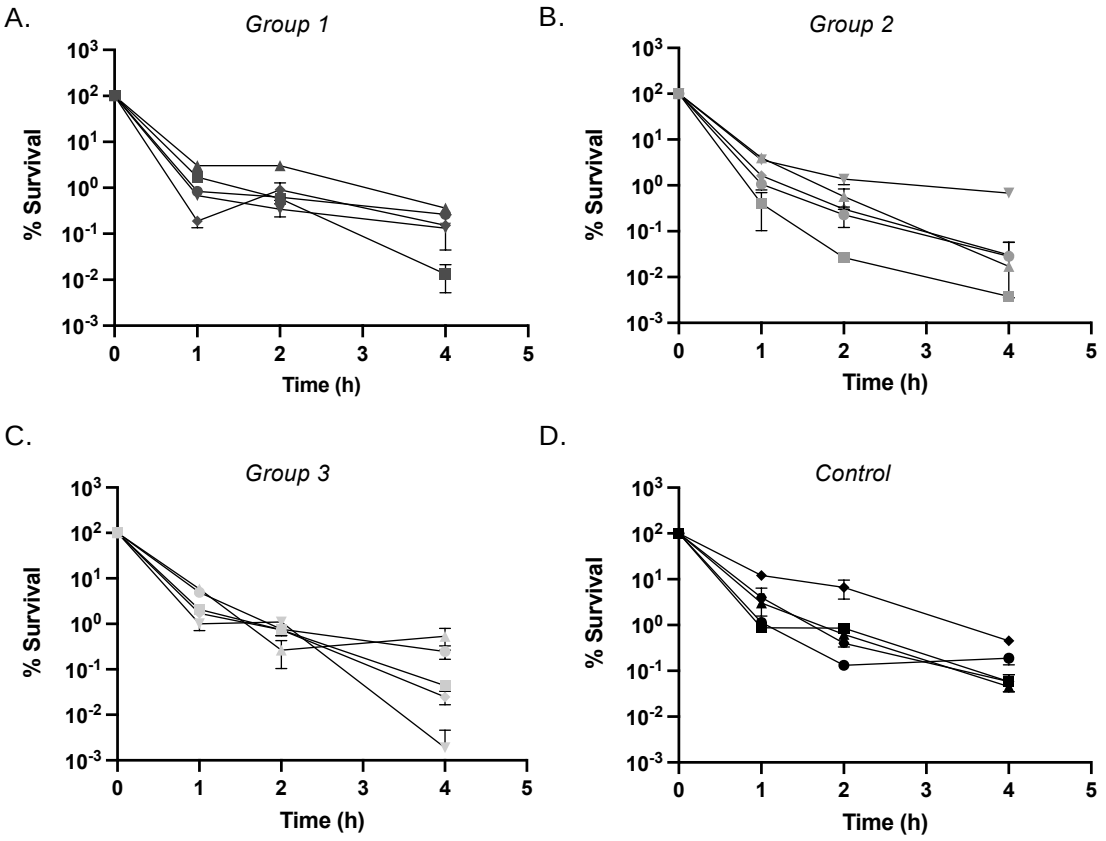

Figure 3-3. Blood from immunized mice kills S. aureus
Longitudinal survival of *S. aureus* measured by an in vitro whole blood killing assay using blood from each immunization group: (A) group 1, (B) group 2, (C) group 3, and (D) control. Each line represents a unique mouse. Data shown as percent survival at each sampled timepoint.

serological antibody response to each individual immunogen using ELISA (**Figure 3-2A–D**) and quantified antigen-specific antibody titers (**Figure 3-2E**). With the exception of SstD, mice developed high IgG antibody titers against all vaccine immunogens (**Figure 3-2E**). By contrast, mice immunized with SstD did not develop high antibody titers, and this antigen elicited the lowest response across groups (**Figure 3-2**). Curiously however, mice vaccinated with all six antigens (group 3) demonstrated a significantly more robust antibody response to SstD, suggesting that this cocktail administration enhanced immunogenicity (**Figure 3-2C, E**). Finally, we note that mock-immunized mice did not demonstrate IgG reactivity to any of the vaccine antigens (**Figure 3-2D**). Overall, mice vaccinated with metal acquisition antigens elicited variable IgG antibody responses.

Immunized blood kills S. aureus

As mentioned above, one barrier to the development of a *S. aureus* vaccine is the failure of small animal models to predict protection in human clinical trials (Proctor, 2012). To circumvent differences in *S. aureus* infection between mouse models and humans, many have noted that using in vitro opsonophagocytosis or killing assays are more reliable indicators of translatable vaccine-induced protection (Paschall et al., 2019; Pozzi et al., 2017). We therefore next sought to investigate the ability of blood from immunized mice to kill *S. aureus* in a whole blood killing assay (**Figure 3-3**). We found that blood from all mice tested were able to decrease *S. aureus* survival at least 100-fold by assay conclusion, including mock-immunized mice (**Figure 3-3A-D**). Notably however, mice vaccinated with all iron, or all metal antigens achieved higher maximum endpoint killing, decreasing *S. aureus* survival more than 10,000-fold by assay conclusion (**Figure 3-3B, C**).

Mice vaccinated with all metal acquisition immunogens kills *S. aureus* equally well without complement

To investigate the relative effect of complement on immunization-induced *S. aureus* killing, we inactivated the plasma before performing additional whole blood killing assays as previously described (**Figure 3-4A-D**). Only mice vaccinated with all six

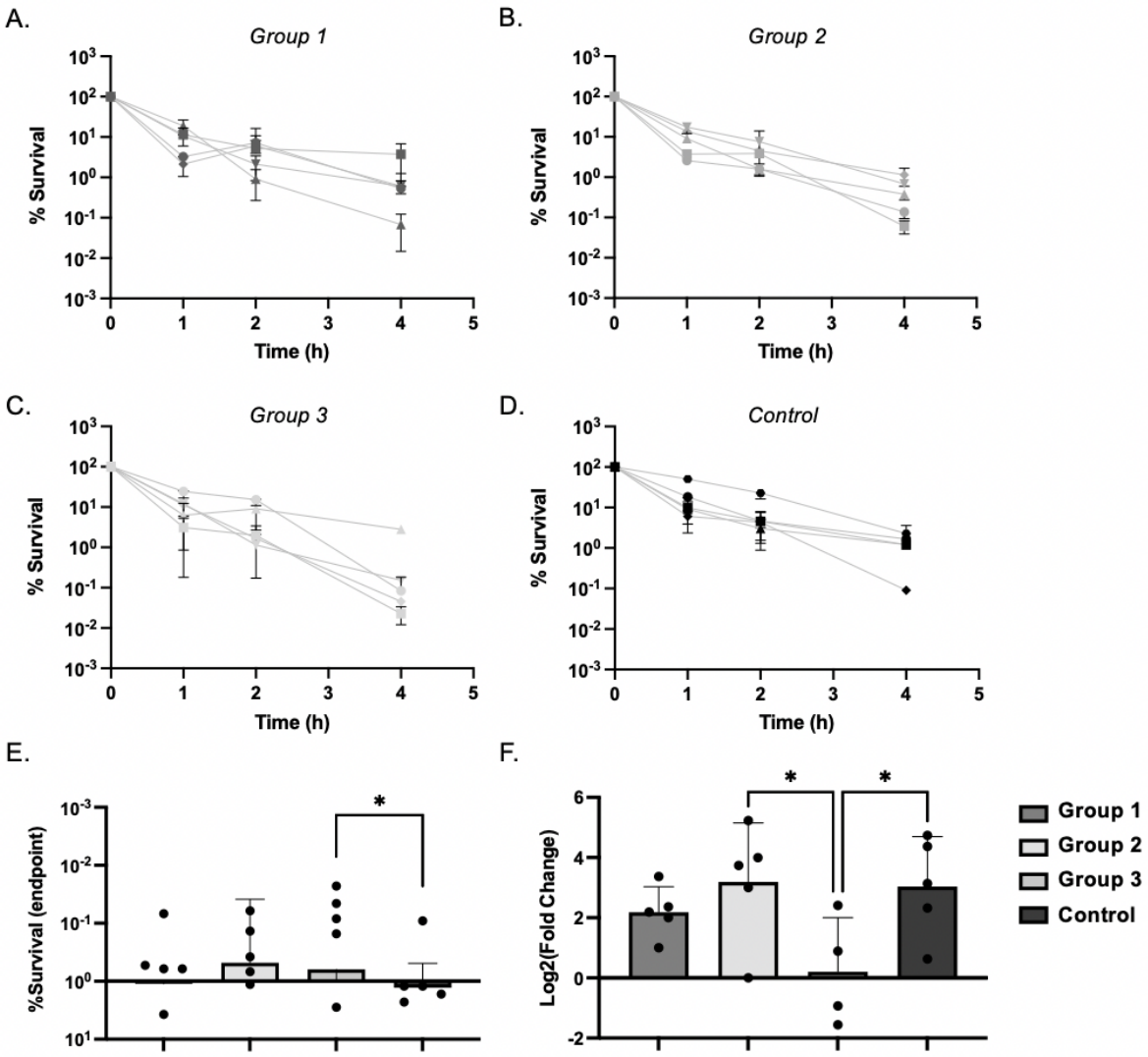

Figure 3-4. Mice vaccinated with all metal acquisition immunogens kills *S. aureus* equally well without complement

Longitudinal survival of *S. aureus* measured by an in vitro whole blood killing assay using blood with heat-inactivated plasma from each immunization group: (A) group 1, (B) group 2, (C) group 3, and (D) control. Data shown as percent survival at each sampled timepoint. (E) Endpoint survival comparison by group. (F) The relative contribution of complement was calculated by dividing (endpoint survival-whole blood/endpoint survival-blood+ inactivated plasma). Data is shown as Log_2(survival change). Statistical significance was determined by Kruskal-Wallis test. * denotes $p<0.05$.

immunogens decreased *S. aureus* survival significantly more than controls (**Figure 3-4E**). Further, we found that *S. aureus* killing was decreased by more than half when plasma was inactivated, apart from mice immunized with all metal antigens, which killed *S. aureus* equally well in assays including inactivated plasma (**Figure 3-4F**). These results suggest that complement strongly contributes to the observed *S. aureus* killing, but that immunization with all metal antigens helps bypass this requirement by eliciting immunity that works via additional mechanisms.

DISCUSSION

S. aureus is one of the leading causes of invasive community- and hospital-acquired infection, costing the US nearly $15 billion annually (Gould et al., 2010). Although immunization has proven successful in lessening the significant morbidity and mortality of other pathogens, traditional strategies have fallen short of designing a protective *S. aureus* vaccine (Proctor, 2015). Previous studies have suggested that a successful *S. aureus* vaccine will need to include multiple antigens, but that the optimal combination has yet to be determined (Broughan et al., 2011). Here we describe the design and testing of a six-antigen cocktail vaccine targeting *S. aureus* nutrient metal acquisition in BALB/c mice. We discovered that mice vaccinated with antigens involved in iron, zinc, and manganese acquisition elicited superior antigen-specific IgG antibody responses and *S. aureus* killing over all other groups, particularly when plasma was inactivated.

Metal starvation is an important host defense mechanism and the ability of bacteria to overcome nutritional immunity is critical to survival, pathogenicity, and establishment of infection (Hood & Skaar, 2012). As such, *S. aureus* possess multiple systems to acquire metal ions from the environment. Previous strategies have included IsdB either

alone or in combination, or MntC with other antigens, but our study is the first to combine both antigens in a single cocktail. Further, we describe the immunogenicity of four additional metal acquisition antigens: SstD, SirA, HtsA, and CntA. Interestingly, SstD alone did not elicit a strong IgG antibody response, but when this antigen was administered as a six-antigen cocktail, SstD-specific titers more than doubled.

In addition to more robust IgG antibody responses, mice immunized with all metal acquisition antigens reduced *S. aureus* survival significantly more than control mice when plasma was inactivated. We found that complement plays a significant role in the observed *S. aureus* killing mediated by all groups except when mice were vaccinated with all six antigens. Notably, mice immunized with all iron acquisition antigens were not able to significantly reduce *S. aureus* survival in either condition, supporting that the addition of all metal acquisition pathway antigens contributed to the elicitation of superior immunity.

In this study, we show that cocktail vaccination enhances both antigen-specific antibody responses and *S. aureus* killing. Together, our results suggest that vaccination targeting metal acquisition could be a promising approach for the development of a *S. aureus* vaccine.

MATERIALS AND METHODS

Antigen gene cloning from *S. aureus* DNA

Genes encoding each antigen were amplified out of the *S. aureus* (strain: Newman) genome using Q5 Hot Start DNA polymerase and the PCR primers shown below (Table 1). Primers were designed with a CACC overhang to facilitate directional TOPO cloning. Fresh, unpurified PCR product was incubated with the pET100/D-TOPO

vector according to manufacturer's instructions and transformed into chemically competent E. coli. In addition to each antigen, the pET100/D-TOPO vector encodes an N-terminal 6X HisTag, Xpress Epitope, and enterokinase (EK) cleavage site. Plasmid DNA from the resulting colonies was sequenced to confirm successful integration and directional orientation of each gene of interest into the pET100/D-TOPO vector.

Antigen expression and purification

For protein expression, plasmids described above were transformed into BL21 (DE3) pLysS E. coli cells and cultured in Luria Broth with 50 μg/mL Kanamycin (+25 μg/mL chloramphenicol). Recombinant protein expression from pET100/D-TOPO was induced at OD600 = 0.8 with the addition of 1 M isopropyl β-D-1-thiogalactopyranoside (IPTG) (added to a final concentration of 1 mM) for 6 h at 37 °C with shaking.

Induced cultures were harvested by centrifugation (8000× g, 4 °C, 20 min) and pellets frozen at −80 °C overnight. Pellets were then thawed on ice and resuspended in 5 mL/g pellet weight with binding buffer (20 mM sodium phosphate, 0.5 M NaCl, 10 mM imidazole, pH 7.4 +EDTA-free protease-inhibitor) before lysis by 6 × 30 s rounds of sonication. Lysate was cleared by centrifugation (10,000× g, 4 °C, 20 min) and filtered using a 0.45 μm PES filter before purification. Each antigen was then purified by nickel affinity chromatography using an equilibrated, 5 mL pre-packed HisTrap HP column (GE Healthcare, IL, USA). The column was washed with 50mL of binding buffer, and purified protein was eluted from the column with a 25 mL gradient into binding buffer +0.5 M Imidazole, pH = 7.4. Each antigen was further purified by gel filtration using a Superdex 200 Increase 10/300 GL column, and eluted fractions corresponding to correctly folded protein were collected for further analysis.

Finally, purification tags were removed before immunization using EKMax enterokinase cleavage according to manufacturer's instructions. Cleavage enzyme was removed using EK-Away purification resin, and purified antigen preparations were buffer-exchanged into PBS. The concentration of all final antigen samples was estimated using BCA Assay.

Vaccination

Six- to eight-week-old female BALB/c mice (n = 5/ group) were used for these studies, and animals were ≤15 weeks old at study conclusion. All procedures were conducted according to protocols approved by Institutional Animal Care and Use Committee at Vanderbilt University Medical Center.

Purified protein combinations were diluted in sterile PBS and emulsified 1:1 in TiterMax Gold for intraperitoneal injection. Isoflurane-anaesthetized mice were immunized on day 0 and received booster injections on days 21 and 42 of either a) PBS, b) 66.7pmol: SstD, c) 66.7pmol/ antigen: SstD, HtsA, SirA, IsdB, or d) 66.7pmol/antigen: SstD, HtsA, SirA, IsdB, CntA, and MntC.

At study conclusion (day 56), mice were sacrificed by CO2 overdose and cardiac puncture exsanguination. Blood was collected in sodium heparin-coated tubes and stored at room temperature on a rotator until use. An additional aliquot of blood was collected for serum separation, blood was allowed to clot at room temperature and serum separated by centrifugation (10,000×g, 4°C, 10 min). Serum was transferred to a new tube and stored at −80 °C until use. Finally, spleens were extracted, pulverized, and strained to create single cell suspensions. Splenocytes were washed 3X with 1% BSA+DPBS, before being resuspended in freezing medium. Splenocytes were stored in liquid nitrogen (-196°C) until use.

Enzyme-Linked Immunosorbent Assay (ELISA)

For indirect serum Enzyme-linked Immunosorbent Assay (ELISA), Immulon 2HB plates (Nunc) were coated with 2 µg/mL of purified recombinant antigen diluted in PBS overnight at 4 °C. Excess antigen was removed with 3X wash with PBS+ 0.05% Tween-20 (PBS-T). This washing step was repeated after each subsequent incubation step. Non-specific binding was blocked with 5% non-fat dried milk (NFDM) in PBS for 1 h at 37 °C, followed by washing. Hyperimmune sera was serially diluted in 1% NFDM in PBS-T, added to wells, and incubated for 1 h at 37 °C. Plates were washed, and incubated with anti-mouse IgG-HRP diluted 1:10,000 in 1% NFDM in PBS-T for 1 h at 37 °C. After washing, plates were developed with 3,3′,5,5′Tetramethylbenzidine for 10 min in the dark, reaction stopped with 1N sulfuric acid, and absorbance read at 450 nm. All ELISA data shown and used for calculations was blank subtracted.

Whole Blood Killing Assay (WBKA)

Whole blood and inactivated plasma killing assays were performed as previously described. Briefly, 100µL of heparin-anticoagulated blood was added per well in a 96-well plate. Bacterial suspensions prepared in PBS, containing 1.10E5 colony forming units (CFU), were added in a maximum volume of 5 µL immediately to the blood. The 96-well plate was incubated for the indicated time at 37 °C under continuous shaking. The number of bacterial CFU was determined at start and after incubation by plating serial 10-fold dilutions and percent survival calculated.

For plasma inactivation, 100µL of heparin-anticoagulated blood was added per well in a 96-well plate and centrifuged at 1000×g for 5 min. Plasma was removed and heat-inactivated for 20 min at 56 °C. Blood cells were washed by adding 100 µL DPBS

and centrifuged with 1000× g for 5 min. PBS was removed and heat-inactivated plasma was mixed with the pelleted cells and used for the killing assay as described above.

Statistics

All graphing and statistical analyses were done using GraphPad Prism 9. Significance between all immunization groups was determined using Kruskal–Wallis test (with Dunn's test for multiple comparisons). ELISA antibody endpoint titers were determined by interpolating a standard curve using GraphPad Prism 9. All statistics were conducted using 95% confidence intervals where applicable.

Chapter 4: Simultaneous Immunization with Multiple Diverse Immunogens Alters Development of Antigen-Specific Antibody-Mediated Immunity

This chapter is adapted from the following published manuscript:

Pilewski, Kelsey A et al. “Simultaneous Immunization with Multiple Diverse Immunogens Alters Development of Antigen-Specific Antibody-Mediated Immunity.” Vaccines vol. 9,9 964. 28 Aug. 2021, doi:10.3390/vaccines9090964

CONTRIBUTIONS: Ivelin Georgiev and I designed the study and wrote the paper. I expressed and purified all antigens, wrote and performed the mouse immunization protocol, mouse euthanasia and sample collection, ELISA binding assays, and analyzed all data. Kevin Kramer helped with mouse euthanasia and sample collection.

INTRODUCTION

The design and implementation of successful immunization regimens worldwide have cemented vaccination as one of the most important human medical interventions in history (Greenwood, 2014; Hajj Hussein et al., 2015; Jones & Helmreich, 2020; Nandi & Shet, 2020; Rodrigues & Plotkin, 2020). However, traditional vaccination strategies utilizing immunization with a live-attenuated or inactivated agent have proven insufficient in the face of many contemporary epidemic, highly mutable, and emerging pathogens (Piot et al., 2019; Pollard & Bijker, 2021). By contrast, modern strategies aim to rationally engineer a single antigen or cocktail of antigens to generate a more focused, protective immune response (Andreano et al., 2019; Delany et al., 2013; Mascola & Fauci, 2020;

Sette & Rappuoli, 2010). Further, although vaccine platform and formulation have been shown to have a profound effect on the magnitude and quality of the elicited immune response (Gebre et al., 2021; Liu, 2019; Zhang et al., 2015), the effect cocktail vaccination (simultaneous immunization with multiple immunogens) has on the antibody response to each individual antigen within the combination remains largely unstudied.

In this study, we sought to characterize the effect of cocktail vaccination on the immunogenicity of pathogen-derived protein antigens. We hypothesized that immunization with a cocktail of structurally, and functionally diverse antigens would result in decreased antibody titer against each unique antigen in the cocktail, compared to mice immunized with each antigen alone. To investigate this, we immunized mice with cell surface-exposed proteins from uropathogenic Escherichia coli, Mycobacterium tuberculosis, and Neisseria meningitides, and monitored the development of antigen-specific IgG antibody responses in BALB/c mice.

RESULTS

Simultaneous Immunization with Multiple Diverse Immunogens

To investigate the effect of cocktail (vs. single antigen) immunization on the development of humoral immunity, we immunized BALB/c mice (n = 5/group) with equimolar quantities of either three diverse immunogens, each unique combination of two, or each immunogen alone, and monitored the development of antigen-specific IgG antibodies. We selected three functionally diverse antigens from divergent pathogens that had either previously been tested or approved as vaccination targets against their native hosts after eliciting protective antibody responses in mice. Specifically, we chose the iron-regulated outer membrane protein IreA, from uropathogenic Escherichia coli, which is exclusively expressed by pathogenic strains of E. coli and facilitates nutrient metal

acquisition (Alteri et al., 2009; Hagan & Mobley, 2007; Russo et al., 2001); the heparin-binding hemagglutinin protein HBHA from Mycobacterium tuberculosis, which facilities bacterial dissemination from the lung (Hart et al., 2018; Parra et al., 2004; Pethe et al., 2001); and the factor H-binding protein fHbp from Neisseria meningitides, which facilitates bacterial innate immune evasion (Donald et al., 2017; McNeil et al., 2013; Scarselli et al., 2011) (**Figure 4-1A**). Consistent with their divergent cellular functions, these proteins share low sequence identity (**Figure 4-1B**). We immunized mice with each combination of antigens described above followed by two booster immunizations, and collected serum 14 days after each immunization for serological analysis (**Figure 4-1C,D**).

A.

Antigen	Pathogen	Function	Ref
IreA	Uropathogenic *Escherichia coli*	Nutrient acquisition	[16]
HBHA	*Mycobacterium tuberculosis*	Dissemination from the lung	[20]
fHbp	*Neisseria meningitides*	Host evasion	[15]

B.

	IreA	HBHA	fHbp
IreA	100%	4.8%	8.3%
HBHA		100%	16.9%
fHbp			100%

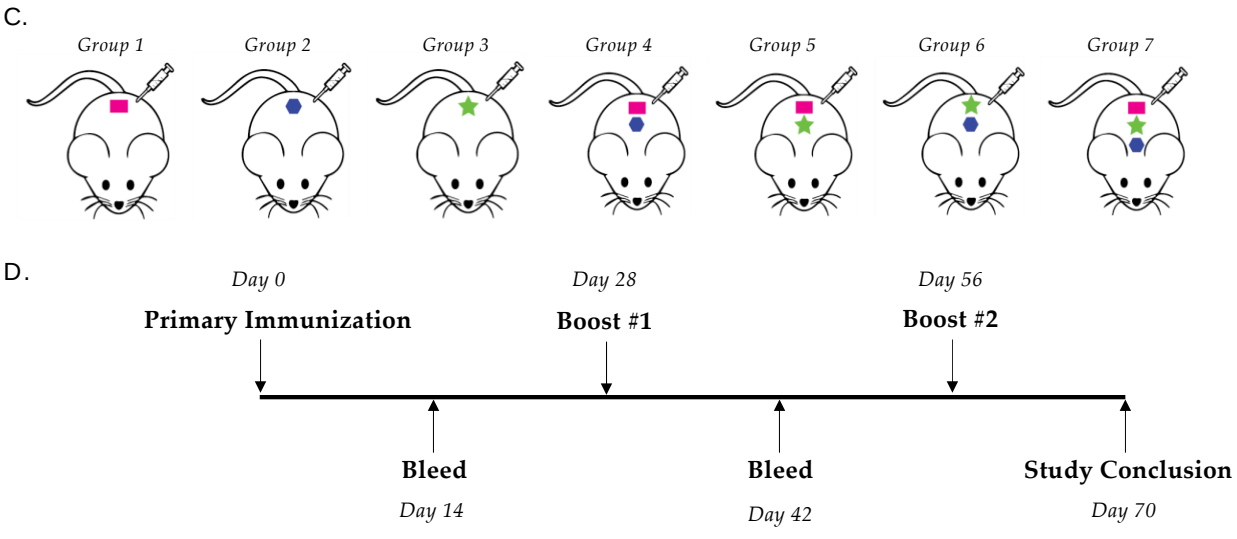

Figure 4-1. Study Design for Simultaneous Immunization with Diverse Antigens
(A) Table of antigens used for immunization in this study. Each of these antigens has been tested at least pre-clinically as a vaccine candidate against their respective native host. (B) Percent sequence identity overlap between each of the immunogens utilized. (C) Immunization schedule and antigen groups for this study denoted by colored symbols (Pink: IreA, Blue: HBHA, Green: fHbp). n=5 female BALB/c mice/group. (D) Immunization and bleed regimens used for all groups.

Antigen Immunization Combinations Elicit Comparable Antibody Titers by Study Conclusion

After completion of the described vaccination regimens with diverse antigen combinations, we sought to compare the elicitation of antigen-specific IgG antibody responses between each immunization group. We measured the serological antibody response to each individual immunogen using ELISA (**Figure 4-2A–C**) and quantified antigen-specific antibody titers (**Figure 4-2D–F**). We observed that IgG titers elicited against both IreA and HBHA were comparable by the end of the study regardless of vaccination group (**Figure 4-2A,B,D,E**). By contrast, responses to fHbp showed more

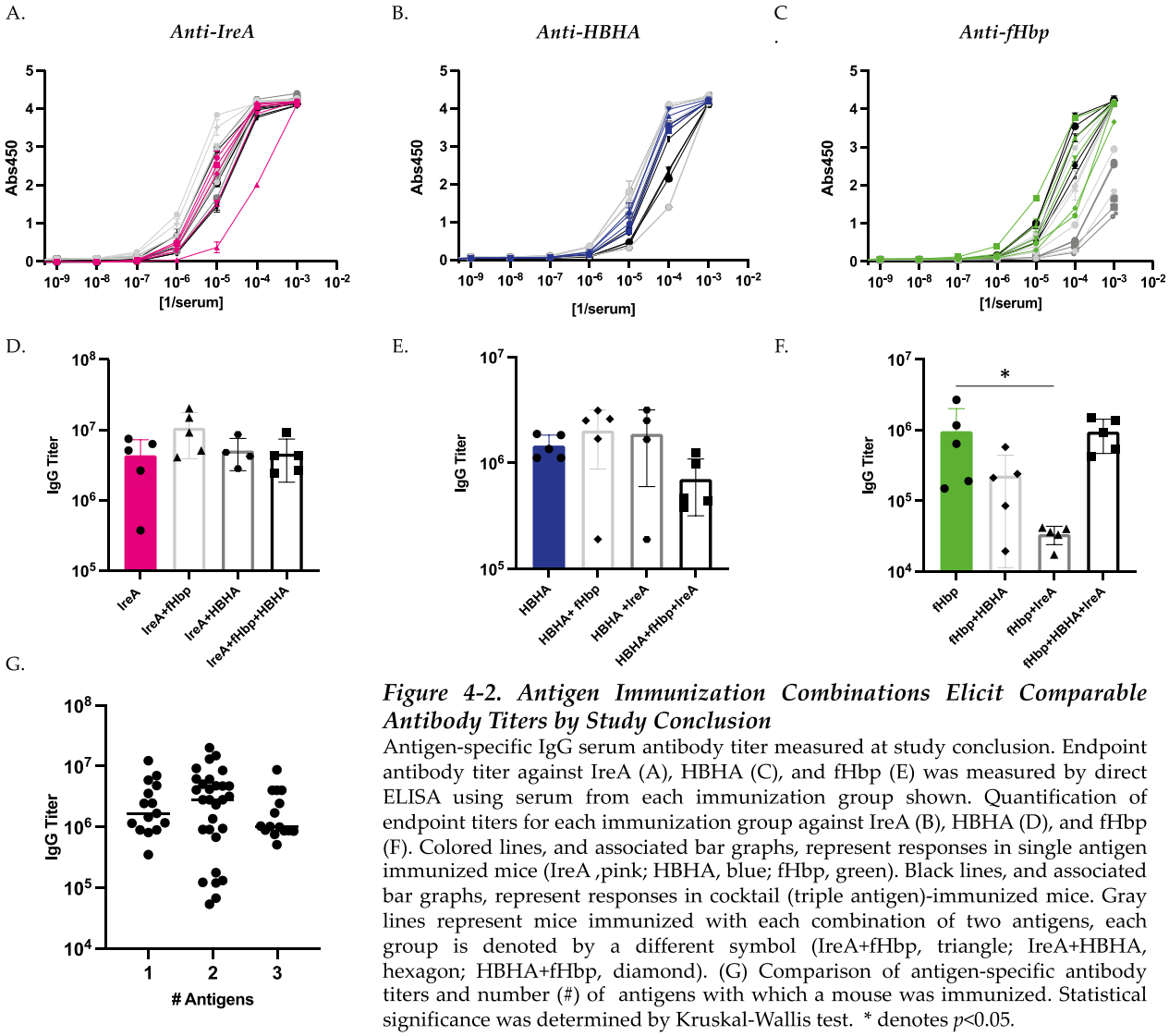

Figure 4-2. Antigen Immunization Combinations Elicit Comparable Antibody Titers by Study Conclusion

Antigen-specific IgG serum antibody titer measured at study conclusion. Endpoint antibody titer against IreA (A), HBHA (C), and fHbp (E) was measured by direct ELISA using serum from each immunization group shown. Quantification of endpoint titers for each immunization group against IreA (B), HBHA (D), and fHbp (F). Colored lines, and associated bar graphs, represent responses in single antigen immunized mice (IreA ,pink; HBHA, blue; fHbp, green). Black lines, and associated bar graphs, represent responses in cocktail (triple antigen)-immunized mice. Gray lines represent mice immunized with each combination of two antigens, each group is denoted by a different symbol (IreA+fHbp, triangle; IreA+HBHA, hexagon; HBHA+fHbp, diamond). (G) Comparison of antigen-specific antibody titers and number (#) of antigens with which a mouse was immunized. Statistical significance was determined by Kruskal-Wallis test. * denotes $p<0.05$.

variability between groups, and mice immunized with IreA+fHbp displayed significantly decreased fHbp-specific antibody titers compared to mice immunized with fHbp alone (**Figure 4-2C,F**). Overall, we did not observe a relationship between the number of antigens with which each mouse was immunized and the magnitude of the elicited antibody response, with no statistically significant correlation between immunization groups with different numbers of antigens (**Figure 4-2G**).

Vaccination Type Affects Development of Antigen-Specific Antibody Titers

After discovering comparable antigen-specific endpoint antibody titers against each individual immunogen across vaccination groups, we next sought to examine the development of this response across over time. We investigated the effect of vaccination type (single subunit vs. cocktail) on the serological antibody response to each antigen ~14 days after each immunization (**Figure 4-3**). We measured serum antibody responses against each individual immunogen using ELISA and quantified the antigen-specific antibody response elicited to each vaccination group over time (**Figure 4-3A–C**). Most mice immunized with IreA and HBHA displayed peak titer responses at day 42 (after boost #1) regardless of vaccination group (**Figure 4-3A, B**). Comparatively, we observed greater fluctuations in the fHbp-specific response between groups over time, with many mice achieving peak titers at day 70 (**Figure 4-3C**). We next compared the antigen-specific antibody titers elicited by mice immunized with a single antigen or all three antigens (cocktail-immunized) over time (**Figure 4-3D–F**). Interestingly, after primary vaccination, cocktail-immunized mice elicited more robust antibody responses against all three antigens (**Figure 4-3D–F**). Further, after boost #1 cocktail-immunized mice elicited more robust antibody responses against both IreA and fHbp, and although not statistically significant, anti-HBHA responses followed a similar trend (**Figure 4-3D–F**). In summary,

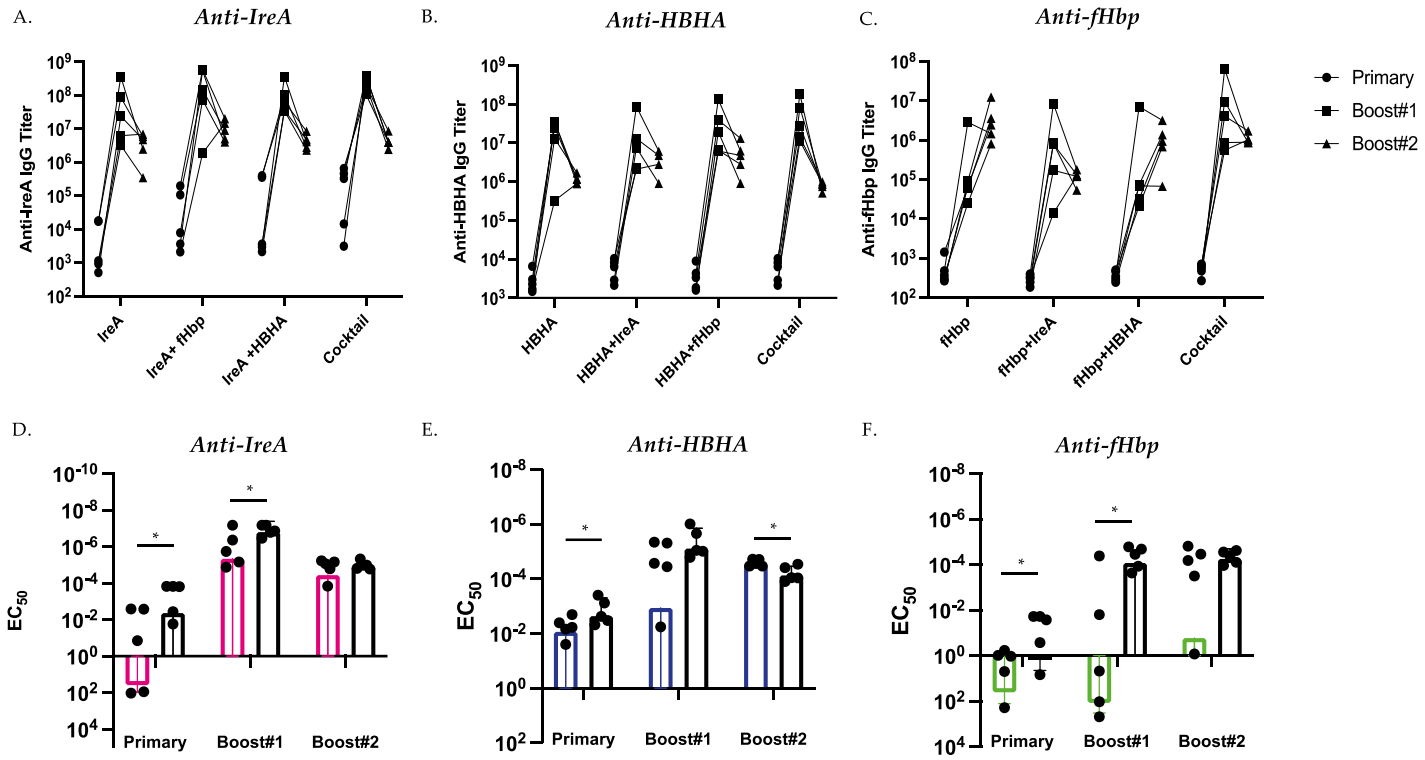

Figure 4-3. Cocktail Immunization Initially Elicits Higher Antibody Titers
Development of antigen-specific serum IgG antibody titers against IreA (A), HBHA (B), and fHbp (C) by each immunization group. Comparison of endpoint titer between single antigen (colored line)- or triple antigen (black line)-immunized mice determined by ELISA 14 days after primary immunization (left), boost #1 (middle), and boost #2 (right). (D) The EC_{50} (concentration of serum at which the half-maximal response is observed) against IreA is quantified over time for both IreA-immunized (pink line) and HBHA+fHbp+IreA-immunized (black lines). (E) The EC_{50} against HBHA is quantified over time for both HBHA-immunized (blue lines) and HBHA+fHbp+IreA-immunized (black lines). (F) The EC_{50} against fHbp is quantified over time for both fHbp-immunized (green line) and HBHA+fHbp+IreA-immunized (black lines). Statistical significance was determined by Mann-Whitney U test. * denotes $p<0.05$.

we discovered that although antigen-specific antibody titers were comparable by study conclusion, cocktail immunization initially elicited more robust antibody titers than single antigen-immunized mice.

Cocktail Immunization Alters Development of Antigen-Specific Antibody-Mediated Immunity

Although we found that antigen-specific antibody titer was not influenced by vaccination group at study conclusion, we discovered that cocktail-immunized mice initially elicited more robust serological antibody responses. In order to evaluate endpoint titer independent of timepoint, we compared the maximum antibody titer reached by mice

immunized with either a single antigen or cocktail of antigens. We observed similar maximum titers across single- and cocktail-immunized mice (**Figure 4-4A–D**). We also compared the rate of antigen-specific IgG antibody development (change in titer over time) between single antigen and cocktail-immunized mice (**Figure 4-4E–P**). When we considered the change in titer between primary immunization and boost #2 as a function of antigen specificity, we observed an increased rate of titer development against both IreA and HBHA, although there was no difference in anti-fHbp responses (**Figure 4-4E–G**). We next combined these data to evaluate the change in titer as a function of immunization group, and discovered that over the length of the study, mice immunized with a single antigen showed an increased rate of antigen-specific IgG antibody titer over cocktail (triple antigen)-immunized mice (**Figure 4-4H**). When comparing antigen-specific antibody titer development between primary vaccination and boost #1, we observed no differences between immunization groups (**Figure 4-4I–L**). Finally, between boost #1 and the study conclusion, we found that cocktail-immunized mice showed a significant decrease in antibody titer change compared to single antigen-immunized mice (**Figure 4-4M–P**). Taken together, these findings suggest that cocktail immunization initially elicited more robust antibody responses but that the change in antibody titer development of these responses tapers more quickly over time.

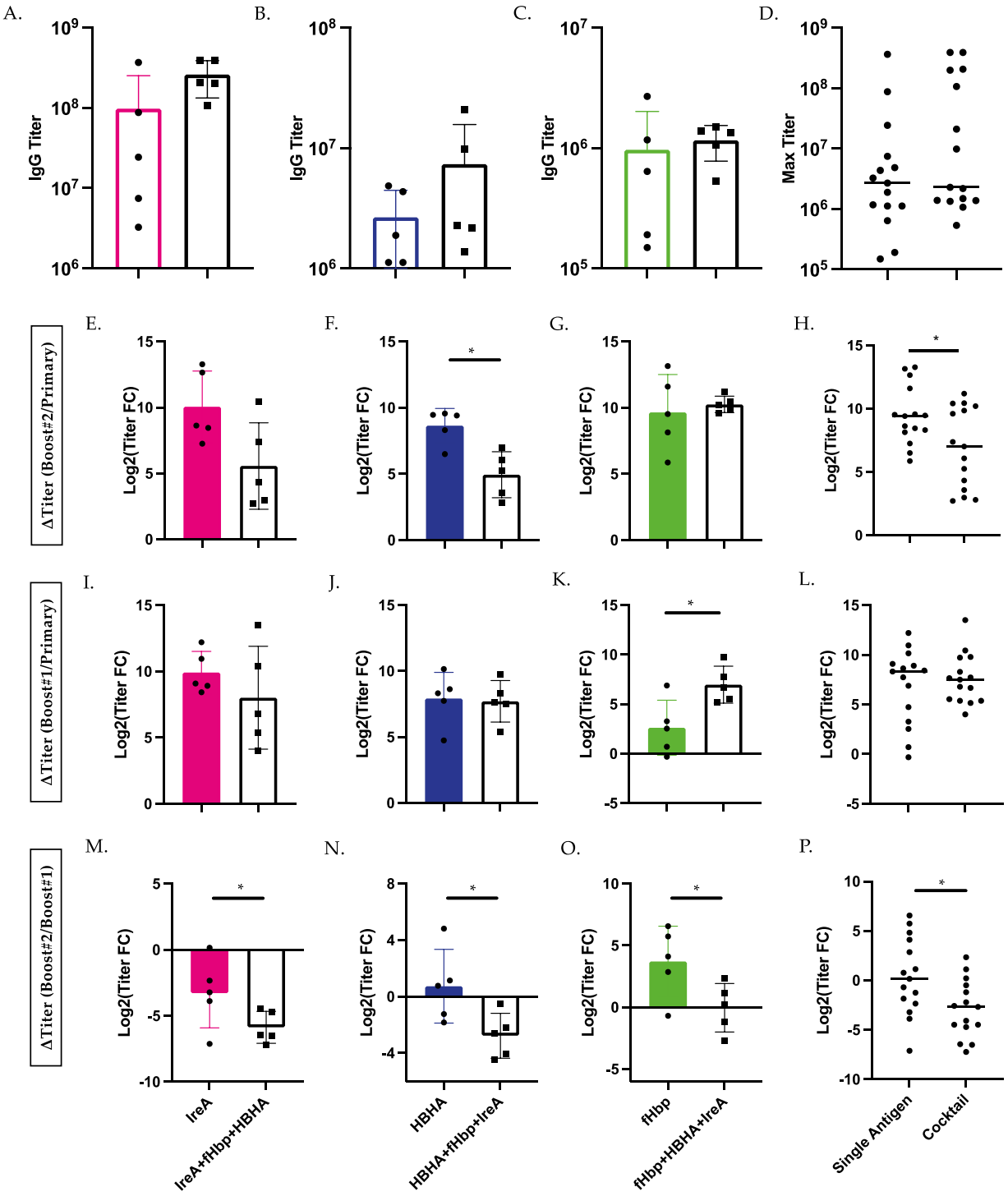

Figure 4-4. Cocktail Immunization Alters Development of Antigen-Specific Antibody-Mediated Immunity

Max endpoint serum antibody titer against IreA (A), HBHA (B), and fHbp (C) measured by ELISA in either single antigen- (color) or cocktail-immunized (IreA+fHbp+HBHA; black). Max serum antibody titer observed in all single antigen vs. cocktail-immunized mice (D). Change in serum antibody titers over the course of vaccination. Change in antibody titer between primary immunization and boost #1 (E), between boost #1 and boost #2 (I), and between primary immunization and boost #2 (M) in IreA- vs. IreA+fHbp+HBHA-immunized mice. (F, J, N) As described for IreA, observed changes in HBHA-specific antibody titers. (G, K, O) As described for HBHA, observed changes in fHbp-specific antibody titers. Change in antibody titer between primary immunization and boost #1 (H), between boost #1 and boost #2 (L), and between primary immunization and boost #2 (P) in all single antigen- vs. cocktail-immunized mice. Statistical significance was determined by Mann-Whitney U test. * denotes $p<0.05$.

DISCUSSION

Vaccines represent one of the most successful medical interventions in history, and their efficacy is dependent on the induction of a robust and long-lasting immune response, traditionally through the elicitation of neutralizing antibodies (Plotkin, 2010; Pulendran & Ahmed, 2011). Modern vaccinology strategies are often focused on the rational design of a single antigen or a cocktail of antigens to generate a more focused, protective immune response (Du et al., 2016; Kwong et al., 2011; Sanders et al., 2013; Swanson et al., 2020). In this study, we examined how simultaneous immunization with multiple diverse antigens affects the development of antigen-specific IgG antibody responses using a prime/two boost vaccination regimen in mice as a model. We discovered that primary immunization followed by two booster immunizations with different combinations of up to three soluble bacterial antigens elicited comparable endpoint antibody titers by study conclusion (day 70). However, after prime and boost #1, mice vaccinated with all three antigens elicited significantly higher antigen-specific IgG antibody responses than mice immunized with a single antigen, while double antigen-immunized mice displayed an intermediate phenotype. When we compared the fold change in antigen-specific IgG antibodies over the course of the study, we found that single antigen-immunized mice showed an in-creased rate of antibody development over triple antigen-immunized mice. Finally, we observed that this difference could largely be traced to a significant decrease in antibody titers between booster immunizations #1 and #2 in triple antigen-immunized compared to single antigen-immunized mice.

Our observations described here, along with previous studies, suggest that cocktail administration of subunit immunogens alters the development of antigen-specific

antibody responses (Galli et al., 2013). Specifically, our results imply that immunization with multiple diverse antigens provides an initial boost to the immune response, and this strategy could be used to quickly elicit high IgG antibody titers against several immunogens. Multiple processes could explain these findings, including that immune exposure to increased antigenic diversity, in this case via cocktail immunization, recruits a greater heterogeneity of immune cells, leading to the formation of more robust germinal center reactions and class-switched antibody responses. By contrast, it could be that cocktail immunization elicits more cross-reactive and polyreactive antibodies, engendering higher apparent titers. However, to elucidate the mechanisms behind our observations, it will be important for future studies to investigate markers of immune activation, induction of memory cells and hallmark cytokines. Moreover, what effect this has on long-term immunological memory and recall in the context of human vaccination will need to be further examined.

Finally, we note several limitations to our study that may have influenced our observations, including the usage of all female mice, one mouse strain (BALB/c), and inconsistent total immunization mass between groups. This investigation was designed such that each mouse group received the same quantity of each unique antigen, although this means that cocktail-immunized mice received the greatest total antigen mass, which could indeed account for the high antibody titers elicited by this group. Nonetheless, we discovered that mice in groups 5 and 6 (IreA+fHbp, HBHA+fHbp) elicited lower endpoint antibody titers against fHbp than mice immunized with fHbp alone, despite being vaccinated with a larger total protein mass. These data suggest that our results cannot solely be explained by total vaccine antigen mass and could indeed be influenced by immunodominance or antigen-specific factors.

In summary, we observed that immunization with multiple diverse bacterial antigens initially induces more robust IgG antibody responses, but that this response wanes more quickly over time, compared with single antigen-immunized mice. Investigating the effect of antigenic properties and formulations on vaccination response, such as those described in this study, contributes both to our basic understanding of factors governing the development of antigen-specific immunity, as well as serves to inform future immunization regimens.

MATERIALS AND METHODS

Antigen Expression and Purification

The gene encoding the bacterial antigen HBHA (GenBank: AAC26052.1) was synthesized by Genscript (Genscript, NJ, USA) and cloned in the pET9a bacterial expression vector. The gene encoding a rationally designed fHbp construct with a 6X HisTag was synthesized by Genscript and cloned in the pET9a bacterial expression vector (Scarselli et al., 2011). The pET30b+ plasmid containing the gene for HisTagged-IreA was a gift from Harry T. Mobley (University of Michigan) (Alteri et al., 2009).

For protein expression, plasmids described above were transformed into the appropriate E. coli strains and cultured in Luria Broth with 50 µg/mL Kanamycin (+25 µg/mL chloramphenicol for BL21 (DE3) pLysS cell culture). Recombinant protein expression from pET9a was induced in Rosetta (DE3) cells at OD600 = 0.6 with the addition of 1 M isopropyl β-D-1-thiogalactopyranoside (IPTG) (added to a final concentration of 1 mM) for 6 h at 37 °C with shaking. Recombinant protein expression from pET30b+ was induced in BL21 (DE3) pLysS cells at OD600 = 0.8 with the addition of 1 M isopropyl β-D-1-thiogalactopyranoside (IPTG) (added to a final concentration of 1 mM) for 6 h at 37 °C with shaking.

Induced cultures were harvested by centrifugation (8000× g, 4 °C, 20 min) and pellets frozen at −80 °C overnight. Pellets were then thawed on ice and resuspended in 5 mL/g pellet weight with the appropriate binding buffer (+EDTA-free protease-inhibitor (Roche)) before lysis by 6 × 30 s rounds of sonication. Lysate was cleared by centrifugation (10,000× g, 4 °C, 20 min) and filtered using a 0.22 µm PES filter before protein purification.

Purification of HBHA: Pellets containing HBHA expressed from pET9a were re-suspended in binding buffer (10 mM sodium phosphate, pH = 7) and lysate prepared as described above. HBHA was purified by multiple rounds of heparin affinity purification using an equilibrated 5 mL pre-packed Heparin HiTrap HP column (GE Healthcare, IL, USA). The column was washed with 10 column volumes (CV) of binding buffer, and purified protein was eluted from the column with a 25 mL gradient into binding buffer +2 M NaCl, pH = 7.

Purification of fHbp: Pellets containing fHbp expressed from pET9a were resus-pended in binding buffer (20 mM sodium phosphate, 0.5 M NaCl, 10 mM imidazole, pH 7.4) and lysate prepared as described above. fHbp was purified by nickel affinity chromatography using an equilibrated, 5 mL pre-packed HisTrap HP column (GE Healthcare, IL, USA). The column was washed with 10 CV of binding buffer, and purified protein was eluted from the column with a 25 mL gradient into binding buffer +0.5 M Imidazole, pH = 7.4.

Purification of IreA: Pellets containing IreA expressed from pET30b+ were resus-pended in denaturing binding buffer (20 mM Tris-Cl, 0.5 M NaCl, 10 mM imidazole, 6 M guanidine-HCl, 1 mM β-mercaptoethanol, 1% Triton X-100, pH 8), and allowed to incubate with stirring for 1 h, before clearing the lysate as described above. IreA was purified using an equilibrated, 5 mL pre-packed HisTrap HP column (GE Healthcare, IL,

USA). The column was washed with 10 CV wash buffer (20 mM Tris-Cl, 0.5 M NaCl, 10 mM imidazole, 6 M Urea, 1 mM β-mercaptoethanol, 1% Triton X-100, pH = 8), before on-column protein re-folding using a 50 mL gradient into renaturation buffer (20 mM Tris-Cl, 0.5 M NaCl, 10 mM imidazole, 1 mM BME, 1% Triton X-100, pH = 8). Finally, purified protein was eluted from the column with a 25 mL gradient into 20 mM Tris-Cl, 0.5 M NaCl, 0.5 M imidazole, 1 mM BME, 0.05% Triton X-100, pH = 8.

All purified recombinant proteins were buffer-exchanged 5X into sterile phosphate-buffered saline (PBS), and their concentrations determined by BCA assay (Pierce, MA, USA).

Vaccination

Six- to eight-week-old female BALB/c mice (n = 5/group) were used for these studies, and animals were ≤15 weeks old at study conclusion. All procedures were conducted according to protocols approved by Institutional Animal Care and Use Committee at Vanderbilt University Medical Center.

Purified protein combinations were diluted in sterile PBS and emulsified 1:1 in TiterMax Gold (Sigma-Aldrich, MO, USA) for intraperitoneal injection. Isoflurane-anaesthetized mice were immunized on day 0 and received booster injections on days 28 and 56 with either 267pmol of each antigen alone, each combination of two antigens, or all three antigens according to vaccination group (see table 1 below). Blood was collected 14 days after each immunization (days 14, 42, and 70) by submandibular puncture. At study conclusion, mice were sacrificed by CO2 overdose and cardiac puncture exsanguination. Blood was allowed to clot at room temperature and serum separated by centrifugation (10,000× g, 4 °C, 10 min). Serum was transferred to a new tube and stored at −80 °C until use.

Antigen	Group	1	2	3	4	5	6	7
IreA		20			20	20		20
HBHA			5.9		5.9		5.9	5.9
fHbp				7.4		7.4	7.4	7.4
	Total (μg)	20	5.9	7.4	25.9	27.4	13.3	33.3

Table 1. Total Immunization Mass Varies Between Groups
Mass of each antigen utilized for immunization across groups such that ~267pmol of each unique antigen is administered per relevant group. Total immunization mass differs across groups.

Enzyme-Linked Immunosorbent Assay (ELISA)

For indirect serum Enzyme-linked Immunosorbent Assay (ELISA), Immulon 2HB plates (Nunc) were coated with 2 μg/mL of purified recombinant antigen diluted in PBS overnight at 4 °C. Excess antigen was removed with 3X wash with PBS+ 0.05% Tween-20 (PBS-T). This washing step was repeated after each subsequent incubation step. Non-specific binding was blocked with 5% non-fat dried milk (NFDM) in PBS for 1 h at 37 °C, followed by washing. Hyperimmune sera was serially diluted in 1% NFDM in PBS-T, added to wells, and incubated for 1 h at 37 °C. Plates were washed, and incubated with anti-mouse IgG-HRP diluted 1:10,000 in 1% NFDM in PBS-T for 1 h at 37 °C. After washing, plates were developed with 3,3′,5,5′-Tetramethylbenzidine for 10 min in the dark, reaction stopped with 1N sulfuric acid, and absorbance read at 450 nm. All ELISA data shown and used for calculations was blank subtracted. Endpoint dilution titer was defined as the serum dilution at which binding reached the lower limit of detection (OD450 = 0.1).

Statistical Analysis

All graphing and statistical analyses were done using GraphPad Prism 9. Significance between all immunization groups was determined using Kruskal–Wallis test (with Dunn's test for multiple comparisons). Significance between pairwise combinations of immunization groups was determined by Mann–Whitney U test. ELISA antibody endpoint titers were determined by interpolating a standard curve using GraphPad Prism 9. Half maximal effective concentrations (EC50) were determined by interpolating a standard curve using GraphPad Prism 9. All statistics were conducted using 95% confidence intervals where applicable.

Chapter 5: Conclusions and Future Directions

Summary

Vaccination is the most effective human medical intervention in history, saving an estimated 100 million lives worldwide in 2000-2019 alone (Toor et al., 2021). Although traditional vaccine strategies have utilized live-attenuated or inactivated versions of the pathogen, this approach has fallen short of generating effective vaccines against modern emerging, and highly mutable pathogens. Advancements in high-throughput antibody discovery, next-generation sequencing, and structural characterization technologies have enabled the contemporary era of vaccinology, often referred to as Reverse Vaccinology 2.0 (Moxon et al.; Rappuoli et al.; Sette & Rappuoli). Modern strategies aim to identify protective epitopes and correlates of immunity from natural infection or vaccination models to inform the rational design of immunogens that elicit sterilizing immunity against previously indomitable pathogens. In this dissertation, I sought to apply recent advancements in antigen-specific B cell sorting and analysis towards the rational design of protective vaccines or antibody therapeutics against Human Immunodeficiency Virus (HIV-1), Hepatitis C Virus (HCV), and *Staphylococcus aureus*.

CONCLUSIONS

First, I investigated the antibody repertoire of a chronically HIV-1/HCV co-infected individual using LIBRA-seq, a technology that enables the simultaneous screening of B cells against a diverse library of antigen targets. I describe the application of LIBRA-seq to discover hundreds of HIV-1 envelope- and HCV envelope-specific BCR sequences from a chronic HIV-1/HCV co-infection sample. Notably, I also discovered five, genetically unique BCR sequences that were positive for at least one HIV-1 and at least 1 HCV

envelope antigen predicted by LIBRA-seq score. I recombinantly expressed and purified these five antibodies (mAb180, mAb692, mAb688, mAb803, mAbKP1-8) and confirmed their HIV-1/HCV cross-reactive binding phenotype by ELISA. Interestingly, I found that three of the five antibodies cross reacted with epitopes on the gp120 subunit of HIV-1 envelope and the E2 subunit of the HCV envelope (mAb688, mAb803, mAbKP1-8), while the remaining two antibodies cross-reacted with epitopes on the gp41 subunit of the HIV-1 envelope and the E2 subunit of the HCV envelope (mAb180, mAb692). Additionally, I found that mAb688 recognized a mannose-dependent glycan region on the highly glycosylated viral subunits. Further glycan microarray analysis mapped mAb688 binding to immature glycans. Notably, all five antibodies showed exceptional HCV neutralization breadth, as well as diverse IgG effector functions against both HIV-1 and HCV. One of these antibodies, mAb688, also cross-reacted with antigens from influenza and diverse coronaviruses, including SARS-CoV-2. Cross-reactive antibodies provide an intriguing new direction for therapeutic and vaccine development against current and emerging infectious diseases.

Next, I designed and tested vaccines targeting metal acquisition against *S. aureus*. In this effort, I chose, designed and tested novel *S. aureus* immunogens in a BALB/c mouse model and assessed immunogenicity and *S. aureus* killing by blood from immunized animals. I found that all antigens elicited robust IgG antibody responses when they were administered as a cocktail. Notably, *S. aureus* killing assays revealed that the six-antigen combination targeting iron, zinc, and manganese acquisition reduced *S. aureus* significantly more than control groups. Further, the vaccine targeting multiple metal acquisition pathways reduced *S. aureus* survival equally well without complement. This is in contrast to the vaccine that included only iron-acquisition antigens, which

reduced *S. aureu*s survival at levels equal to mock-immunized mice when complement was inactivated. Together these data suggest targeting metal acquisition pathways could represent an effective strategy for the design of a protective *S. aureus* vaccine.

Finally, I sought to characterize the effect of cocktail vaccination on the individual immunogenicity of surface-accessible antigens from uropathogenic *Escherichia coli*, *Mycobacterium tuberculosis*, and *Neisseria meningitides* (IreA, HBHA, fHbp). In this study, I immunized BALB/c mice with equimolar quantities of either all three diverse immunogens, each unique combination of two, or each immunogen alone, and monitored the development of antigen-specific IgG antibodies. I found that although antigen-specific endpoint antibody titers were comparable across immunization groups by study conclusion (day 70), cocktail-immunized mice initially elicited more robust antibody responses. Further, I discovered that single antigen-immunized mice showed an increased rate of IgG antibody development over triple antigen-immunized mice and that this difference could largely be traced to a significant decrease in antibody titers between booster immunizations #1 and #2 in triple antigen-immunized compared to single antigen-immunized mice. Investigating the basic properties that govern the development of antigen-specific antibody responses will help inform the design of future combination immunization regimens.

FUTURE DIRECTIONS

Development of HIV-1/HCV cross-reactive vaccines and therapeutics

Chapter 2 details the discovery and characterization of the first HIV-1/HCV cross-reactive antibodies using LIBRA-seq. Further investigation will be needed to determine whether these antibodies can be used therapeutically or to design cross-reactive vaccine

candidates. We discovered these antibodies in a single HIV-1/HCV co-infected donor, and whether these antibody specificities require co-infection, are common, or difficult to elicit, will require additional study. To begin to test this, I propose to use LIBRA-seq to profile a cohort of both HIV-1/HCV co-infected, as well as HIV-1 and HCV mono-infected, donors to assess the relative frequency and requirements for developing HIV-1/HCV cross-reactive specificity. Moreover, whether the order of infection (HIV-1 or HCV first) influences the development of antigen-specific antibodies will need to be studied. It will be important to investigate how infection or administration with HIV-1 before HCV, vice versa, or HIV-1/HCV simultaneously, affects the development of antigen-specific immunity using LIBRA-seq. Further, it will be critical to examine whether these antibodies could be elicited by vaccination. To this end, I propose to immunize humanized mice with different combinations of HIV-1 envelope and HCV envelope proteins and analyze the development of HIV-1/HCV cross-reactive antibodies. Beyond informing the design of novel vaccines, these antibodies could be used as therapeutic candidates themselves. Antibody therapeutics have shown significant promise in both preventing and treating HIV-1 and HCV infections. There are unfortunately no animal models of HIV-1/HCV co-infection but examining protection in mono-infection models would provide critical data. Notably, we have already tested the ability of glycan-reactive mAb688 to treat influenza A infection in mice and found that mAb688 had no effect on protection or mouse pathology.

Multispecific antibodies for highly mutable viruses

Antibodies are often utilized for their incredible specificity, though polyreactive or non-specific antibodies are also found. The description of HIV-1/HCV cross-reactive antibodies in Chapter 2, highlights the potential for an intermediate, multispecific, binding

phenotype. Multi-specific binding is distinct, in that these antibodies can recognize multiple targets (HIV-1, HCV), without displaying typical signs of polyreactivity, or promiscuous binding. These observations prompt multiple outstanding questions, particularly about antibodies mAbKP1-8 and mAb803. Although we know these antibodies recognize epitopes on both HIV-1 gp120 (CD4-induced), HCV E2 (overlapping CD81 binding site), further epitope mapping will be needed to define mechanisms of this mode of binding. For example, I propose to map the epitopes targeted by these antibodies with single-residue resolution on both HIV-1 and HCV. We can then compare the epitopes targeted on each viral envelope to assess how sequence and structural homology affect the mechanism of this HIV-1/HCV multi-specific binding. Further, I propose to generate antibody paratope mutants of mAb803 and mAbKP1-8 to determine which mutations or sequences are important for recognition of HIV-1 vs. HCV.

Antibody mAb688 also demonstrated unique binding patterns, where it recognized multiple viral envelope antigens, but did not show reactivity to a panel of unrelated autoantigens. Notably, de-glycosylation and mannose-inhibition experiments never completely abrogated mAb688 binding to HIV-1 and HCV envelope. It is of course possible this observation was due to incomplete glycan removal or inhibition, but pursuing structural studies with mAb688 could provide critical information about protein vs. glycan contacts made at the epitope:paratope interface. This surprising discovery also prompts further study to examine whether mAb688 could be used to design broadly antiviral vaccines or therapeutics. For example, we could engineer viral immunogens that are enriched for the immature, hybrid type glycans recognized by mAb688, and assess both whether mAb688-like antibodies can be elicited and further examine the extent to which these immunogens induce cross-protective immunity.

Harnessing polyreactive antibodies for good

Polyreactive, or promiscuous antibodies can sometimes provide a selective advantage in the fight against highly mutable pathogens. However, factors contributing to their elicitation-including how they break develop to break immune tolerance- remain incompletely understood. This is particularly highlighted by our discovery of mAb180 and mAb692 in Chapter 2. These antibodies demonstrated typical traits of polyreactivity, but are also cross-functional, prompting the investigation of how these antibodies might influence infection or pathology *in vivo*. In **figure 2-11**, we showed that mAb180 and mAb692 acquire mutations that establish or enhance cross-reactive binding to HIV-1 envelope vs. HCV envelope. However, polyreactivity was only measured in the mature antibodies. It will be important to measure the polyreactivity of the germline-reversion and antibody paratope mutants to assess whether (and how) polyreactivity is introduced by SHM. We could then detangle antibody mutations required for antigen binding vs. polyreactivity to engineer antibodies with more desirable effects.

More generally, it will be important for future vaccination or therapeutic strategies to consider how to engage, or avoid, the auto/polyreactive repertoire. Studies of the poly/autoreactive repertoire has largely been limited to autoimmune diseases, but a detailed investigation of the healthy human repertoire is lacking. To this end, I propose to profile the human auto/polyreactive B cell repertoire before and after infection or vaccination (e.g. with HIV-1) to trace the activation of pre-existing polyreactive B cells by infectious agent or immunogen. Specifically, I would use an approach described in the subsequent section (LIBRA-seq with antigen discovery) to accomplish these studies.

Extended applications of LIBRA-seq

*Ligand-blocking (*LIBRA-seq with ligand blocking)

The experiments and discoveries described in Chapter 2 highlight the utility and power of LIBRA-seq to identify rare, antigen-specific antibodies from diverse repertoires. However, in some antibody discovery efforts, it is important to identify functional (as opposed to binding-only) antibodies, and in many cases the function of interest could be the identification of antibodies that can block antigen interactions with its cognate ligand. For example, HCV neutralizing antibodies often function by blocking HCV envelope interaction with its receptor CD81. By adding CD81 (or other receptors) to the LIBRA-seq workflow, I hypothesize we will preferentially identify neutralizing antibodies. In proof-of-concept experiments, I used oligo-labeled HIV-1 envelope protein and oligo-labeled CD4 protein to identify CD4 binding-site-specific antibody sequences, as well as oligo-labeled HCV envelope protein and oligo-labeled CD81 protein to identify CD81 binding site-specific antibody sequences from HIV-1- and HIV-1/HCV co-infected donor samples. We are still working on the bioinformatic analysis of these samples.

Paired antibody-antigen discovery (LIBRA-seq with antigen discovery)

As previously discussed, LIBRA-seq enables high throughput antigen specificity mapping of the BCR repertoire by leveraging individually expressed, DNA-barcoded soluble antigens and next generation sequencing. Individually expressing, purifying, and barcoding antigens for these experiments is time consuming, biases the data, and requires prior knowledge of the sample reactivities. To expand the capacity of LIBRA-seq, I have designed an approach that leverages advances in high-throughput screening

techniques (yeast, phage, ribosome display) to enable discovery of both BCR and its respective antigen sequences for tens of thousands of B cells.

Specifically, I propose to adapt a recently described technology that involves the molecular indexing of self-assembled proteins (MIPSA; Credle et al., Biorxiv, 2021), for the simultaneous discovery of both antigen and antibody sequences. Briefly, a plasmid library encoding full length proteins associated with a unique barcode sequence will be linearized and transcribed in vitro. The N-terminus of the RNA library is then reverse transcribed using a HaloLigand-tagged primer, which recognizes the HaloTag translated along with each full-length protein. Each unique cDNA barcode is attached to its associated full-length protein via this HaloTag-HaloLigand interaction and allows for high throughput protein identification by sequencing. Staining human PBMCs with the DNA-barcoded library will enable the unbiased identification of tens of thousands of B cell receptor sequences along with their cognate antigen specificities. Development of this technology would enable us to ask unprecedented, essential questions about human immunity.

Fine mapping of *S. aureus* vaccine-induced immunity

Chapter 3 describes the design and application of a *S. aureus* vaccine targeting metal acquisition. We found that mice immunized with antigens targeting iron, zinc, and manganese more effectively killed *S. aureus* than all other groups, but there is much left to learn about how this observation contributes to protection from live infection. We found that immunization with all metal antigens was superior to immunization with all iron antigens, but there are several mechanisms that could explain this difference. I propose to examine *S. aureus* survival in the presence of vaccine-induced sera to determine the direct effect of antibody binding (in the absence of other blood components) on *S. aureus*

survival. Further, we could measure if and how *S. aureus* upregulates metal starvation pathways by qPCR. Interestingly, I found no correlation between antibody titers against a single antigen and *S. aureus* killing, suggesting it is the cooperation of immune responses to the cocktail that provides enhanced killing. Immunizing animals with larger antigen cocktails could provide increasingly better protection and future studies could consider including additional metal acquisition antigens.

All of the experiments described in Chapter 3 involved the characterization of serological antibody responses. However, splenocytes were also collected from each of these animals in pursuit of characterizing the B cell response to these vaccination strategies. Although each immunogen used in this study was sequentially distinct, they perform similar functions and could therefore potentially elicit cross-reactive antibodies to structurally homologous regions. To investigate antigen-specificity and differences in cross-reactivity elicited by each vaccine, I would use flow cytometry and LIBRA-seq with barcoded metal acquisition antigens. Further, these experiments would enable the identification of monoclonal antibodies recognizing the novel metal acquisition antigens we utilized in the study, which could be characterized as therapeutics themselves. Together, these experiments would contribute towards the development of a sorely needed *S. aureus* vaccine.

Maximizing antigen-specific antibody responses with antigen cocktails

Chapter 4 describes our observation that simultaneous immunization with multiple diverse antigens (cocktail immunization) alters the development and maintenance of antigen-specific antibodies. However, we only investigated the serological IgG response, leaving many outstanding questions. Specifically, it will be important to examine how the serological IgM and B cell responses are affected by vaccination strategy, and how each

of these immune markers correlates with protection from infection. Next, our study used a maximum of three antigens in the cocktail vaccine group, but whether the antigen-specific IgG response would increase linearly as the number of antigens in the cocktail remains to be studied. Notably, in Chapter 3 we also observed that the administration of SstD as a four-antigen and six-antigen cocktail significantly increased the SstD-specific IgG response over injection with SstD alone. These data support the theory that more antigens correlates with a more robust antibody response, though there is likely a maximum number of antigens at which the immune response plateaus. Further, we discovered that cocktail-immunized mice displayed a more rapid decay in serum antibody titers compared to single antigen-immunized mice. It will be interesting to examine the effect of cocktail vaccination on the memory and recall response to each of these antigens. Investigating the effect of antigenic combinations on vaccination-induced responses is critical to engineer the optimal immune responses and inform future immunization regimens.

REFERENCES

Allen, D., Cumano, A., Dildrop, R., Kocks, C., Rajewsky, K., Rajewsky, N., Roes, J., Sablitzky, F., & Siekevitz, M. (1987, Apr). Timing, genetic requirements and functional consequences of somatic hypermutation during B-cell development. *Immunol Rev, 96*, 5-22. https://doi.org/10.1111/j.1600-065x.1987.tb00506.x

Allman, D., Wilmore, J. R., & Gaudette, B. T. (2019). The continuing story of T-cell independent antibodies. *Immunological Reviews, 288*(1), 128-135. https://doi.org/10.1111/imr.12754

Alteri, C. J., Hagan, E. C., Sivick, K. E., Smith, S. N., & Mobley, H. L. (2009, Sep). Mucosal immunization with iron receptor antigens protects against urinary tract infection. *PLoS Pathog, 5*(9), e1000586. https://doi.org/10.1371/journal.ppat.1000586

Amanna, I. J., & Slifka, M. K. (2011, 2011/03/15/). Contributions of humoral and cellular immunity to vaccine-induced protection in humans. *Virology, 411*(2), 206-215. https://doi.org/https://doi.org/10.1016/j.virol.2010.12.016

Andreano, E., D'Oro, U., Rappuoli, R., & Finco, O. (2019). Vaccine Evolution and Its Application to Fight Modern Threats. *Front Immunol, 10*, 1722. https://doi.org/10.3389/fimmu.2019.01722

Ansari, S., Jha, R. K., Mishra, S. K., Tiwari, B. R., & Asaad, A. M. (2019). Recent advances in Staphylococcus aureus infection: focus on vaccine development. *Infection and drug resistance, 12*, 1243-1255. https://doi.org/10.2147/IDR.S175014

Astronomo, R. D., Santra, S., Ballweber-Fleming, L., Westerberg, K. G., Mach, L., Hensley-McBain, T., Sutherland, L., Mildenberg, B., Morton, G., Yates, N. L., Mize, G. J., Pollara, J., Hladik, F., Ochsenbauer, C., Denny, T. N., Warrier, R., Rerks-Ngarm, S., Pitisuttithum, P., Nitayapan, S., Kaewkungwal, J., Ferrari, G., Shaw, G. M., Xia, S.-M., Liao, H.-X., Montefiori, D. C., Tomaras, G. D., Haynes, B. F., &

McElrath, M. J. (2016, 2016/12/01/). Neutralization Takes Precedence Over IgG or IgA Isotype-related Functions in Mucosal HIV-1 Antibody-mediated Protection. *EBioMedicine, 14*, 97-111. https://doi.org/https://doi.org/10.1016/j.ebiom.2016.11.024

Bachmann, M. F., & Zinkernagel, R. M. (1997). NEUTRALIZING ANTIVIRAL B CELL RESPONSES. *Annual Review of Immunology, 15*(1), 235-270. https://doi.org/10.1146/annurev.immunol.15.1.235

Bagnoli, F., Bertholet, S., & Grandi, G. (2012, 2012-February-22). Inferring Reasons for the Failure of Staphylococcus aureus Vaccines in Clinical Trials [Opinion]. *Frontiers in Cellular and Infection Microbiology, 2*. https://doi.org/10.3389/fcimb.2012.00016

Bailey, J. R., Flyak, A. I., Cohen, V. J., Li, H., Wasilewski, L. N., Snider, A. E., Wang, S., Learn, G. H., Kose, N., Loerinc, L., Lampley, R., Cox, A. L., Pfaff, J. M., Doranz, B. J., Shaw, G. M., Ray, S. C., & Crowe, J. E. (2017). Broadly neutralizing antibodies with few somatic mutations and hepatitis C virus clearance. *JCI Insight, 2*. https://doi.org/10.1172/jci.insight.92872

Balazs, A. B., Chen, J., Hong, C. M., Rao, D. S., Yang, L., & Baltimore, D. (2012, Jan 5). Antibody-based protection against HIV infection by vectored immunoprophylaxis [Research Support, N.I.H., Extramural

Research Support, Non-U.S. Gov't]. *Nature, 481*(7379), 81-84. https://doi.org/10.1038/nature10660

Beasley, F. C., Marolda, C. L., Cheung, J., Buac, S., & Heinrichs, D. E. (2011, Jun). Staphylococcus aureus transporters Hts, Sir, and Sst capture iron liberated from human transferrin by Staphyloferrin A, Staphyloferrin B, and catecholamine stress hormones, respectively, and contribute to virulence. *Infect Immun, 79*(6), 2345-2355. https://doi.org/10.1128/IAI.00117-11

Begier, E., Seiden, D. J., Patton, M., Zito, E., Severs, J., Cooper, D., Eiden, J., Gruber, W. C., Jansen, K. U., Anderson, A. S., & Gurtman, A. (2017, 2017/02/22/). SA4Ag, a 4-antigen Staphylococcus aureus vaccine, rapidly induces high levels of bacteria-killing antibodies. *Vaccine, 35*(8), 1132-1139. https://doi.org/https://doi.org/10.1016/j.vaccine.2017.01.024

Blattner, F. R., & Tucker, P. W. (1984, 1984/02/01). The molecular biology of immunoglobulin D. *Nature, 307*(5950), 417-422. https://doi.org/10.1038/307417a0

Breitfeld, D., Ohl, L., Kremmer, E., Ellwart, J., Sallusto, F., Lipp, M., & Förster, R. (2000). Follicular B Helper T Cells Express Cxc Chemokine Receptor 5, Localize to B Cell Follicles, and Support Immunoglobulin Production. *Journal of Experimental Medicine, 192*(11), 1545-1552. https://doi.org/10.1084/jem.192.11.1545

Bricault, C. A., Yusim, K., Seaman, M. S., Yoon, H., Theiler, J., Giorgi, E. E., Wagh, K., Theiler, M., Hraber, P., Macke, J. P., Kreider, E. F., Learn, G. H., Hahn, B. H., Scheid, J. F., Kovacs, J. M., Shields, J. L., Lavine, C. L., Ghantous, F., Rist, M., Bayne, M. G., Neubauer, G. H., McMahan, K., Peng, H., Chéneau, C., Jones, J. J., Zeng, J., Ochsenbauer, C., Nkolola, J. P., Stephenson, K. E., Chen, B., Gnanakaran, S., Bonsignori, M., Williams, L. D., Haynes, B. F., Doria-Rose, N., Mascola, J. R., Montefiori, D. C., Barouch, D. H., & Korber, B. (2019). HIV-1 Neutralizing Antibody Signatures and Application to Epitope-Targeted Vaccine Design. *Cell Host Microbe, 25*(1), 59-72.e58. https://doi.org/10.1016/j.chom.2018.12.001

Broughan, J., Anderson, R., & Anderson, A. S. (2011, 2011/05/01). Strategies for and advances in the development of Staphylococcus aureus prophylactic vaccines. *Expert Rev Vaccines, 10*(5), 695-708. https://doi.org/10.1586/erv.11.54

Buchacher, A., Predl, R., Strutzenberger, K., Steinfellner, W., Trkola, A., Purtscher, M., Gruber, G., Tauer, C., Steindl, F., Jungbauer, A., & et al. (1994, Apr). Generation of human monoclonal antibodies against HIV-1 proteins; electrofusion and Epstein-Barr virus transformation for peripheral blood lymphocyte immortalization.

AIDS Res Hum Retroviruses, 10(4), 359-369. https://doi.org/10.1089/aid.1994.10.359

Burke, K. P., & Cox, A. L. (2010, Jul). Hepatitis C virus evasion of adaptive immune responses: a model for viral persistence. *Immunol Res, 47*(1-3), 216-227. https://doi.org/10.1007/s12026-009-8152-3

Burton, D. R. (1985, 1985/03/01/). Immunoglobulin G: Functional sites. *Molecular Immunology, 22*(3), 161-206. https://doi.org/https://doi.org/10.1016/0161-5890(85)90151-8

Burton, D. R. (2010, Oct 19). Scaffolding to build a rational vaccine design strategy. *Proc Natl Acad Sci U S A, 107*(42), 17859-17860. https://doi.org/10.1073/pnas.1012923107

Cassat, J. E., & Skaar, E. P. (2012, 2012/03/01). Metal ion acquisition in Staphylococcus aureus: overcoming nutritional immunity. *Seminars in Immunopathology, 34*(2), 215-235. https://doi.org/10.1007/s00281-011-0294-4

Chaplin, D. D. (2010, Feb). Overview of the immune response. *J Allergy Clin Immunol, 125*(2 Suppl 2), S3-23. https://doi.org/10.1016/j.jaci.2009.12.980

Chen, L., Kwon, Y. D., Zhou, T., Wu, X., O'Dell, S., Cavacini, L., Hessell, A. J., Pancera, M., Tang, M., Xu, L., Yang, Z. Y., Zhang, M. Y., Arthos, J., Burton, D. R., Dimitrov, D. S., Nabel, G. J., Posner, M. R., Sodroski, J., Wyatt, R., Mascola, J. R., & Kwong, P. D. (2009, Nov 20). Structural basis of immune evasion at the site of CD4 attachment on HIV-1 gp120. *Science, 326*(5956), 1123-1127. https://doi.org/10.1126/science.1175868

Chen, Z. J., & Amigorena, S. (2015, Feb). Editorial overview: innate immunity. *Curr Opin Immunol, 32*, v-vi. https://doi.org/10.1016/j.coi.2015.01.016

Chiu, M. L., Goulet, D. R., Teplyakov, A., & Gilliland, G. L. (2019, Dec 3). Antibody Structure and Function: The Basis for Engineering Therapeutics. *Antibodies (Basel), 8*(4). https://doi.org/10.3390/antib8040055

Chohan, B., Lavreys, L., Rainwater, S. M. J., & Overbaugh, J. (2005). Evidence for Frequent Reinfection with Human Immunodeficiency Virus Type 1 of a Different Subtype. *Journal of Virology, 79*, 10701-10708. https://doi.org/10.1128/JVI.79.16.10701-10708.2005

Chukwuma, V. U., Kose, N., Sather, D. N., Sapparapu, G., Falk, R., King, H., Singh, V., Lampley, R., Malherbe, D. C., Ditto, N. T., Sullivan, J. T., Barnes, T., Doranz, B. J., Labranche, C. C., Montefiori, D. C., Kalams, S. A., Haigwood, N. L., & Crowe, J. E., Jr. (2018). Increased breadth of HIV-1 neutralization achieved by diverse antibody clones each with limited neutralization breadth. *PLoS ONE, 13*(12), e0209437. https://doi.org/10.1371/journal.pone.0209437

Corti, D., Langedijk, J. P., Hinz, A., Seaman, M. S., Vanzetta, F., Fernandez-Rodriguez, B. M., Silacci, C., Pinna, D., Jarrossay, D., Balla-Jhagjhoorsingh, S., Willems, B., Zekveld, M. J., Dreja, H., O'Sullivan, E., Pade, C., Orkin, C., Jeffs, S. A., Montefiori, D. C., Davis, D., Weissenhorn, W., McKnight, A., Heeney, J. L., Sallusto, F., Sattentau, Q. J., Weiss, R. A., & Lanzavecchia, A. (2010). Analysis of memory B cell responses and isolation of novel monoclonal antibodies with neutralizing breadth from HIV-1-infected individuals. *PLoS ONE, 5*(1), e8805. https://doi.org/10.1371/journal.pone.0008805

Danta, M., Semmo, N., Fabris, P., Brown, D., Pybus, O. G., Sabin, C. A., Bhagani, S., Emery, V. C., Dusheiko, G. M., & Klenerman, P. (2008, Jun 1). Impact of HIV on host-virus interactions during early hepatitis C virus infection. *J Infect Dis, 197*(11), 1558-1566. https://doi.org/10.1086/587843

Davis, S. K., Selva, K. J., Kent, S. J., & Chung, A. W. (2020, Apr). Serum IgA Fc effector functions in infectious disease and cancer. *Immunol Cell Biol, 98*(4), 276-286. https://doi.org/10.1111/imcb.12306

Delany, I., Rappuoli, R., & Seib, K. L. (2013, May 1). Vaccines, reverse vaccinology, and bacterial pathogenesis. *Cold Spring Harb Perspect Med, 3*(5), a012476. https://doi.org/10.1101/cshperspect.a012476

Deng, J., Wang, X., Zhang, B. Z., Gao, P., Lin, Q., Kao, R. Y., Gustafsson, K., Yuen, K. Y., & Huang, J. D. (2019, Sep 4). Broad and Effective Protection against Staphylococcus aureus Is Elicited by a Multivalent Vaccine Formulated with Novel Antigens. *mSphere, 4*(5). https://doi.org/10.1128/mSphere.00362-19

Donald, R. G., Hawkins, J. C., Hao, L., Liberator, P., Jones, T. R., Harris, S. L., Perez, J. L., Eiden, J. J., Jansen, K. U., & Anderson, A. S. (2017, Feb). Meningococcal serogroup B vaccines: Estimating breadth of coverage. *Hum Vaccin Immunother, 13*(2), 255-265. https://doi.org/10.1080/21645515.2017.1264750

Dorrington, K. J., & Klein, M. H. (1982, 1982/10/01/). Binding sites for Fcγ receptors on immunoglobulin G and factors influencing their expression. *Molecular Immunology, 19*(10), 1215-1221. https://doi.org/https://doi.org/10.1016/0161-5890(82)90286-3

Du, L., Tai, W., Yang, Y., Zhao, G., Zhu, Q., Sun, S., Liu, C., Tao, X., Tseng, C. K., Perlman, S., Jiang, S., Zhou, Y., & Li, F. (2016, Nov 22). Introduction of neutralizing immunogenicity index to the rational design of MERS coronavirus subunit vaccines. *Nat Commun, 7*, 13473. https://doi.org/10.1038/ncomms13473

Feuth, T., Arends, J. E., Fransen, J. H., Nanlohy, N. M., van Erpecum, K. J., Siersema, P. D., Hoepelman, A. I., & van Baarle, D. (2013). Complementary role of HCV and HIV in T-cell activation and exhaustion in HIV/HCV coinfection. *PLoS ONE, 8*(3), e59302. https://doi.org/10.1371/journal.pone.0059302

Finney, J., & Kelsoe, G. (2018, Jul 28). Poly- and autoreactivity of HIV-1 bNAbs: implications for vaccine design. *Retrovirology, 15*(1), 53. https://doi.org/10.1186/s12977-018-0435-0

Finney, J., Yang, G., Kuraoka, M., Song, S., Nojima, T., Verkoczy, L., Kitamura, D., Haynes, B. F., & Kelsoe, G. (2019, Dec 15). Cross-Reactivity to Kynureninase Tolerizes B Cells That Express the HIV-1 Broadly Neutralizing Antibody 2F5. *J Immunol, 203*(12), 3268-3281. https://doi.org/10.4049/jimmunol.1900069

Forgacs, D., Abreu, R. B., Sautto, G. A., Kirchenbaum, G. A., Drabek, E., Williamson, K. S., Kim, D., Emerling, D. E., & Ross, T. M. (2021). Convergent antibody evolution and clonotype expansion following influenza virus vaccination. *PLoS ONE, 16*(2), e0247253. https://doi.org/10.1371/journal.pone.0247253

Forthal, D. N. (2014). Functions of Antibodies. *Microbiology Spectrum, 2*(4), 1-17. https://pubmed.ncbi.nlm.nih.gov/25215264
https://www.ncbi.nlm.nih.gov/pmc/articles/PMC4159104/

Frenck, R. W., Jr., Creech, C. B., Sheldon, E. A., Seiden, D. J., Kankam, M. K., Baber, J., Zito, E., Hubler, R., Eiden, J., Severs, J. M., Sebastian, S., Nanra, J., Jansen, K. U., Gruber, W. C., Anderson, A. S., & Girgenti, D. (2017, Jan 5). Safety, tolerability, and immunogenicity of a 4-antigen Staphylococcus aureus vaccine (SA4Ag): Results from a first-in-human randomised, placebo-controlled phase 1/2 study. *Vaccine, 35*(2), 375-384. https://doi.org/10.1016/j.vaccine.2016.11.010

Galli, V., Simionatto, S., Marchioro, S. B., Klabunde, G. H., Conceicao, F. R., & Dellagostin, O. A. (2013, Sep). Recombinant secreted antigens from Mycoplasma hyopneumoniae delivered as a cocktail vaccine enhance the immune response of mice. *Clin Vaccine Immunol, 20*(9), 1370-1376. https://doi.org/10.1128/CVI.00140-13

Gally, J. A., & Edelman, G. M. (1970, 1970/07/01). Somatic Translocation of Antibody Genes. *Nature, 227*(5256), 341-348. https://doi.org/10.1038/227341a0

Gandhi, R. T., & Walker, B. D. (2002). Immunologic control of HIV-1. *Annu Rev Med, 53*, 149-172. https://doi.org/10.1146/annurev.med.53.082901.104011

Garcia, K. C. (2019, 2019/09/19/). Dual Arms of Adaptive Immunity: Division of Labor and Collaboration between B and T Cells. *Cell, 179*(1), 3-7. https://doi.org/https://doi.org/10.1016/j.cell.2019.08.022

Gebre, M. S., Brito, L. A., Tostanoski, L. H., Edwards, D. K., Carfi, A., & Barouch, D. H. (2021, Mar 18). Novel approaches for vaccine development. *Cell, 184*(6), 1589-1603. https://doi.org/10.1016/j.cell.2021.02.030

Giang, E., Dorner, M., Prentoe, J. C., Dreux, M., Evans, M. J., Bukh, J., Rice, C. M., Ploss, A., Burton, D. R., & Law, M. (2012, Apr 17). Human broadly neutralizing antibodies to the envelope glycoprotein complex of hepatitis C virus. *Proc Natl Acad Sci U S A, 109*(16), 6205-6210. https://doi.org/10.1073/pnas.1114927109

Gould, I. M., Reilly, J., Bunyan, D., & Walker, A. (2010, Dec). Costs of healthcare-associated methicillin-resistant Staphylococcus aureus and its control. *Clin Microbiol Infect, 16*(12), 1721-1728. https://doi.org/10.1111/j.1469-0691.2010.03365.x

Greenwood, B. (2014). The contribution of vaccination to global health: past, present and future. *Philos Trans R Soc Lond B Biol Sci, 369*(1645), 20130433. https://doi.org/10.1098/rstb.2013.0433

Grim, K. P., San Francisco, B., Radin, J. N., Brazel, E. B., Kelliher, J. L., Parraga Solorzano, P. K., Kim, P. C., McDevitt, C. A., & Kehl-Fie, T. E. (2017, Oct 31). The Metallophore Staphylopine Enables Staphylococcus aureus To Compete with the Host for Zinc and Overcome Nutritional Immunity. *mBio, 8*(5). https://doi.org/10.1128/mBio.01281-17

Gu, F., He, W., Xiao, S., Wang, S., Li, X., Zeng, Q., Ni, Y., & Han, L. (2020, 2020/04/07). Antimicrobial Resistance and Molecular Epidemiology of Staphylococcus aureus Causing Bloodstream Infections at Ruijin Hospital in Shanghai from 2013 to 2018. *Scientific Reports, 10*(1), 6019. https://doi.org/10.1038/s41598-020-63248-5

Guo, Y., Song, G., Sun, M., Wang, J., & Wang, Y. (2020, 2020-March-17). Prevalence and Therapies of Antibiotic-Resistance in Staphylococcus aureus [Review]. *Frontiers in Cellular and Infection Microbiology, 10*. https://doi.org/10.3389/fcimb.2020.00107

Hagan, E. C., & Mobley, H. L. (2007, Aug). Uropathogenic Escherichia coli outer membrane antigens expressed during urinary tract infection. *Infect Immun, 75*(8), 3941-3949. https://doi.org/10.1128/IAI.00337-07

Hajj Hussein, I., Chams, N., Chams, S., El Sayegh, S., Badran, R., Raad, M., Gerges-Geagea, A., Leone, A., & Jurjus, A. (2015). Vaccines Through Centuries: Major Cornerstones of Global Health. *Front Public Health, 3*, 269. https://doi.org/10.3389/fpubh.2015.00269

Hargrave, A., Mustafa, A. S., Hanif, A., Tunio, J. H., & Hanif, S. N. M. (2021). Current Status of HIV-1 Vaccines. *Vaccines, 9*(9), 1026. https://doi.org/10.3390/vaccines9091026

Harkness, D. R. (1970, 1970/12/01). Structure and Function of Immunoglobulins. *Postgraduate Medicine, 48*(6), 64-69. https://doi.org/10.1080/00325481.1970.11693629

Hart, P., Copland, A., Diogo, G. R., Harris, S., Spallek, R., Oehlmann, W., Singh, M., Basile, J., Rottenberg, M., Paul, M. J., & Reljic, R. (2018, Mar 7). Nanoparticle-Fusion Protein Complexes Protect against Mycobacterium tuberculosis Infection. *Mol Ther, 26*(3), 822-833. https://doi.org/10.1016/j.ymthe.2017.12.016

He, L., Cheng, Y., Kong, L., Azadnia, P., Giang, E., Kim, J., Wood, M. R., Wilson, I. A., Law, M., & Zhu, J. (2015, Aug 4). Approaching rational epitope vaccine design for hepatitis C virus with meta-server and multivalent scaffolding. *Sci Rep, 5*, 12501. https://doi.org/10.1038/srep12501

Hernandez, M. D., & Sherman, K. E. (2011). HIV/hepatitis C coinfection natural history and disease progression. *Current Opinion in HIV and AIDS, 6*(6), 478-482. https://doi.org/10.1097/COH.0b013e32834bd365

Hijazi, K., Wang, Y., Scala, C., Jeffs, S., Longstaff, C., Stieh, D., Haggarty, B., Vanham, G., Schols, D., Balzarini, J., Jones, I. M., Hoxie, J., Shattock, R., & Kelly, C. G. (2011). DC-SIGN Increases the Affinity of HIV-1 Envelope Glycoprotein Interaction with CD4. *PLoS ONE, 6*(12), e28307. https://doi.org/10.1371/journal.pone.0028307

Hood, M. I., & Skaar, E. P. (2012, 2012/08/01). Nutritional immunity: transition metals at the pathogen–host interface. *Nature Reviews Microbiology, 10*(8), 525-537. https://doi.org/10.1038/nrmicro2836

Hultgren, S. J., Schwan, W. R., Schaeffer, A. J., & Duncan, J. L. (1986, 1986/12//). Regulation of production of type 1 pili among urinary tract isolates of Escherichia coli. *Infection and Immunity, 54*(3), 613-620. https://doi.org/10.1128/iai.54.3.613-620.1986

Imkeller, K., & Wardemann, H. (2018). Assessing human B cell repertoire diversity and convergence. *Immunological Reviews, 284*(1), 51-66. https://doi.org/https://doi.org/10.1111/imr.12670

Ingiliz, P., Martin, T. C., Rodger, A., Stellbrink, H. J., Mauss, S., Boesecke, C., Mandorfer, M., Bottero, J., Baumgarten, A., Bhagani, S., Lacombe, K., Nelson, M., Rockstroh, J. K., & group, N. s. (2017, Feb). HCV reinfection incidence and spontaneous clearance rates in HIV-positive men who have sex with men in Western Europe. *J Hepatol, 66*(2), 282-287. https://doi.org/10.1016/j.jhep.2016.09.004

Iwasaki, A., & Medzhitov, R. (2015, 2015/04/01). Control of adaptive immunity by the innate immune system. *Nature Immunology, 16*(4), 343-353. https://doi.org/10.1038/ni.3123

J V Ravetch, a., & Kinet, J. P. (1991). Fc Receptors. *Annual Review of Immunology, 9*(1), 457-492. https://doi.org/10.1146/annurev.iy.09.040191.002325

Jackson, K., Kidd, M., Wang, Y., & Collins, A. (2013, 2013-September-02). The Shape of the Lymphocyte Receptor Repertoire: Lessons from the B Cell Receptor [Review]. *Frontiers in Immunology, 4*. https://doi.org/10.3389/fimmu.2013.00263

Jain, A., & Pasare, C. (2017, May 15). Innate Control of Adaptive Immunity: Beyond the Three-Signal Paradigm. *J Immunol, 198*(10), 3791-3800. https://doi.org/10.4049/jimmunol.1602000

Janeway, C. (2001a). The generation of diversity in immunoglobulins. In *Immunobiology: The Immune System in Health and Disease*. Garland Science.

Janeway, C. (2001b). The recognition and effector mechanisms of adaptive immunity. In *Immunobiology: The Immune System in Health and Disease*. Garland Science.

Jansen, K. U., Girgenti, D. Q., Scully, I. L., & Anderson, A. S. (2013, 2013/06/07/). Vaccine review: "Staphyloccocus aureus vaccines: Problems and prospects". *Vaccine, 31*(25), 2723-2730. https://doi.org/https://doi.org/10.1016/j.vaccine.2013.04.002

Jardine, J. G., Ota, T., Sok, D., Pauthner, M., Kulp, D. W., Kalyuzhniy, O., Skog, P. D., Thinnes, T. C., Bhullar, D., Briney, B., Menis, S., Jones, M., Kubitz, M., Spencer, S., Adachi, Y., Burton, D. R., Schief, W. R., & Nemazee, D. (2015, July 10, 2015). Priming a broadly neutralizing antibody response to HIV-1 using a germline-targeting immunogen. *Science, 349*(6244), 156-161. https://doi.org/10.1126/science.aac5894

Jefferis, R., Lund, J., & Pound, J. D. (1998). IgG-Fc-mediated effector functions: molecular definition of interaction sites for effector ligands and the role of glycosylation. *Immunological Reviews, 163*(1), 59-76. https://doi.org/https://doi.org/10.1111/j.1600-065X.1998.tb01188.x

Jenkins, A., Diep, B. A., Mai, T. T., Vo, N. H., Warrener, P., Suzich, J., Stover, C. K., & Sellman, B. R. (2015, Feb 17). Differential expression and roles of Staphylococcus aureus virulence determinants during colonization and disease. *mBio, 6*(1), e02272-02214. https://doi.org/10.1128/mBio.02272-14

Jones, D., & Helmreich, S. (2020). A history of herd immunity. *The Lancet, 396*(10254), 810-811. https://doi.org/10.1016/s0140-6736(20)31924-3

Kang, C. I., Song, J. H., Ko, K. S., Chung, D. R., & Peck, K. R. (2011, Jan). Clinical features and outcome of Staphylococcus aureus infection in elderly versus younger adult patients. *Int J Infect Dis, 15*(1), e58-62. https://doi.org/10.1016/j.ijid.2010.09.012

Keck, Z. Y., Pierce, B. G., Lau, P., Lu, J., Wang, Y., Underwood, A., Bull, R. A., Prentoe, J., Velazquez-Moctezuma, R., Walker, M. R., Luciani, F., Guest, J. D., Fauvelle, C., Baumert, T. F., Bukh, J., Lloyd, A. R., & Foung, S. K. H. (2019, May). Broadly neutralizing antibodies from an individual that naturally cleared multiple hepatitis C virus infections uncover molecular determinants for E2 targeting and vaccine design. *PLoS Pathog, 15*(5), e1007772. https://doi.org/10.1371/journal.ppat.1007772

Kehl-Fie, T. E., Zhang, Y., Moore, J. L., Farrand, A. J., Hood, M. I., Rathi, S., Chazin, W. J., Caprioli, R. M., & Skaar, E. P. (2013). MntABC and MntH contribute to systemic Staphylococcus aureus infection by competing with calprotectin for nutrient manganese. *Infection and Immunity, 81*(9), 3395-3405. https://doi.org/10.1128/IAI.00420-13

Kelsoe, G., & Haynes, B. F. (2017, Jan). Host controls of HIV broadly neutralizing antibody development. *Immunol Rev, 275*(1), 79-88. https://doi.org/10.1111/imr.12508

Kennedy, R. B., Ovsyannikova, I. G., Palese, P., & Poland, G. A. (2020). Current Challenges in Vaccinology. *Frontiers in Immunology, 11*, 1181-1181. https://doi.org/10.3389/fimmu.2020.01181

Klimka, A., Mertins, S., Nicolai, A. K., Rummler, L. M., Higgins, P. G., Günther, S. D., Tosetti, B., Krut, O., & Krönke, M. (2021, 2021/01/18). Epitope-specific immunity against Staphylococcus aureus coproporphyrinogen III oxidase. *NPJ Vaccines, 6*(1), 11. https://doi.org/10.1038/s41541-020-00268-2

Krismer, B., Weidenmaier, C., Zipperer, A., & Peschel, A. (2017, 2017/11/01). The commensal lifestyle of Staphylococcus aureus and its interactions with the nasal microbiota. *Nature Reviews Microbiology, 15*(11), 675-687. https://doi.org/10.1038/nrmicro.2017.104

Kwong, P. D., Mascola, J. R., & Nabel, G. J. (2011, Sep). Rational design of vaccines to elicit broadly neutralizing antibodies to HIV-1. *Cold Spring Harb Perspect Med, 1*(1), a007278. https://doi.org/10.1101/cshperspect.a007278

Lambers, F. A., Prins, M., Thomas, X., Molenkamp, R., Kwa, D., Brinkman, K., van der Meer, J. T., Schinkel, J., & group, M. s. (2011, Nov 13). Alarming incidence of hepatitis C virus re-infection after treatment of sexually acquired acute hepatitis C virus infection in HIV-infected MSM. *Aids, 25*(17), F21-27. https://doi.org/10.1097/QAD.0b013e32834bac44

Lara, J., Teka, M. A., Sims, S., Xia, G. L., Ramachandran, S., & Khudyakov, Y. (2018, Nov). HCV adaptation to HIV coinfection. *Infect Genet Evol, 65*, 216-225. https://doi.org/10.1016/j.meegid.2018.07.039

Lee, C. D., Watanabe, Y., Wu, N. C., Han, J., Kumar, S., Pholcharee, T., Seabright, G. E., Allen, J. D., Lin, C. W., Yang, J. R., Liu, M. T., Wu, C. Y., Ward, A. B., Crispin, M., & Wilson, I. A. (2021, Mar). A cross-neutralizing antibody between HIV-1 and influenza virus. *PLoS Pathog, 17*(3), e1009407. https://doi.org/10.1371/journal.ppat.1009407

Li, D., Huang, Z., & Zhong, J. (2015). Hepatitis C virus vaccine development: old challenges and new opportunities. *National Science Review, 2*(3), 285-295. https://doi.org/10.1093/nsr/nwv040

Lin, W., Weinberg, E. M., & Chung, R. T. (2013, Mar). Pathogenesis of accelerated fibrosis in HIV/HCV co-infection. *J Infect Dis, 207 Suppl 1*, S13-18. https://doi.org/10.1093/infdis/jis926

Liu, M., Yang, G., Wiehe, K., Nicely, N. I., Vandergrift, N. A., Rountree, W., Bonsignori, M., Alam, S. M., Gao, J., Haynes, B. F., & Kelsoe, G. (2015, Jan). Polyreactivity and autoreactivity among HIV-1 antibodies. *J Virol, 89*(1), 784-798. https://doi.org/10.1128/jvi.02378-14

Liu, M. A. (2019, Apr 24). A Comparison of Plasmid DNA and mRNA as Vaccine Technologies. *Vaccines (Basel), 7*(2). https://doi.org/10.3390/vaccines7020037

Lowy, F. D. (1998, 1998/08/20). Staphylococcus aureus Infections. *New England Journal of Medicine, 339*(8), 520-532. https://doi.org/10.1056/NEJM199808203390806

Lu, L. L., Suscovich, T. J., Fortune, S. M., & Alter, G. (2018, Jan). Beyond binding: antibody effector functions in infectious diseases. *Nat Rev Immunol, 18*(1), 46-61. https://doi.org/10.1038/nri.2017.106

Martinello, M., Hajarizadeh, B., Grebely, J., Dore, G. J., & Matthews, G. V. (2017). HCV Cure and Reinfection Among People With HIV/HCV Coinfection and People Who Inject Drugs. *Current HIV/AIDS Reports, 14*, 110-121. https://doi.org/10.1007/s11904-017-0358-8

Mascola, J. R., & Fauci, A. S. (2020, Feb). Novel vaccine technologies for the 21st century. *Nat Rev Immunol, 20*(2), 87-88. https://doi.org/10.1038/s41577-019-0243-3

Mastronarde, D. N. (2003). SerialEM: A Program for Automated Tilt Series Acquisition on Tecnai Microscopes Using Prediction of Specimen Position. *Microscopy and Microanalysis, 9*(S02), 1182-1183. https://doi.org/10.1017/S1431927603445911

McHutchison, J. G., Gordon, S. C., Schiff, E. R., Shiffman, M. L., Lee, W. M., Rustgi, V. K., Goodman, Z. D., Ling, M. H., Cort, S., & Albrecht, J. K. (1998, Nov 19). Interferon alfa-2b alone or in combination with ribavirin as initial treatment for chronic hepatitis C. Hepatitis Interventional Therapy Group. *N Engl J Med, 339*(21), 1485-1492. https://doi.org/10.1056/nejm199811193392101

McNeil, L. K., Zagursky, R. J., Lin, S. L., Murphy, E., Zlotnick, G. W., Hoiseth, S. K., Jansen, K. U., & Anderson, A. S. (2013, Jun). Role of factor H binding protein in Neisseria meningitidis virulence and its potential as a vaccine candidate to broadly protect against meningococcal disease. *Microbiol Mol Biol Rev, 77*(2), 234-252. https://doi.org/10.1128/MMBR.00056-12

Miller, L. S., Fowler, V. G., Shukla, S. K., Rose, W. E., & Proctor, R. A. (2020, Jan 1). Development of a vaccine against Staphylococcus aureus invasive infections: Evidence based on human immunity, genetics and bacterial evasion mechanisms. *FEMS Microbiol Rev, 44*(1), 123-153. https://doi.org/10.1093/femsre/fuz030

Mintz, M. A., & Cyster, J. G. (2020). T follicular helper cells in germinal center B cell selection and lymphomagenesis. *Immunological Reviews, 296*(1), 48-61. https://doi.org/https://doi.org/10.1111/imr.12860

Mitchison, N. A. (1971a). The carrier effect in the secondary response to hapten-protein conjugates. I. Measurement of the effect with transferred cells and objections to the local environment hypothesis. *European Journal of Immunology, 1*(1), 10-17. https://doi.org/https://doi.org/10.1002/eji.1830010103

Mitchison, N. A. (1971b). The carrier effect in the secondary response to hapten-protein conjugates. II. Cellular cooperation. *European Journal of Immunology, 1*(1), 18-27. https://doi.org/https://doi.org/10.1002/eji.1830010104

Mitchison, N. A. (1971c). The carrier effect in the secondary response to hapten-protein conjugates. V. Use of antilymphocyte serum to deplete animals of helper cells. *European Journal of Immunology, 1*(2), 68-75. https://doi.org/https://doi.org/10.1002/eji.1830010204

Mouquet, H., & Nussenzweig, M. C. (2012). Polyreactive antibodies in adaptive immune responses to viruses. *Cellular and Molecular Life Sciences, 69*, 1435-1445. https://doi.org/10.1007/s00018-011-0872-6

Moxon, R., Reche, P. A., & Rappuoli, R. (2019, 2019-December-03). Editorial: Reverse Vaccinology [Editorial]. *Frontiers in Immunology, 10*. https://doi.org/10.3389/fimmu.2019.02776

Nandi, A., & Shet, A. (2020, Aug 2). Why vaccines matter: understanding the broader health, economic, and child development benefits of routine vaccination. *Hum Vaccin Immunother, 16*(8), 1900-1904. https://doi.org/10.1080/21645515.2019.1708669

Nemazee, D. (2017, 2017/05/01). Mechanisms of central tolerance for B cells. *Nature Reviews Immunology, 17*(5), 281-294. https://doi.org/10.1038/nri.2017.19

Nicholson, L. B. (2016). The immune system. *Essays in biochemistry, 60*(3), 275-301. https://doi.org/10.1042/EBC20160017

Notidis, E., Heltemes, L., & Manser, T. (2002). Dominant, Hierarchical Induction of Peripheral Tolerance during Foreign Antigen-Driven B Cell Development. *Immunity, 17*(3), 317-327. https://doi.org/10.1016/S1074-7613(02)00392-8

Ofek, G., Guenaga, F. J., Schief, W. R., Skinner, J., Baker, D., Wyatt, R., & Kwong, P. D. (2010, Oct 19). Elicitation of structure-specific antibodies by epitope scaffolds. *Proc Natl Acad Sci U S A, 107*(42), 17880-17887. https://doi.org/10.1073/pnas.1004728107

Ohi, M., Li, Y., Cheng, Y., & Walz, T. (2004). Negative Staining and Image Classification - Powerful Tools in Modern Electron Microscopy. *Biol Proced Online, 6*, 23-34. https://doi.org/10.1251/bpo70

Operskalski, E. A., & Kovacs, A. (2011). HIV/HCV co-infection: Pathogenesis, clinical complications, treatment, and new therapeutic technologies. *Current HIV/AIDS Reports, 8*, 12-22. https://doi.org/10.1007/s11904-010-0071-3

Parra, M., Pickett, T., Delogu, G., Dheenadhayalan, V., Debrie, A. S., Locht, C., & Brennan, M. J. (2004, Dec). The mycobacterial heparin-binding hemagglutinin is a protective antigen in the mouse aerosol challenge model of tuberculosis. *Infect Immun, 72*(12), 6799-6805. https://doi.org/10.1128/IAI.72.12.6799-6805.2004

Paschall, A. V., Middleton, D. R., & Avci, F. Y. (2019). Opsonophagocytic Killing Assay to Assess Immunological Responses Against Bacterial Pathogens. *Journal of visualized experiments : JoVE*(146), 10.3791/59400. https://doi.org/10.3791/59400

Pethe, K., Alonso, S., Biet, F., Delogu, G., Brennan, M. J., Locht, C., & Menozzi, F. D. (2001, 2001/07/01). The heparin-binding haemagglutinin of M. tuberculosis is required for extrapulmonary dissemination. *Nature, 412*(6843), 190-194. https://doi.org/10.1038/35084083

Pierce, B. G., Boucher, E. N., Piepenbrink, K. H., Ejemel, M., Rapp, C. A., Thomas, W. D., Sundberg, E. J., Weng, Z., & Wang, Y. (2017). Structure-Based Design of Hepatitis C Virus Vaccines that Elicit Neutralizing Antibody Responses to a Conserved Epitope. *Journal of Virology, 91*, JVI.01032-01017. https://doi.org/10.1128/JVI.01032-17

Pineda, J. A., Garcia-Garcia, J. A., Aguilar-Guisado, M., Rios-Villegas, M. J., Ruiz-Morales, J., Rivero, A., del Valle, J., Luque, R., Rodriguez-Bano, J., Gonzalez-Serrano, M., Camacho, A., Macias, J., Grilo, I., Gomez-Mateos, J. M., & Grupo

para el Estudio de las Hepatitis Viricas de la Sociedad Andaluza de Enfermedades, I. (2007, Sep). Clinical progression of hepatitis C virus-related chronic liver disease in human immunodeficiency virus-infected patients undergoing highly active antiretroviral therapy. *Hepatology, 46*(3), 622-630. https://doi.org/10.1002/hep.21757

Piot, P., Larson, H. J., O'Brien, K. L., N'Kengasong, J., Ng, E., Sow, S., & Kampmann, B. (2019, Nov). Immunization: vital progress, unfinished agenda. *Nature, 575*(7781), 119-129. https://doi.org/10.1038/s41586-019-1656-7

Pizarro-Cerda, J., & Cossart, P. (2006, Feb 24). Bacterial adhesion and entry into host cells. *Cell, 124*(4), 715-727. https://doi.org/10.1016/j.cell.2006.02.012

Planchais, C., Kok, A., Kanyavuz, A., Lorin, V., Bruel, T., Guivel-Benhassine, F., Rollenske, T., Prigent, J., Hieu, T., Prazuck, T., Lefrou, L., Wardemann, H., Schwartz, O., Dimitrov, J. D., Hocqueloux, L., & Mouquet, H. (2019, Apr 9). HIV-1 Envelope Recognition by Polyreactive and Cross-Reactive Intestinal B Cells. *Cell Rep, 27*(2), 572-585 e577. https://doi.org/10.1016/j.celrep.2019.03.032

Platt, L., Easterbrook, P., Gower, E., McDonald, B., Sabin, K., McGowan, C., Yanny, I., Razavi, H., & Vickerman, P. (2016). Prevalence and burden of HCV co-infection in people living with HIV: A global systematic review and meta-analysis. *The Lancet Infectious Diseases, 16*, 797-808. https://doi.org/10.1016/S1473-3099(15)00485-5

Plotkin, S. (2014). History of vaccination. *Proceedings of the National Academy of Sciences, 111*(34), 12283-12287. https://doi.org/10.1073/pnas.1400472111

Plotkin, S. A. (2010, Jul). Correlates of protection induced by vaccination. *Clin Vaccine Immunol, 17*(7), 1055-1065. https://doi.org/10.1128/CVI.00131-10

Pohlmann, S., Baribaud, F., Lee, B., Leslie, G. J., Sanchez, M. D., Hiebenthal-Millow, K., Munch, J., Kirchhoff, F., & Doms, R. W. (2001, May). DC-SIGN interactions with

human immunodeficiency virus type 1 and 2 and simian immunodeficiency virus. *J Virol, 75*(10), 4664-4672. https://doi.org/10.1128/JVI.75.10.4664-4672.2001

Pöhlmann, S., Zhang, J., Baribaud, F., Chen, Z., Leslie, G. J., Lin, G., Granelli-Piperno, A., Doms, R. W., Rice, C. M., & McKeating, J. A. (2003, Apr). Hepatitis C virus glycoproteins interact with DC-SIGN and DC-SIGNR. *J Virol, 77*(7), 4070-4080. https://doi.org/10.1128/jvi.77.7.4070-4080.2003

Pollard, A. J., & Bijker, E. M. (2021, Feb). A guide to vaccinology: from basic principles to new developments. *Nat Rev Immunol, 21*(2), 83-100. https://doi.org/10.1038/s41577-020-00479-7

Pöyhönen, L., Bustamante, J., Casanova, J.-L., Jouanguy, E., & Zhang, Q. (2019, 2019/05/01). Life-Threatening Infections Due to Live-Attenuated Vaccines: Early Manifestations of Inborn Errors of Immunity. *Journal of Clinical Immunology, 39*(4), 376-390. https://doi.org/10.1007/s10875-019-00642-3

Pozzi, C., Olaniyi, R., Liljeroos, L., Galgani, I., Rappuoli, R., & Bagnoli, F. (2017). Vaccines for Staphylococcus aureus and Target Populations. In F. Bagnoli, R. Rappuoli, & G. Grandi (Eds.), *Staphylococcus aureus: Microbiology, Pathology, Immunology, Therapy and Prophylaxis* (pp. 491-528). Springer International Publishing. https://doi.org/10.1007/82_2016_54

Proctor, R. A. (2012). Challenges for a Universal Staphylococcus aureus Vaccine. *Clinical Infectious Diseases, 54*(8), 1179-1186. https://doi.org/10.1093/cid/cis033

Proctor, R. A. (2015, Dec 2). Recent developments for Staphylococcus aureus vaccines: clinical and basic science challenges. *Eur Cell Mater, 30*, 315-326. https://doi.org/10.22203/ecm.v030a22

Pugach, P., Ozorowski, G., Cupo, A., Ringe, R., Yasmeen, A., de Val, N., Derking, R., Kim, H. J., Korzun, J., Golabek, M., de los Reyes, K., Ketas, T. J., Julien, J.-P., Burton, D. R., Wilson, I. A., Sanders, R. W., Klasse, P. J., Ward, A. B., & Moore,

J. P. (2015). A Native-Like SOSIP.664 Trimer Based on an HIV-1 Subtype B env Gene. *Journal of Virology, 89*, 3380-3395. https://doi.org/10.1128/JVI.03473-14

Pulendran, B., & Ahmed, R. (2011, Jun). Immunological mechanisms of vaccination. *Nat Immunol, 12*(6), 509-517. https://doi.org/10.1038/ni.2039

Punjani, A., Rubinstein, J. L., Fleet, D. J., & Brubaker, M. A. (2017, Mar). cryoSPARC: algorithms for rapid unsupervised cryo-EM structure determination. *Nat Methods, 14*(3), 290-296. https://doi.org/10.1038/nmeth.4169

Rappuoli, R., Bottomley, M. J., D'Oro, U., Finco, O., & De Gregorio, E. (2016). Reverse vaccinology 2.0: Human immunology instructs vaccine antigen design. *The Journal of experimental medicine, 213*(4), 469-481. https://doi.org/10.1084/jem.20151960

Reiche, S., Nestler, C., Sieg, M., Schulz, K., Cordes, C., Krznaric, I., & Jassoy, C. (2014, Apr). Hepatitis C virus (HCV)-specific memory B-cell responses in transiently and chronically infected HIV positive individuals. *J Clin Virol, 59*(4), 218-222. https://doi.org/10.1016/j.jcv.2014.01.023

Rodrigues, C. M. C., & Plotkin, S. A. (2020). Impact of Vaccines; Health, Economic and Social Perspectives. *Front Microbiol, 11*, 1526. https://doi.org/10.3389/fmicb.2020.01526

Rose, D. R. (1982). The generation of antibody diversity. *American Journal of Hematology, 13*(1), 91-99. https://doi.org/https://doi.org/10.1002/ajh.2830130111

Russo, T. A., Carlino, U. B., & Johnson, J. R. (2001, Oct). Identification of a new iron-regulated virulence gene, ireA, in an extraintestinal pathogenic isolate of Escherichia coli. *Infect Immun, 69*(10), 6209-6216. https://doi.org/10.1128/IAI.69.10.6209-6216.2001

Rustgi, V. K. (2007, Jul). The epidemiology of hepatitis C infection in the United States. *J Gastroenterol, 42*(7), 513-521. https://doi.org/10.1007/s00535-007-2064-6

Sakano, H., Maki, R., Kurosawa, Y., Roeder, W., & Tonegawa, S. (1980, 1980/08/01). Two types of somatic recombination are necessary for the generation of complete immunoglobulin heavy-chain genes. *Nature, 286*(5774), 676-683. https://doi.org/10.1038/286676a0

Salazar, N., Castiblanco-Valencia, M. M., da Silva, L. B., de Castro, Í. A., Monaris, D., Masuda, H. P., Barbosa, A. S., & Arêas, A. P. M. (2014). Staphylococcus aureus manganese transport protein C (MntC) is an extracellular matrix- and plasminogen-binding protein. *PLoS ONE, 9*(11), e112730-e112730. https://doi.org/10.1371/journal.pone.0112730

Salgado-Pabón, W., & Schlievert, P. M. (2014, 2014/08/01). Models matter: the search for an effective Staphylococcus aureus vaccine. *Nature Reviews Microbiology, 12*(8), 585-591. https://doi.org/10.1038/nrmicro3308

Sanders, R. W., Derking, R., Cupo, A., Julien, J. P., Yasmeen, A., de Val, N., Kim, H. J., Blattner, C., de la Pe??a, A. T., Korzun, J., Golabek, M., de los Reyes, K., Ketas, T. J., van Gils, M. J., King, C. R., Wilson, I. A., Ward, A. B., Klasse, P. J., & Moore, J. P. (2013). A Next-Generation Cleaved, Soluble HIV-1 Env Trimer, BG505 SOSIP.664 gp140, Expresses Multiple Epitopes for Broadly Neutralizing but Not Non-Neutralizing Antibodies. *PLoS Pathogens, 9*. https://doi.org/10.1371/journal.ppat.1003618

Sarzotti-Kelsoe, M., Bailer, R. T., Turk, E., Lin, C. l., Bilska, M., Greene, K. M., Gao, H., Todd, C. A., Ozaki, D. A., Seaman, M. S., Mascola, J. R., & Montefiori, D. C. (2014). Optimization and validation of the TZM-bl assay for standardized assessments of neutralizing antibodies against HIV-1. *Journal of Immunological Methods, 409*, 131-146. https://doi.org/10.1016/j.jim.2013.11.022

Sather, D. N., Armann, J., Ching, L. K., Mavrantoni, A., Sellhorn, G., Caldwell, Z., Yu, X., Wood, B., Self, S., Kalams, S., & Stamatatos, L. (2009, Jan). Factors associated with the development of cross-reactive neutralizing antibodies during human immunodeficiency virus type 1 infection. *J Virol, 83*(2), 757-769. https://doi.org/JVI.02036-08 [pii]
10.1128/JVI.02036-08

Sather, D. N., Carbonetti, S., Malherbe, D. C., Pissani, F., Stuart, A. B., Hessell, A. J., Gray, M. D., Mikell, I., Kalams, S. A., Haigwood, N. L., & Stamatatos, L. (2014, Nov). Emergence of broadly neutralizing antibodies and viral coevolution in two subjects during the early stages of infection with human immunodeficiency virus type 1. *J Virol, 88*(22), 12968-12981. https://doi.org/10.1128/JVI.01816-14

Sautto, G. A., Kirchenbaum, G. A., Abreu, R. B., Ecker, J. W., Pierce, S. R., Kleanthous, H., & Ross, T. M. (2020, Jan 15). A Computationally Optimized Broadly Reactive Antigen Subtype-Specific Influenza Vaccine Strategy Elicits Unique Potent Broadly Neutralizing Antibodies against Hemagglutinin. *J Immunol, 204*(2), 375-385. https://doi.org/10.4049/jimmunol.1900379

Scarselli, M., Aricò, B., Brunelli, B., Savino, S., Di Marcello, F., Palumbo, E., Veggi, D., Ciucchi, L., Cartocci, E., Bottomley, M. J., Malito, E., Lo Surdo, P., Comanducci, M., Giuliani, M. M., Cantini, F., Dragonetti, S., Colaprico, A., Doro, F., Giannetti, P., Pallaoro, M., Brogioni, B., Tontini, M., Hilleringmann, M., Nardi-Dei, V., Banci, L., Pizza, M., & Rappuoli, R. (2011). Rational Design of a Meningococcal Antigen Inducing Broad Protective Immunity. *Science Translational Medicine, 3*(91), 91ra62-91ra62. https://doi.org/10.1126/scitranslmed.3002234

Setliff, I., Shiakolas, A. R., Pilewski, K. A., Murji, A. A., Mapengo, R. E., Janowska, K., Richardson, S., Oosthuysen, C., Raju, N., Ronsard, L., Kanekiyo, M., Qin, J. S., Kramer, K. J., Greenplate, A. R., McDonnell, W. J., Graham, B. S., Connors, M., Lingwood, D., Acharya, P., Morris, L., & Georgiev, I. S. (2019, Dec 12). High-Throughput Mapping of B Cell Receptor Sequences to Antigen Specificity. *Cell, 179*(7), 1636-1646 e1615. https://doi.org/10.1016/j.cell.2019.11.003

Sette, A., & Rappuoli, R. (2010, Oct 29). Reverse vaccinology: developing vaccines in the era of genomics. *Immunity, 33*(4), 530-541. https://doi.org/10.1016/j.immuni.2010.09.017

Sheldon, J., & Heinrichs, D. (2012, 2012-April-04). The iron-regulated staphylococcal lipoproteins [Review]. *Frontiers in Cellular and Infection Microbiology, 2*. https://doi.org/10.3389/fcimb.2012.00041

Swanson, K. A., Rainho-Tomko, J. N., Williams, Z. P., Lanza, L., Peredelchuk, M., Kishko, M., Pavot, V., Alamares-Sapuay, J., Adhikarla, H., Gupta, S., Chivukula, S., Gallichan, S., Zhang, L., Jackson, N., Yoon, H., Edwards, D., Wei, C.-J., & Nabel, G. J. (2020). A respiratory syncytial virus (RSV) F protein nanoparticle vaccine focuses antibody responses to a conserved neutralization domain. *Science Immunology, 5*(47), eaba6466. https://doi.org/10.1126/sciimmunol.aba6466

Tang, D., Kang, R., Coyne, C. B., Zeh, H. J., & Lotze, M. T. (2012). PAMPs and DAMPs: signal 0s that spur autophagy and immunity. *Immunological Reviews, 249*(1), 158-175. https://doi.org/10.1111/j.1600-065X.2012.01146.x

Tester, I., Smyk-Pearson, S., Wang, P., Wertheimer, A., Yao, E., Lewinsohn, D. M., Tavis, J. E., & Rosen, H. R. (2005, Jun 6). Immune evasion versus recovery after acute hepatitis C virus infection from a shared source. *J Exp Med, 201*(11), 1725-1731. https://doi.org/10.1084/jem.20042284

Teymournejad, O., & Montgomery, C. P. (2021, 2021-February-22). Evasion of Immunological Memory by S. aureus Infection: Implications for Vaccine Design [Review]. *Frontiers in Immunology, 12*. https://doi.org/10.3389/fimmu.2021.633672

Tonegawa, S. (1983, Apr 14). Somatic generation of antibody diversity. *Nature, 302*(5909), 575-581. https://doi.org/10.1038/302575a0

Tong, S. Y. C., Davis, J. S., Eichenberger, E., Holland, T. L., & Fowler, V. G., Jr. (2015). Staphylococcus aureus infections: epidemiology, pathophysiology, clinical manifestations, and management. *Clinical microbiology reviews, 28*(3), 603-661. https://doi.org/10.1128/CMR.00134-14

Toor, J., Echeverria-Londono, S., Li, X., Abbas, K., Carter, E. D., Clapham, H. E., Clark, A., de Villiers, M. J., Eilertson, K., Ferrari, M., Gamkrelidze, I., Hallett, T. B., Hinsley, W. R., Hogan, D., Huber, J. H., Jackson, M. L., Jean, K., Jit, M., Karachaliou, A., Klepac, P., Kraay, A., Lessler, J., Li, X., Lopman, B. A., Mengistu, T., Metcalf, C. J. E., Moore, S. M., Nayagam, S., Papadopoulos, T., Perkins, T. A., Portnoy, A., Razavi, H., Razavi-Shearer, D., Resch, S., Sanderson, C., Sweet, S., Tam, Y., Tanvir, H., Tran Minh, Q., Trotter, C. L., Truelove, S. A., Vynnycky, E., Walker, N., Winter, A., Woodruff, K., Ferguson, N. M., & Gaythorpe, K. A. (2021, Jul 13). Lives saved with vaccination for 10 pathogens across 112 countries in a pre-COVID-19 world. *eLife, 10*. https://doi.org/10.7554/eLife.67635

Trkola, A., Purtscher, M., Muster, T., Ballaun, C., Buchacher, A., Sullivan, N., Srinivasan, K., Sodroski, J., Moore, J. P., & Katinger, H. (1996, Feb). Human monoclonal antibody 2G12 defines a distinctive neutralization epitope on the gp120 glycoprotein of human immunodeficiency virus type 1. *J Virol, 70*(2), 1100-1108. https://doi.org/10.1128/jvi.70.2.1100-1108.1996

Verkoczy, L., & Diaz, M. (2014, May). Autoreactivity in HIV-1 broadly neutralizing antibodies: implications for their function and induction by vaccination. *Curr Opin HIV AIDS, 9*(3), 224-234. https://doi.org/10.1097/COH.0000000000000049

Vestergaard, M., Frees, D., Ingmer, H., Fischetti Vincent, A., Novick Richard, P., Ferretti Joseph, J., Portnoy Daniel, A., Braunstein, M., & Rood Julian, I. (2019, 2019/03/22). Antibiotic Resistance and the MRSA Problem. *Microbiology Spectrum, 7*(2), 7.2.18. https://doi.org/10.1128/microbiolspec.GPP3-0057-2018

Vivithanaporn, P., Nelles, K., DeBlock, L., Newman, S. C., Gill, M. J., & Power, C. (2012, Jan 15). Hepatitis C virus co-infection increases neurocognitive impairment

severity and risk of death in treated HIV/AIDS. *J Neurol Sci, 312*(1-2), 45-51. https://doi.org/10.1016/j.jns.2011.08.025

Wareing, M. D., & Tannock, G. A. (2001, 2001/05/14/). Live attenuated vaccines against influenza; an historical review. *Vaccine, 19*(25), 3320-3330. https://doi.org/https://doi.org/10.1016/S0264-410X(01)00045-7

Williams, W. B., Han, Q., & Haynes, B. F. (2018, Jan). Cross-reactivity of HIV vaccine responses and the microbiome. *Curr Opin HIV AIDS, 13*(1), 9-14. https://doi.org/10.1097/COH.0000000000000423

Williams, W. B., Liao, H. X., Moody, M. A., Kepler, T. B., Alam, S. M., Gao, F., Wiehe, K., Trama, A. M., Jones, K., Zhang, R., Song, H., Marshall, D. J., Whitesides, J. F., Sawatzki, K., Hua, A., Liu, P., Tay, M. Z., Seaton, K. E., Shen, X., Foulger, A., Lloyd, K. E., Parks, R., Pollara, J., Ferrari, G., Yu, J. S., Vandergrift, N., Montefiori, D. C., Sobieszczyk, M. E., Hammer, S., Karuna, S., Gilbert, P., Grove, D., Grunenberg, N., McElrath, M. J., Mascola, J. R., Koup, R. A., Corey, L., Nabel, G. J., Morgan, C., Churchyard, G., Maenza, J., Keefer, M., Graham, B. S., Baden, L. R., Tomaras, G. D., & Haynes, B. F. (2015, Aug 14). HIV-1 VACCINES. Diversion of HIV-1 vaccine-induced immunity by gp41-microbiota cross-reactive antibodies. *Science, 349*(6249), aab1253. https://doi.org/10.1126/science.aab1253

Williams, W. B., Meyerhoff, R. R., Edwards, R. J., Li, H., Manne, K., Nicely, N. I., Henderson, R., Zhou, Y., Janowska, K., Mansouri, K., Gobeil, S., Evangelous, T., Hora, B., Berry, M., Abuahmad, A. Y., Sprenz, J., Deyton, M., Stalls, V., Kopp, M., Hsu, A. L., Borgnia, M. J., Stewart-Jones, G. B. E., Lee, M. S., Bronkema, N., Moody, M. A., Wiehe, K., Bradley, T., Alam, S. M., Parks, R. J., Foulger, A., Oguin, T., Sempowski, G. D., Bonsignori, M., LaBranche, C. C., Montefiori, D. C., Seaman, M., Santra, S., Perfect, J., Francica, J. R., Lynn, G. M., Aussedat, B., Walkowicz, W. E., Laga, R., Kelsoe, G., Saunders, K. O., Fera, D., Kwong, P. D., Seder, R. A., Bartesaghi, A., Shaw, G. M., Acharya, P., & Haynes, B. F. (2021, May 27). Fab-dimerized glycan-reactive antibodies are a structural category of

natural antibodies. *Cell, 184*(11), 2955-2972 e2925. https://doi.org/10.1016/j.cell.2021.04.042

Zhang, L., Wang, W., & Wang, S. (2015). Effect of vaccine administration modality on immunogenicity and efficacy. *Expert Rev Vaccines, 14*(11), 1509-1523. https://doi.org/10.1586/14760584.2015.1081067